

SSP

DEVELOPMENT OF MODELS FOR PREDICTING WATER AND SEDIMENT ROUTING AND YIELD FROM STORMS ON SMALL WATERSHEDS

Prepared for

USDA FOREST SERVICE
ROCKY MOUNTAIN FOREST AND RANGE
EXPERIMENT STATION

Flagstaff Arizona



Prepared by

Civil Engineering Department
Engineering Research Center
Colorado State University
Fort Collins, Colorado

D. B. Simons
R. M. Li
M. A. Stevens

August, 1975

CER 74 - 75 DBS - RML - MAS 24

TABLE OF CONTENTS

DEVELOPMENT OF MODELS FOR PREDICTING WATER AND SEDIMENT ROUTING AND YIELD FROM STORMS ON SMALL WATERSHEDS

Prepared for

USDA FOREST SERVICE
ROCKY MOUNTAIN FOREST AND RANGE
EXPERIMENT STATION

Flagstaff Arizona



Prepared by

Civil Engineering Department
Engineering Research Center
Colorado State University
Fort Collins, Colorado

D. B. Simons
R. M. Li
M. A. Stevens

TABLE OF CONTENTS

	Page	Page
AUTHORIZATION	50	iv
LIST OF TABLES	51	v
LIST OF FIGURES	56	vi
1. INTRODUCTION	59	1
GENERAL	59	1
OBJECTIVES	61	3
SCOPE OF THE PRESENT STUDY	62	4
MODEL STRUCTURE		5
2. GEOMETRY OF A WATERSHED	65	8
SEGMENTATION OF THE WATERSHED	65	8
RELATION BETWEEN WETTED PERIMETER AND FLOW AREA	66	9
3. ESTIMATION OF EXCESS RAINFALL	72	12
NET RAINFALL	72	13
GROUND RESPONSE TO RAINFALL	73	18
INFILTRATION	77	22
SOIL MOISTURE ADJUSTMENT		27
MEAN RAINFALL EXCESS RATE	79	29
4. WATER ROUTING	81	
CONTINUITY EQUATION FOR WATER	81	30
MOMENTUM EQUATION	93	30
RESISTANCE EQUATIONS	101	31
Overland flow resistance		32
Channel flow resistance	107	34
Grain resistance factor		38
Overall resistance factor		41
DISCHARGE AND FLOW AREA RELATION	109	42
NUMERICAL SCHEME	110	43
Nonlinear scheme		45
Linear scheme		49

	<u>Page</u>
5. SEDIMENT ROUTING	50
CONTINUITY FOR SEDIMENT	50
SEDIMENT TRANSPORT EQUATIONS	51
EQUATIONS FOR SEDIMENT SUPPLY	56
Soil detachment by raindrop impact	56
Soil detachment by surface runoff	58
NUMERICAL PROCEDURE FOR SEDIMENT ROUTING	59
Bed-material load routing	59
Wash load routing	61
Degradation or aggradation	62
6. MODEL APPLICATION AND VERIFICATION	65
INPUT DATA	65
Basin characteristics data	66
Geometry data	66
Soil data	71
Vegetation and ground cover data	74
Flow resistance parameters	75
Sediment routing parameters	76
Storm characteristics data	76
Antecedent conditions	77
MODEL CALIBRATION	79
TESTS RESULTS	81
Comparisons of the simulated and measured results	81
Discussion of test results	93
Applications to predict watershed treatment effects	101
7. SUMMARY	107
8. FUTURE WORK	109
PLANNED WORK	109
OTHER CONSIDERATIONS	110
REFERENCES	112
APPENDIX	114

AUTHORIZATION

This research was sponsored by the USDA Forest Service, Rocky Mountain Forest and Range Experiment Station under Grant PL 89-106 and supported with Colorado State University matching funds. The investigations were conducted in accordance with the Research Agreement No. 16-289-GR between the Rocky Mountain Forest and Range Experiment Station and Colorado State University. Harry E. Brown and D. Ross Carder were authorized departmental officers for the Rocky Mountain Forest and Range Experiment Station and Daryl B. Simons was the principal investigator. The period of agreement was from May 15, 1972 to June 30, 1975.

LIST OF TABLES

		<u>Page</u>
Table 3.1	Rain reaching the ground	15
Table 6.1	Geometry of Watershed 1	69
Table 6.2	Geometry of Watershed 2	70
Table 6.3	Computational Sequence for Watershed 1	72
Table 6.4	Computational Sequence for Watershed 17	73
Table 6.5	Antecedent moisture contents	81
Table 6.6	Errors in Simulation	84
Fig. 3.1	Representation of the soil-moisture depletion curve	20
Fig. 4.1	Resistance to flow in overland flow units results from ground cover as well as from the soil	33
Fig. 4.2	Resistance to flow in channel flow units	35
Fig. 4.3	Rectangular network in the x-t plane	44
Fig. 5.1	Geometric segmentation of Watershed 1	57
Fig. 5.2	Geometric segmentation of Watershed 17	58
Fig. 5.3	Water hydrograph from Watershed 17 for the September 5, 1970 storm	61
Fig. 5.4	Water hydrograph from Watershed 1 for the September 5, 1970 storm	64
Fig. 5.5	Water hydrograph from Watershed 1 for the September 6, 1967 storm	64
Fig. 5.6	Water hydrograph from Watershed 1 for the November 22, 1965 storm	65
Fig. 5.7	Water hydrograph from Watershed 1 for the November 24, 1965 storm	66
Fig. 5.8	Water hydrograph from Watershed 1 for the November 25, 1965 storm	67
Fig. 5.9	Comparison of measured and simulated water yield	68
Fig. 5.10	Comparison of measured and simulated peak water flows	69
Fig. 5.11	Comparison of measured and simulated time to peak water flow	90
Fig. 5.12	Comparison of measured and simulated sediment yields	91
Fig. 5.13	Computed infiltration capacity in Watershed 1 during the September 5, 1970 storm	92
Fig. 5.14	Aggradation and degradation of channels in Watershed 1 during the September 5, 1970 storm	97

LIST OF FIGURES

		<u>Page</u>
Fig. 1.1	Flow chart for the water and sediment routing model	6
Fig. 2.1	Examples of watershed segmentation	10
Fig. 2.2	Wetted perimeter versus flow area for the main channel in Watershed 1	11
Fig. 3.1	Rain reaching the ground	14
Fig. 3.2	Ground response to net rainfall	19
Fig. 3.3	Soil moisture profile	24
Fig. 3.4	Representation of the soil-moisture depletion curve	26
Fig. 4.1	Resistance to flow in overland flow units results from ground cover as well as from the soil	35
Fig. 4.2	Resistance to flow in channel flow units	35
Fig. 4.3	Rectangular network in the x-t plane	44
Fig. 6.1	Geometric segmentation of Watershed 1	67
Fig. 6.2	Geometric segmentation of Watershed 17	68
Fig. 6.3	Water hydrograph from Watershed 17 for the September 5, 1970 storm	83
Fig. 6.4	Water hydrograph from Watershed 1 for the September 5, 1970 storm	84
Fig. 6.5	Water hydrograph from Watershed 1 for the September 6, 1967 storm	84
Fig. 6.6	Water hydrograph from Watershed 1 for the November 22, 1965 storm	85
Fig. 6.7	Water hydrograph from Watershed 1 for the November 24, 1965 storm	86
Fig. 6.8	Water hydrograph from Watershed 1 for the November 25, 1965 storm	87
Fig. 6.9	Comparison of measured and simulated water yield	88
Fig. 6.10	Comparison of measured and simulated peak water flows	89
Fig. 6.11	Comparison of measured and simulated time to peak water flow	90
Fig. 6.12	Comparison of measured and simulated sediment yields	91
Fig. 6.13	Computed infiltration capacity in Watershed 1 during the September 6, 1967 storm	92
Fig. 6.14	Aggradation and degradation of channels in Watershed 1 during the September 5, 1970 storm	96
		97

Fig. 6.15	Computed hydrographs for the September 5, 1970 storm on Watershed 1	97
Fig. 6.16	Computed hydrographs for the November 22, 1965 storm on Watershed 1	98
Fig. 6.17	Sediment yields from a sequence of storms over Watershed 1	99
Fig. 6.18	Effect of canopy cover density on the water hydrograph from Watershed 1	101
Fig. 6.19	Effect of canopy cover density on the sediment hydrograph from Watershed 1	102
Fig. 6.20	Effect of ground cover density on the water hydrograph from Watershed 1	103
Fig. 6.21	Effect of ground cover density on the sediment yield from Watershed 1	104

A_c	Area covered by trees in an overland flow unit	L^2
A_g	Area with ground cover within area A_c	L^2
A_o	Area without trees in an overland flow unit	L^2
δ	Thickness of bed layer	L
α_1	Coefficient in P vs. A relation	
α_2	Coefficient in resistance equation	
α_3	Coefficient in raindrop soil detachment equation	
k	Constant depending on roughness	
β_1	Exponent in P vs. A relation	
β_2	Exponent in resistance equation	
β_3	Exponent in raindrop soil detachment equation	
C	Sediment concentration by volume	
C_a	Sediment concentration at a distance a above the bed	
C_b	Concentration of suspended bed material load	
C_d	Drag coefficient	
C_g	Channel-flow ground cover density	
C_w	Concentration of wash load	
C_{aL}	Sediment concentration at distance L from the bed	
C_{bL}	Potential bed material load concentration	
C_{wL}	Potential wash load concentration	

LIST OF SYMBOLS

<u>Symbol</u>	<u>Description</u>	<u>Unit</u>
A	Cross-sectional area of flow	L^2
A_g	Area with ground cover within a specific area	L^2
A_h	Cross-sectional area of flow occupied by the high ground cover	L^2
A_g^c	Area with ground cover within area A_t^c	L^2
A_t^c	Area covered by trees in an overland flow unit	L^2
A_g^o	Area with ground cover within area A_t^o	L^2
A_t^o	Area without trees in an overland flow unit	L^2
a	Thickness of bed layer	L
a_1	Coefficient in P vs. A relation	
a_2	Coefficient in resistance equation	
a_3	Coefficient in raindrop soil detachment equation	
B	Constant depending on roughness	
b_1	Exponent in P vs. A relation	
b_2	Exponent in resistance equation	
b_3	Exponent in raindrop soil detachment equation	
C	Sediment concentration by volume	
C_a	Known concentration at a distance a above the bed	
C_b	Concentration of suspended bed material load	
C_d	Drag coefficient	
C_g	Channel-flow ground cover density	
C_w	Concentration of wash load	
C_ξ	Sediment concentration at distance ξ from the bed	
C_b^p	Potential bed material load concentration	
C_w^p	Potential wash load concentration	

LIST OF SYMBOLS - Continued

<u>Symbol</u>	<u>Description</u>	<u>Unit</u>
D_b	Amount of detached bed material	L
D_c	Canopy cover density	
D_f	Detachment coefficient of runoff	
D_g	Overland flow ground cover density	
D_i	Potential rate of soil detachment	L/T
D_p	Maximum depth to which a raindrop can penetrate the soil layer	L
d_s	Size of sediment	L
E	Mean evaporation rate from the interception storage	L/T
e_g	Evaporation rate from the water on the ground	L/T
F_b	Percent of bed-material load size in a typical soil sample	
F_w	Percent of wash-load size in a typical soil sample	
f	Darcy-Weisbach friction factor for grain resistance only	
f'	Overall Darcy-Weisbach friction factor	
f_i	Infiltration rate	L/T
f_m	Average infiltration capacity	L/T
f_o	Darcy-Weisbach grain resistance factor without rainfall	
f_i^c	Average infiltration rates for areas under canopy	L/T
f_i^o	Average infiltration rates for areas without trees	L/T
f_m^c	Average infiltration capacity for areas under canopy	L/T
f_m^o	Average infiltration capacity for areas without trees	L/T
G_b	Bed-material load transport rate	L^3/T
G_c	Sediment transport capacity	L^3/T
G_s	Total sediment transport rate	L^3/T

LIST OF SYMBOLS - Continued

<u>Symbol</u>	<u>Description</u>	<u>Unit</u>
G_w	Wash load transport rate	L^3/T
g	Gravitational acceleration	L/T^2
g_b	Lateral inflow rate of bed material load per unit length of channel	L^2/T
g_s	Lateral inflow rate of sediment per unit length of channel	L^2/T
g_w	Lateral inflow rate of wash load per unit length of channel	L^2/T
h	Magnitude of ponded water head at the surface	L
I_s	Initial interception storage content, defined as the ratio of the initial interception storage capacity to the total interception storage capacity	
i	Rainfall rate or intensity	L/T
i_c	Crown cover interception rate	L/T
i_e	Excess rainfall rate	L/T
i_g	Ground cover interception rate	L/T
i_n	Net rainfall rate, rate of rainfall reaching the ground	L/T
i_o	Through fall rate	L/T
i_e^c	Average excess rainfall rate for areas under canopy	L/T
i_e^o	Average excess rainfall rate for areas without trees	L/T
i_n^c	Average net rainfall rate for areas under canopy	L/T
i_n^o	Average net rainfall rate for areas without trees	L/T
\bar{i}	Average rainfall intensity	L/T
\bar{i}_e	Overall mean rainfall excess rate	L/T
J_1, J_2	Integrals in evaluating total suspended load	
K_o	Constant representing grain resistance without rainfall for $N_r \leq 900$	

LIST OF SYMBOLS - Continued

<u>Symbol</u>	<u>Description</u>	<u>Unit</u>
K_r	Number describing the added friction resulting from rainfall	
K_1	Parameter describing grain resistance with rainfall for $N_r \leq 900$	
K_2	Constant describing grain resistance for $2,000 \leq N_r \leq 25,000$	
K_3	Constant describing grain resistance for $N_r \geq 100,000$	
K'_1, K'_2, K'_3	Modified value of K_1, K_2 and K_3 including ground cover resistance	
k_s	Saturated hydraulic conductivity	L/T
L	Length of an overland flow plot	L
ℓ_c	Average length of ground cover in the channel in the direction of flow	L
ℓ_o	Average length of overland flow ground cover in the direction of flow	L
m_o	Soil moisture content	
m_s	Soil moisture content at saturation	
m_w	Soil moisture content at wilting point	
m_o^c	Soil moisture content for areas under canopy	
m_o^o	Soil moisture content for areas without trees	
$m_o(0)$	Antecedent moisture content	
N_r	Flow Reynolds number $\frac{QR}{\nu A}$	
n	Manning's roughness coefficient	
P	Wetted perimeter	L
P_c	Magnitude of the capillary potential head	L
P_h	Average wetted perimeter occupied by the high ground cover	L

LIST OF SYMBOLS - Continued

<u>Symbol</u>	<u>Description</u>	<u>Unit</u>
P_ℓ	Average wetted perimeter occupied by the low ground cover	L
P_w	Magnitude of capillary potential head at wilting point	L
Q	Water discharge	L^3/T
q_b	Bed-load transport rate per unit width of channel	L^2/T
q_ℓ	Lateral inflow rate per unit length of channel	L^2/T
R	Hydraulic radius, A/P	L
r	Variable	
r_v	Ratio of V_c to V_g	
S_c	Ratio of the evaporation surface to the horizontal projected area for a tree canopy	
S_f	Friction slope	
S_g	Ratio of the evaporation surface to the horizontal projected area for a typical ground cover	
S_o	Bed slope	
t	Time	T
U_*	Shear velocity of the flow	L/T
u_ξ	Point mean velocity at the distance ξ from the bed	L/T
V_c	Mean velocity of water flow	L/T
V_g	Interception storage capacity of a tree canopy per unit area	L
V	Interception storage capacity of the ground cover per unit area of ground cover	L
V_e	Mean velocity in the vicinity of the low ground cover	L/T
v_s	Settling velocity of the sediment particle	
v_n	Hypothetical infiltration velocity, defined as the local flow rate average over a finite area of the porous medium	L/T

LIST OF SYMBOLS - Continued

<u>Symbol</u>	<u>Description</u>	<u>Unit</u>
\bar{v}_η	Average value of v_η	L/T
W	Width of an overland flow plot	L
w	Parameter of sediment suspension	
x	Downslope distance	L
y	Depth of flow	L
y'	Average depth of depression storage in an unit area of overland flow unit	L
z_m	Equivalent maximum penetration depth of raindrop impact	L
z	Net depth of loose soil	L
z_b	Depth of loose soil for bed material load size	L
z_w	Depth of loose soil for wash load size	L
α	Coefficient in A vs. Q relation	
β	Exponent in A vs. Q relation	
γ	Specific weight of water	F/L ³
γ_s	Specific weight of sediment	F/L ³
Δt	Time increment in computation	T
Δx	Space increment in computation	L
ΔZ	Mean elevation change	L
Δz_b^P	Potential change in loose soil storage for bed material size	L
$\bar{\epsilon}$	Effective height of the low ground cover	L
ϵ_b	Porosity of the bed material sediment	
ϵ_ℓ	Average height of the low ground cover	L
ϵ_w	Porosity of the wash load sediment	
η	Magnitude of the gravitational potential head of the wetted front in the soil column	L

LIST OF SYMBOLS - Continued

<u>Symbol</u>	<u>Description</u>	<u>Unit</u>
η_a	Depth of the aeration zone	L
η_s	Roughness height	L
λ	Ratio of high ground cover density to total ground cover density	
ν	Kinematic viscosity of water	L^2/T
ξ	Depth above the bed	L
ρ	Density of water	M/L^3
τ_c	Critical tractive force	F/L^2
τ_o	Boundary shear stress acting on the grain	F/L^2
τ_*	Effective overall resistance force	F/L^2
ψ_c	Channel ground-cover resistance descriptor	L^{-1}
ψ_o	Overland flow ground-cover resistance descriptor	L^{-1}
$(\cdot)_j^n$	Quantity of the variable at grid point $x = j\Delta x$ and $t = n\Delta t$	

1. INTRODUCTION

GENERAL

The management of watersheds and river basins for the optimum benefit of the people in general requires a complete knowledge of the interrelations between ecology and environment. The watershed response to developments, either natural or man-induced, must be anticipated correctly if progress is to be made towards wise use of our nation's watersheds.

In recognition of the complex interrelations between all factors in watersheds, the U.S. Forest Service implemented a program to conduct multiple-use evaluations of watershed treatments on lands in the Beaver Creek drainage on the Coconino National Forest in north-central Arizona. Started in the late 1950's the project was established as part of the Arizona Watershed Program and is known as the Beaver Creek National Multiple Use Evaluation Project.

The Beaver Creek drainage contains 37 instrumented watersheds. Work programs on Beaver Creek are being conducted by the U.S. Forest Service with the cooperation of the Arizona Game and Fish Department, the Arizona Water Resources Committee, the Arizona Land Department, the U.S. Geological Survey, the University of Arizona, Northern Arizona University and Colorado State University.

While many of the forest management practices being tested on Beaver Creek were designed primarily to increase water yield, the results of the treatments are being evaluated in terms of effects on sedimentation and flood damage, timber and forage yields, wildlife and aesthetics as well as streamflow. Results of the Multiple Use Evaluation Project

management studies are being used by land managers and water users in Arizona and elsewhere in the Southwest. Moreover the studies are providing input for economic analyses being undertaken to assess alternative management schemes for watersheds.

One of the major problems in land-use and water resource planning in managing watersheds is predicting the erosion of the land surface and the subsequent transport of the eroded sediment through the downstream conveyance channels. To our dismay in the past, the excess yields of sediment from watersheds have resulted in filling of lakes and reservoirs plugging irrigation systems, pollution of river waters, killing of aquatic life, destruction of water and land vegetation, changing of the riverine and watershed morphology, as well as indirectly aggravating other problems such as flood hazards. It is towards the prediction of these erosion problems that Colorado State University has directed its efforts for the Multiple Use Evaluation Project.

Because the physical processes governing watershed behavior are very complicated, many past studies have utilized a statistical interpretation of observed watershed response data. The Unit Hydrograph Method for water routing and the Universal Soil-loss Equation for soil erosion are examples of these types of statistical studies. However, it is difficult to predict the response of a watershed to various watershed developments or treatments using statistical methods because the methods are based on the assumption of homogeneity in time and space. These homogeneities occur rarely if at all over entire natural watersheds.

In spite of the complexity of the physical processes governing watershed response, numerical modeling of the physical process system promises to be the most viable way to estimate the time-dependent

responses of watersheds to various management programs such as varying forest cover or varying land use. Therefore, as a part of the Multiple Use Evaluation Project, Colorado State University has developed a numerical computer program employing the formulation of the basic physical processes to determine water and sediment yield and transport in small watersheds. The mathematical model is presented in this report.

OBJECTIVES

The overall objective of Colorado State University's efforts on behalf of the Beaver Creek National Multiple-Use Evaluation Project is to develop prediction models for estimating sediment yield from a broad spectrum of source areas and watersheds. The prediction models are being tested on study areas within the Beaver Creek drainage. These areas range in size from under 100 to several thousand acres and include a variety of treated and untreated conditions in the ponderosa pine and pinyon-juniper type forest. The models are also to be tested on watersheds in other parts of the United States having far different climates, soils, and vegetation, ranging from desert to sub-alpine conditions.

In developing a validated sediment prediction model, the following tasks were specified:

1. Estimate the amount of soil loss from specified resource response units (land units with homogeneous slope, aspect, soil, precipitation and timber density) as well as from other source areas such as roads.
2. Estimate the amount of sediment transported out of the watersheds by the principal drainage networks.
3. Estimate aggradation and degradation at different points in the channel system.

In most cases, the movement of sediment from watersheds results from the movement of water. In fact, the same physical processes

are at work in moving sediment and water. Early studies indicated the most feasible way of developing a sediment routing and sediment yield model would be to couple the sediment model directly to the water routing and yield model. The Forest Service was not able to supply a suitable water yield and routing model to Colorado State University in time to meet the schedule for developing the sediment model. In an effort to produce a viable sediment yield and routing model on schedule, Colorado State University developed a water routing model which was coupled directly to the sediment model. In recognition of this additional work, the completion date for the present phase of the research was extended one year.

SCOPE OF THE PRESENT STUDY

In a meeting held at Flagstaff, Arizona on October 2, 3 and 4, 1971 the current status of the Colorado State University sediment and water yield and routing model was discussed. At that time, the model had been validated with field data collected on Watershed 17, a 300 acre ponderosa pine watershed, during the Labor Day weekend storm in 1970. That storm matched closely those measured in the field. Also, yields for this same storm were computed for Watershed 17 for different assumed amounts of canopy and ground cover.

In the meeting, the arrangements were made that Colorado State University would prepare a document describing the progress to date on developing the water and sediment routing model. The report would contain the validation achieved on Watershed 17 data. It was suggested that the model should be tested on one of the pinyon-juniper watersheds (Watershed 1 was subsequently selected) and the results presented in this

report. Also, suggestions for future activities would be outlined in this report.

This report covers the progress made under Cooperative Research Agreement No. 16-289-GR between the Rocky Mountain Forest and Range Experiment Station and Colorado State University on developing a water and sediment routing model.

MODEL STRUCTURE

The Colorado State University model simulates the land surface hydrologic cycle, sediment production, and water and sediment movement on small watersheds. Conceptually the watershed is divided into an overland flow part and a channel system part. Different physical processes are important for the two different environments. In the overland flow part, processes of interception, evaporation, infiltration, raindrop impact detachment of soil, erosion by overland flow, and overland flow water and sediment routing to the nearest channel are simulated. In channel system part, water and sediment contributed by overland flow are routed and the amount of channel erosion or sediment deposition through the channel system is determined. The main functions in the model are shown in Fig. 1.1. The details of the model structure are given in the following chapters.

In this model emphasis is on the mechanics of water and sediment routing. The model is set up for single storm hydrograph computations. No attempt has been made to simulate the long-term water balance in the watershed, as this is to be achieved through coupling this model with another model being developed by the Multiple Use Evaluation Project.

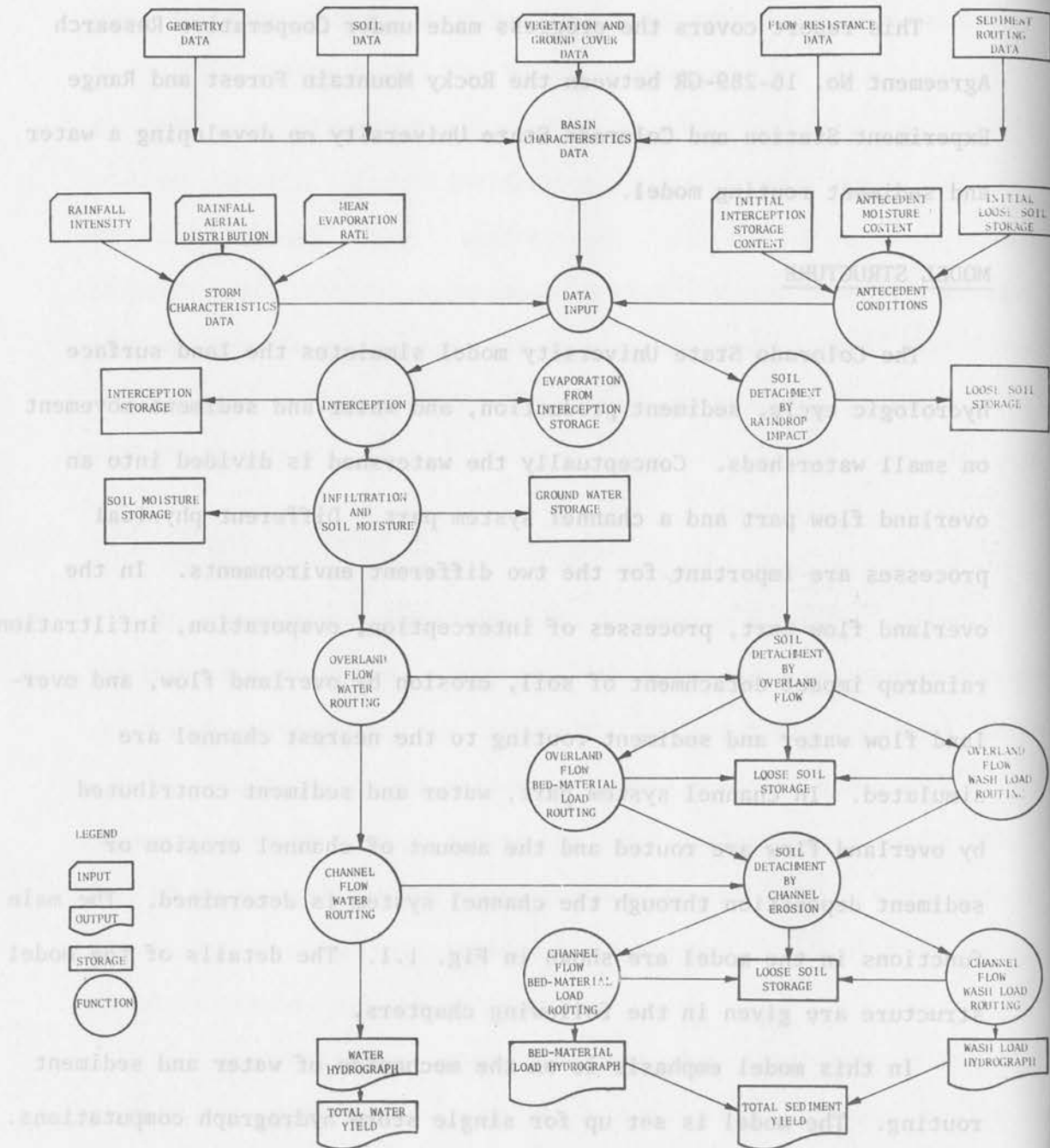


Fig. 1.1 Flow chart for the water and sediment routing model

The viability of the water and sediment routing model was verified with data from 5 storms on Watershed 1 and 1 storm on Watershed 17.

The computed results demonstrate the utility of the model in predicting water and sediment yields, synthesizing water and sediment hydrographs, and forecasting the effect of various watershed treatments on water and sediment yields. In addition, from this preliminary effort the future work necessary to further this cooperative study program has been identified.

The details of the Colorado State University water and sediment routing model are given in the following chapter.

follows:

1. A rectangular grid system is superimposed on the topographic map of the watershed. The size of the grid is chosen so that the watershed boundaries and channels can be approximated by grid segments. The overland flow units are the grid units inside the watershed boundary and the channel units are segments between grid intersection points.
2. The principal flow direction is determined for each overland flow unit. The principal flow direction is identified by the magnitude and azimuth of the bed slope (or land slope). The azimuth is normal to the elevation contours and is in the direction of decreasing elevation. The bed slope is estimated along the azimuth.
3. It is assumed that the water flows in the direction of the bed-slope azimuth to the next overland flow unit or to the

2. GEOMETRY OF A WATERSHED

Because most watersheds are nonhomogeneous in topography, soils, vegetation and other features, it is necessary to segment each watershed into smaller units which can be considered homogeneous. Then the smaller units can be treated easily in a mathematical manner. Similarly the channel system in a watershed can be represented by segments, each having a different location, shape, slope and roughness.

SEGMENTATION OF THE WATERSHED

The watershed is decomposed into overland flow units and channel flow units. The sequence in segmenting the watershed into units is as follows:

1. A rectangular grid system is superimposed on the topographic map of the watershed. The size of the grid is chosen so that the watershed boundaries and channels can be approximated by grid segments. The overland flow units are the grid units inside the watershed boundary and the channel units are segments between grid intersection points.
2. The principal flow direction is determined for each overland flow unit. The principal flow direction is identified by the magnitude and azimuth of the bed slope (or land slope). The azimuth is normal to the elevation contours and is in the direction of decreasing elevation. The bed slope is estimated along the azimuth.
3. It is assumed that the water flows in the direction of the bed-slope azimuth to the next overland flow unit or to the

adjacent channel. Thus water cascades from overland flow unit to overland flow unit and then into the channel system.

4. For simplicity, the overland flow units in cascade can be grouped into a larger overland flow unit. The representative slope length for the larger unit is the ratio of total area of the cascade to the width of the overland flow unit where it joins the channel. The bed slope is an average value of the bed slopes of all the small units.
5. The computational sequence for the flow network is established. The method employed is simply to follow the logics of the gravity flow and the flow continuity.

A plan view of a typical segmented watershed is shown in Fig. 2.1.

Both overland flow units and channel segment units are illustrated.

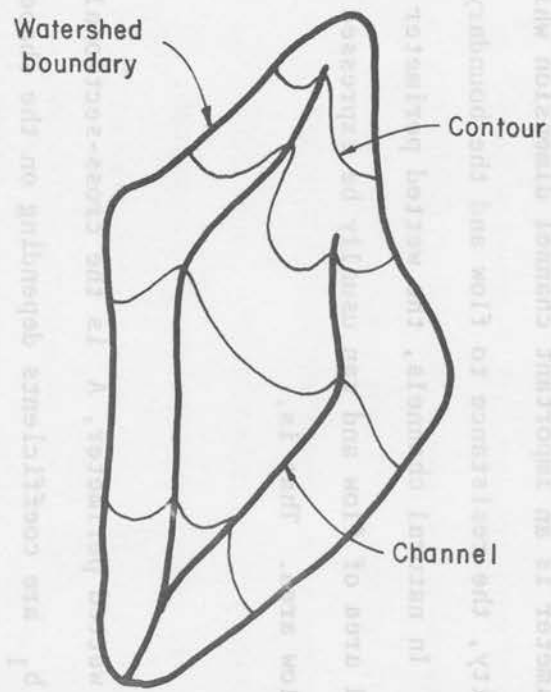
RELATION BETWEEN WETTED PERIMETER AND FLOW AREA

The wetted perimeter is an important channel dimension which governs the mean flow velocity, the resistance to flow and the boundary shear stress in channels. In natural channels, the wetted perimeter changes with cross-sectional area of flow and can usually be expressed as a power function of flow area. That is,

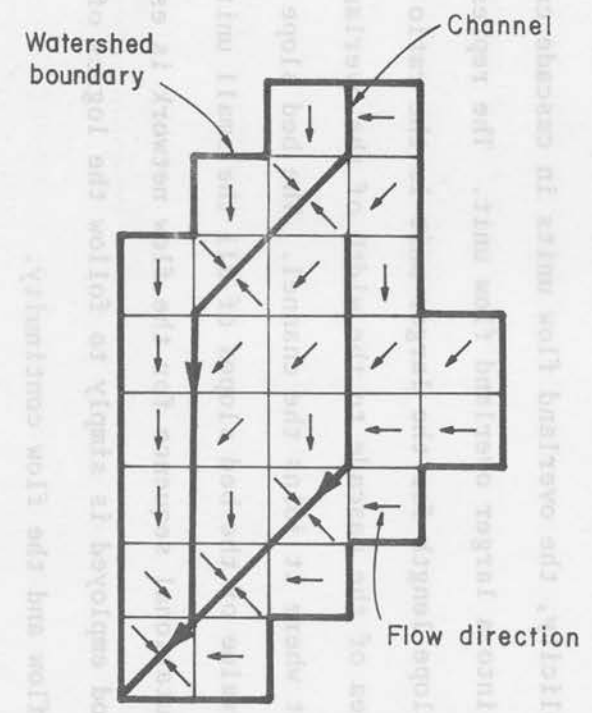
$$P = a_1 A^{b_1} \quad (2-1)$$

in which P is the wetted perimeter, A is the cross-sectional area of flow, and a_1 and b_1 are coefficients depending on the shape of the channel.

An example of wetted perimeter versus flow area relation is shown in Fig. 2.2.



a. Topographic features



b. Segmented watershed

Fig. 2.1 Examples of watershed segmentation

3. ESTIMATION OF EXCESS RAINFALL

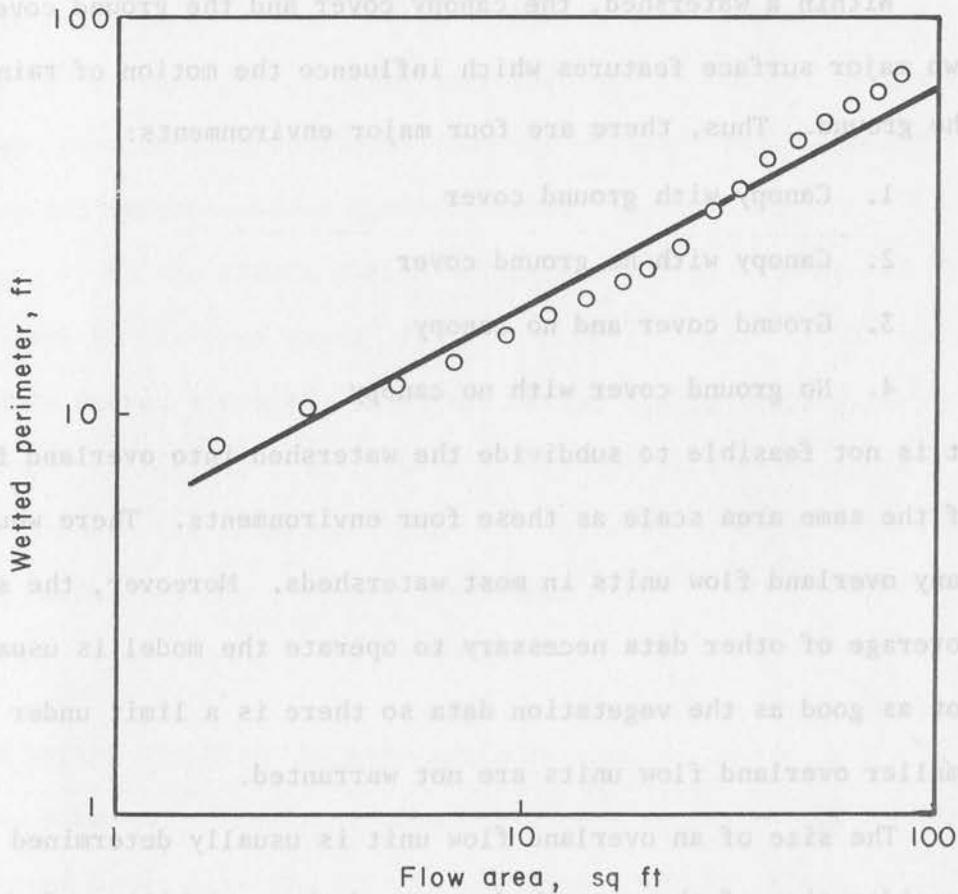


Fig. 2.2 Wetted perimeter versus flow area for the main channel in Watershed 1

3. ESTIMATION OF EXCESS RAINFALL

In this study, the water budget for each overland flow unit is simulated to determine the rainfall excess resulting from an individual storm.

Within a watershed, the canopy cover and the ground cover are the two major surface features which influence the motion of raindrops near the ground. Thus, there are four major environments:

1. Canopy with ground cover
2. Canopy with no ground cover
3. Ground cover and no canopy
4. No ground cover with no canopy

It is not feasible to subdivide the watershed into overland flow units of the same area scale as these four environments. There would be too many overland flow units in most watersheds. Moreover, the spatial coverage of other data necessary to operate the model is usually not as good as the vegetation data so there is a limit under which smaller overland flow units are not warranted.

The size of an overland flow unit is usually determined from consideration of the watershed area and the variability of the surface topography. Thereafter, in each overland flow unit the excess rainfall is determined considering a weighting procedure dependent on the canopy cover density and ground cover density. The canopy cover density is defined as the ratio of the area covered by trees to the total area. The ground cover density is the ratio of the ground area covered with litter, rock, grass etc. to the total area. That is, the ground cover density is the fraction of the ground surface which is not bare soil.

For the four environments, the water balance computations are subdivided into the net rainfall determination and the determination of the ground response to net rainfall.

NET RAINFALL

Net rainfall is defined as the quantity of rainfall which actually reaches the ground. Under trees, net rainfall is the sum of the throughfall and stemflow (Zinke, 1965). The net rainfall rates for different interception conditions are derived below.

Let i be the rainfall rate (or intensity) at time t at the upper level of the tree canopy as shown in Fig. 3.1a. If the rain falls onto trees, a portion is stored in the canopy and the remainder i_o passes through the trees. Let i_c be the rate at which rain is being stored in the canopy at time t . Then, under trees, the rainfall rate is reduced to the throughfall rate or

$$i_o = i - i_c \quad (3.1)$$

In this study, stemflow has been neglected.

The area under the trees consists of a bare portion and a portion with ground cover (litter, tree mulch, rocks, shrubs, grass, etc.)

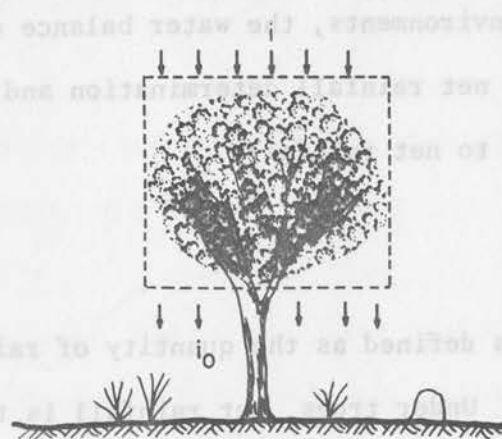
Refer to Fig. 3.1b and let i_g be the rate at which rain is being stored in the ground cover at time t . Then under the tree, the rate at which rain reaches the ground (net rainfall rate) is

$$i_n = i_o - i_g = i - i_c - i_g \quad (3.2)$$

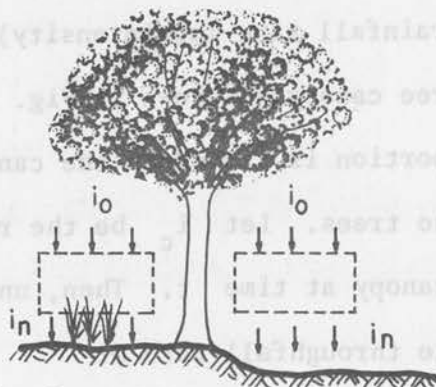
where there is ground cover, and

$$i_n = i_o = i - i_c \quad (3.3)$$

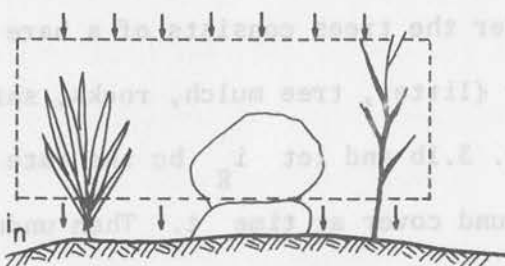
where there is no ground cover.



a. Control volume for a tree canopy



b. Control volumes under canopy



c. Control volume for ground cover only

Fig. 3.1 Rain reaching the ground

The area without trees (see Fig. 3.1c) also consists of a bare portion and a portion with ground cover. Where there are no trees, but there is ground cover, the net rainfall rate is

$$i_n = i - i_g \quad (3.4)$$

Where there are no trees and no ground cover, the net rainfall rate is

$$i_n = i \quad (3.5)$$

A summary of rainfall rate reaching the ground for different interception conditions is given in Table 3.1.

Table 3.1 Rain reaching the ground

<u>Area</u>	<u>Net rainfall rate, i_n</u>
Trees, ground cover	$i - i_c - i_g$
Trees, no ground cover	$i - i_c$
No trees, ground cover	$i - i_g$
No trees, no ground cover	i

Let A_t^c be the area covered by trees in an overland flow unit.

Also let A_g^c be the area with ground cover within area A_t^c . Then the average net rainfall rate under a canopy is

$$i_n^c = i - i_c - \frac{A_g^c}{A_t^c} i_g \quad (3.6)$$

Similarly, the average net rainfall rate in the area of the overland flow unit without trees is

$$i_n^o = i - \frac{A_g^o}{A_t^o} i_g \quad (3.7)$$

in which A_t^O is the total area without trees in an overland flow unit, and A_g^O is the area with ground cover within area A_t^O .

Assume the ground cover has the same density over the entire area of an overland flow unit either under canopy or over the area without trees. One then obtains

$$\frac{A_g^C}{A_t^C} = \frac{A_g^O}{A_t^O} = D_g \quad (3.8)$$

in which D_g is the overland flow ground cover density, the ratio of the area covered with ground cover to the total area in an overland flow unit.

The substitution of Eq. 3.8 into Eqs. 3.6 and 3.7 yields

$$i_n^C = i - i_c - D_g i_g \quad (3.9)$$

for areas under canopy and

$$i_n^O = i - D_g i_g \quad (3.10)$$

for areas without trees.

According to Horton (1919), the total interception equals leaf storage capacity plus evaporation loss during the storm. Zinke (1965) indicated that..."usually for a storm, there is an initial period during which the vegetation cover is wetted and a so-called interception storage capacity is satisfied. This is followed by loss from this storage, and the loss is dependent upon the evaporation opportunity during the remainder of the storm." Accordingly

$$i_c = i \quad (3.11)$$

$$\text{if } \sum_{t'=1}^t i(t') \Delta t \leq (1 - I_s) V_c$$

$$i_c = E S_c \quad (3.12)$$

$$\text{if } \sum_{t'=1}^t i(t') \Delta t > (1 - I_s) V_c$$

and

$$i_g = i \quad (3.13)$$

$$\text{if } \sum_{t'=1}^t i(t') \Delta t \leq (1 - I_s) V_g$$

$$i_g = E S_g \quad (3.14)$$

$$\text{if } \sum_{t'=1}^t i(t') \Delta t > (1 - I_s) V_g$$

Here Δt is the time increment, $i(t')$ is the rainfall at time t' , V_c is the interception storage capacity of a tree canopy per unit area of tree canopy, V_g is the interception storage capacity of the ground cover per unit area of ground cover, E is the mean evaporation rate from the interception storages, S_c and S_g are respectively the ratios of the evaporating surface to the horizontal projected area for a tree canopy and for a typical ground cover, and I_s is the initial interception storage content which is defined as the ratio of the initial storage capacity to the total interception storage capacity.

Let r_v be the ratio of V_c to V_g , or

$$V_c = r_v V_g \quad (3.15)$$

Then one may assume

$$S_c = r_v S_g \quad (3.16)$$

The average net rainfall rate under the canopy at time t can be determined by combining Eqs 3.9, 3.11, 3.12, 3.13, 3.14, 3.15 and 3.16 to yield

$$i_n^c = 0 \quad (3.17)$$

$$\text{if } \sum_{t'=1}^t i(t') \Delta t \leq (r_v + D_g) (1 - I_s) V_g$$

and

$$i_n^c = i - E (r_v + D_g) S_g \quad (3.18)$$

$$\text{if } \sum_{t'=1}^t i(t') \Delta t > (r_v + D_g) (1 - I_s) V_g$$

Similarly, the average net rainfall rate for the area without

trees is

$$i_n^o = 0 \quad (3.19)$$

$$\text{if } \sum_{t'=1}^t i(t') \Delta t \leq (1 - I_s) D_g V_g$$

and

$$i_n^o = i - E D_g S_g \quad (3.20)$$

GROUND RESPONSE TO RAINFALL

In this model, we are concerned with the water yield from a single storm. During the storm, the transpiration from soil through vegetation and evaporation from the soil are small and are therefore neglected.

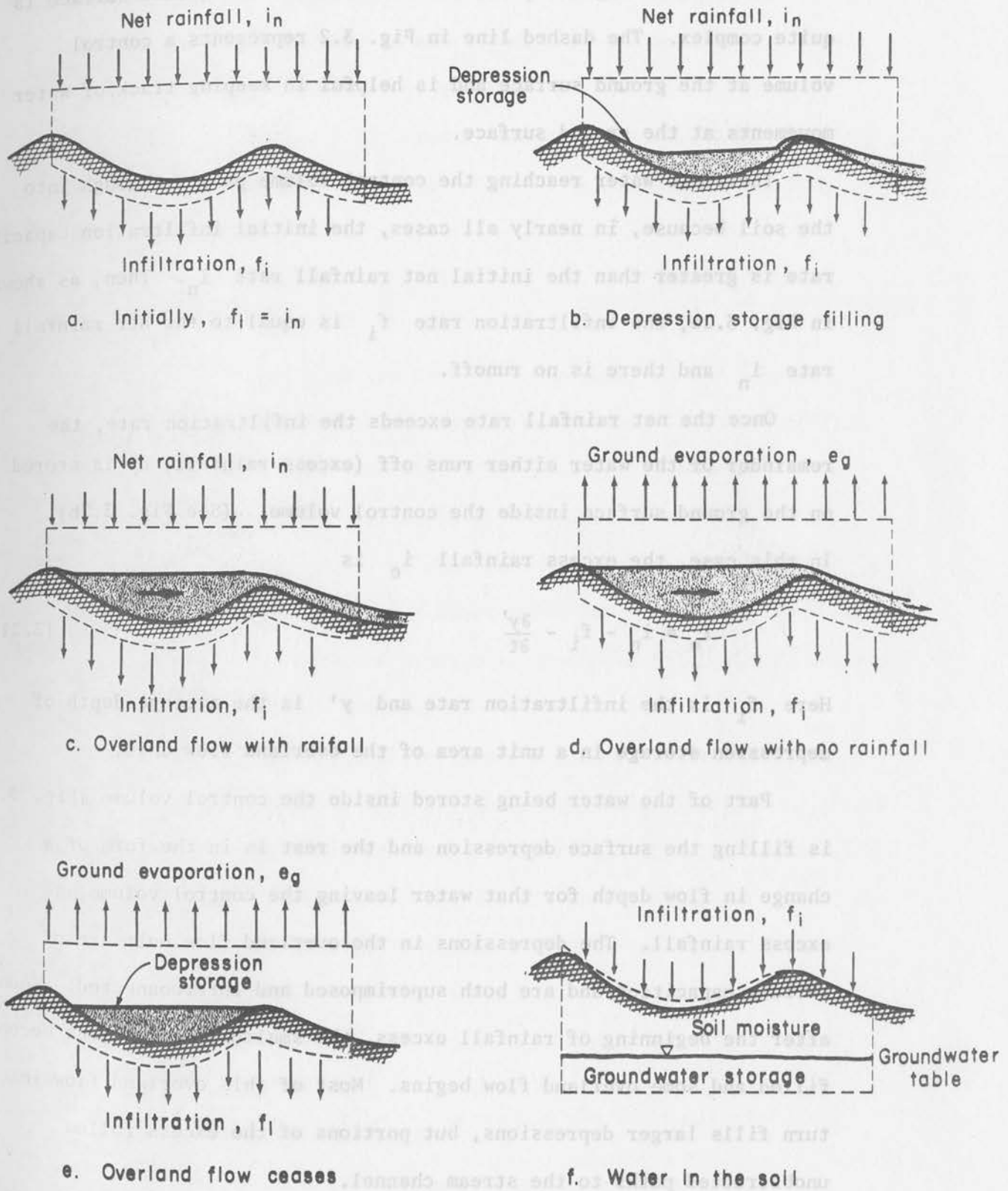


Fig. 3.2 Ground response to net rainfall

As shown in Fig. 3.2, the water balance at the ground surface is quite complex. The dashed line in Fig. 3.2 represents a control volume at the ground surface and is helpful in keeping track of water movements at the ground surface.

The first water reaching the control volume passes through into the soil because, in nearly all cases, the initial infiltration capacity rate is greater than the initial net rainfall rate i_n . Then, as shown in Fig. 3.2a, the infiltration rate f_i is equal to the net rainfall rate i_n and there is no runoff.

Once the net rainfall rate exceeds the infiltration rate, the remainder of the water either runs off (excess rainfall) or is stored on the ground surface inside the control volume. (See Fig. 3.2b). In this case, the excess rainfall i_e is

$$i_e = i_n - f_i - \frac{\partial y'}{\partial t} \quad (3.21)$$

Here f_i is the infiltration rate and y' is the average depth of depression storage in a unit area of the overland flow unit.

Part of the water being stored inside the control volume (Fig. 3.2b) is filling the surface depression and the rest is in the form of a change in flow depth for that water leaving the control volume as excess rainfall. The depressions in the overland flow unit are of various capacities and are both superimposed and interconnected. Soon after the beginning of rainfall excess, the smallest depressions become filled and some overland flow begins. Most of this overland flow in turn fills larger depressions, but portions of the excess follow unobstructed paths to the stream channel.

Once all the depressions are full, all the water is in motion and we have overland flow in all segments of the unit area. (See Fig. 3.2c). Again, the excess rainfall is given by Eq. 3.21.

As shown in Fig. 3.2d, excess rainfall continues even after the net rainfall stops but for this case, the excess is derived from storage or

$$i_e = -f_i - e_g - \frac{\partial y}{\partial t} \quad (3.22)$$

Here e_g is the evaporation rate from the water on the ground.

When the water level has dropped to the level required to fill the depression storage (See Fig. 3.2e) overland flow ceases. The remaining water either evaporates (e_g) or infiltrates (f_i).

The underground phase of the ground response to net rainfall is illustrated in Fig. 3.2f. The water which infiltrates into the soil increases the soil moisture storage in the upper soil profile and may change the groundwater storage.

It is difficult to describe mathematically the entire sequence of events illustrated in Fig. 3.2 because, for one thing, very little is known concerning the magnitude of depression storage. Meaningful observation of depression storage are not easily obtained. Thus, the depression storage is usually combined with interception and treated as initial loss with respect to storm runoff (Linsley, et al., 1958). For simplicity, the depression storage is neglected in this study, but implicitly is included in the interception storage capacity described in the previous section.

Referring to Fig. 3.2 and neglecting depression storage the water balance equation is

$$i_e = i_n - f_i \quad (3.23)$$

in which i_e is the rainfall excess rate, i_n is the net rainfall rate and f_i is the infiltration rate. The average rainfall excess rates under canopy and in the area without trees are respectively,

$$i_e^c = i_n^c - f_i^c \quad (3.24)$$

for areas under canopy and

$$i_e^o = i_n^o - f_i^o \quad (3.25)$$

for areas without trees in which f_i^c and f_i^o are respectively the average infiltration rates for areas under canopy and for areas without trees.

INFILTRATION

Darcy's Law for saturated flow through porous medium (Daily and Harleman, 1966, p. 181) is

$$v_n = k_s \frac{\partial (P_c + h + \eta)}{\partial \eta} \quad (3.26)$$

in which v_n is the hypothetical infiltration velocity defined as the local flow rate averaged over a finite area of the porous medium, k_s is the saturated hydraulic conductivity (coefficient of permeability), P_c is the magnitude of the capillary potential head, h is the magnitude of ponded water head at the surface and η is the magnitude of the gravitational potential head of the wetted front in the soil column.

Assuming one-dimensional flow and neglecting h , Eq. 3.26 becomes

$$v_n = k_s \frac{d(P_c + \eta)}{d\eta} \quad (3.27)$$

Integration of Eq. 3.27 yields

$$\int_0^{\bar{\eta}} v_{\eta} d\eta = k_s (\bar{P}_c + \bar{\eta}) \quad (3.28)$$

in which $\bar{\eta}$ and \bar{P}_c are respectively the magnitudes of the gravitational potential head and the capillary potential head of the wetted front at a particular time t .

Let \bar{v}_{η} denote the average value of v_{η} , so that

$$\int_0^{\bar{\eta}} v_{\eta} d\eta = \bar{v}_{\eta} \bar{\eta} \quad (3.29)$$

From Eqs. 3.28 and 3.29, one obtains

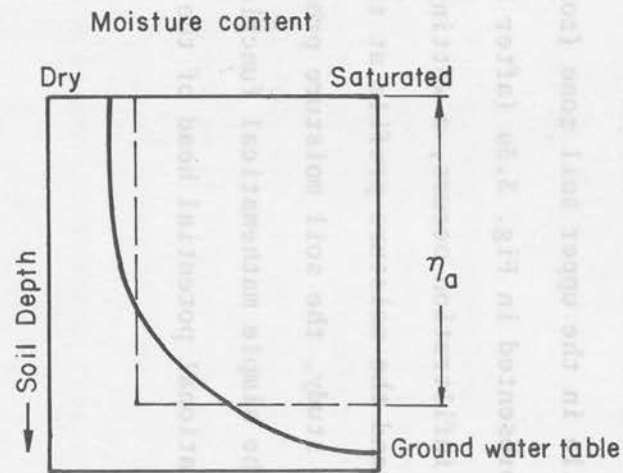
$$\bar{v}_{\eta} = k_s \left(1 + \frac{\bar{P}_c}{\bar{\eta}} \right) \quad (3.30)$$

Assume the average infiltration capacity f_m at time t to be \bar{v}_{η} in Eq. 3.30; i.e.,

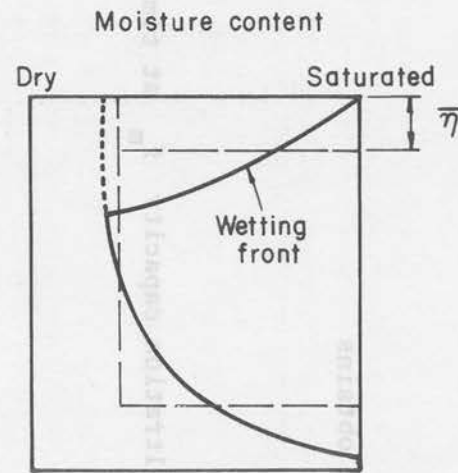
$$f_m = k_s \left(1 + \frac{\bar{P}_c}{\bar{\eta}} \right) \quad (3.31)$$

The soil moisture profile in the upper soil zone (zone of aeration) prior to infiltration is represented in Fig. 3.3a (after Hewlett and Nutter, 1969, p. 57). When infiltration occurs, a wetting front moves through the upper soil zone and the moisture profile at time t is shown in Fig. 3.3b. In this study, the soil moisture profile at time t is represented by the simple mathematical functions shown in Fig. 3.3c. Then, the gravitational potential head of the wetted front at time t is

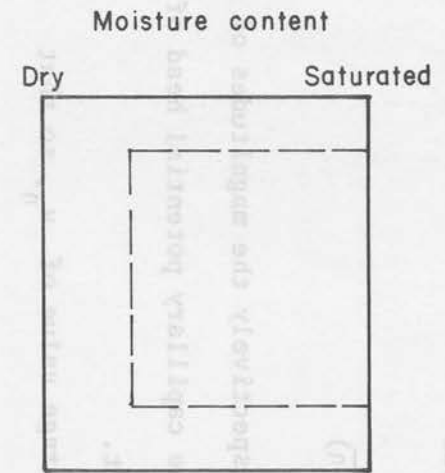
$$\bar{\eta} = \frac{f_m \Delta t}{m_s - m_o} \quad (3.32)$$



a. Moisture profile at time $t - \Delta t$



b. Moisture profile at time t



c. Mathematical representation of the moisture profile at time t

Fig. 3.3 Soil moisture profile

in which m_s is the moisture content at saturation and m_o is the moisture content of the zone of aeration prior to infiltration.

The magnitude of the capillary potential head or the moisture tension head of the wetted front \bar{P}_c is a function of soil moisture content (Zahner, 1965). A typical representation of soil moisture depletion curve is given in Fig. 3.4. The capillary potential head at time t can be approximated by a linear interpolation or

$$\bar{P}_c = \left(\frac{m_s - m_o}{m_s - m_w} \right) P_w \quad (3.33)$$

in which m_w is the soil moisture content at wilting point (defined as the moisture content at which permanent wilting of plants occurs), and P_w is the capillary potential head at wilting point.

The substitution of Eqs. 3.32 and 3.33 into Eq. 3.31 yields

$$f_m = \frac{k_s}{2} \left\{ 1 + \sqrt{1 + \frac{4 P_w (m_s - m_o)^2}{k_s \Delta t (m_s - m_w)}} \right\} \quad (3.34)$$

The moisture contents for areas under canopy and for areas without trees are different due to different rates of water supply to the ground. Thus, the average infiltration capacities are different for the areas under canopy and the areas without trees. They are

$$f_m^c = \frac{k_s}{2} \left\{ 1 + \sqrt{1 + \frac{4 P_w (m_s - m_o^c)^2}{k_s \Delta t (m_s - m_w)}} \right\} \quad (3.35)$$

for areas under canopy and

$$f_m^o = \frac{k_s}{2} \left\{ 1 + \sqrt{1 + \frac{4 P_w (m_s - m_o^o)^2}{k_s \Delta t (m_s - m_w)}} \right\} \quad (3.36)$$

for areas without trees. Here m_o^c and m_o^o are respectively

in which m_s is the moisture content at saturation and m_o is the moisture content of the zone of aeration prior to infiltration. The magnitude of the capillary potential head or the moisture tension head of the wetted front \bar{p}_c is a function of soil moisture content (Zahner, 1962). A typical representation of soil moisture depletion curve is given in Fig. 3.4. The capillary potential head at time t can be approximated by a linear interpolation or

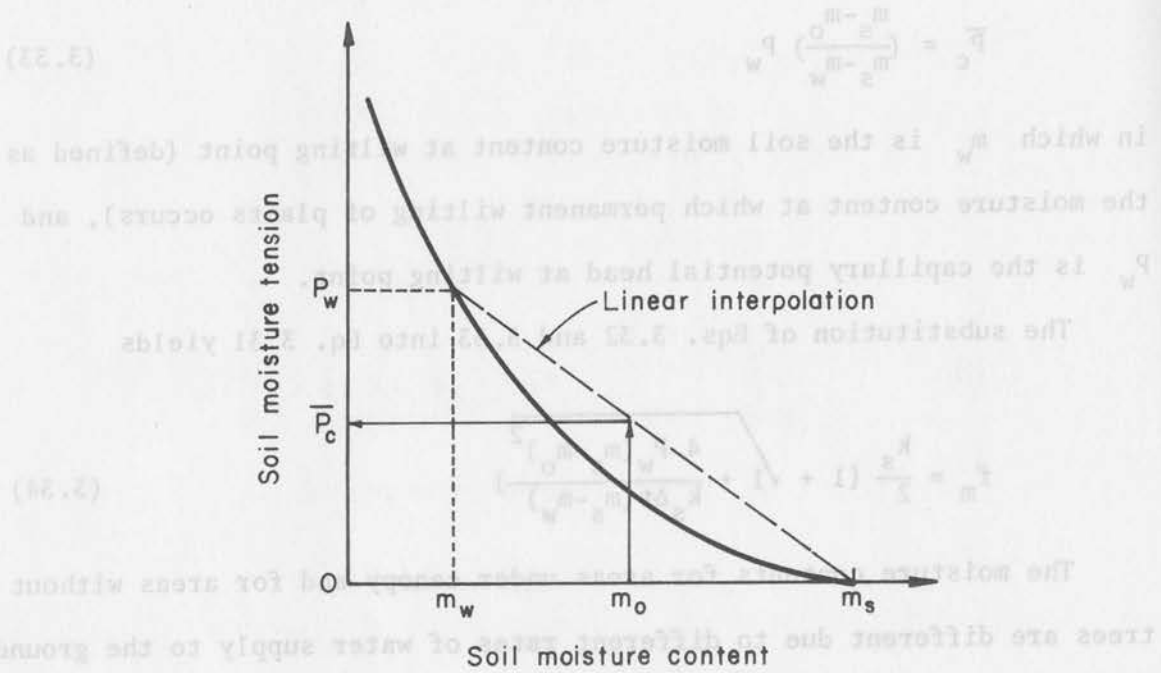


Fig. 3.4 Representation of the soil-moisture depletion curve

the moisture contents for the areas under canopy and the areas without trees.

The actual infiltration rate not only depends on the infiltration capacity but also depends on the moisture supply. The rate of moisture supply is essentially the same as net rainfall rate. Assuming that a threshold condition of runoff production is valid, the actual infiltration rates for areas under canopy and areas without trees are

$$f_i^c = f_m^c \quad (3.37)$$

$$\text{if } i_n^c > f_m^c$$

and

$$f_i^c = i_n^c \quad (3.38)$$

$$\text{if } i_n^c \leq f_m^c$$

for areas under canopy and

$$f_i^o = f_m^o \quad (3.39)$$

$$\text{if } i_n^o > f_m^o$$

and

$$f_i^o = i_n^o \quad (3.40)$$

$$\text{if } i_n^o \leq f_m^o$$

for areas without trees.

SOIL MOISTURE ADJUSTMENT

To account for the fact that rainfall is not continuous and that the infiltration process is actually the flow of water through unsaturated porous media, the value of the soil moisture in the zone

of aeration m_o is adjusted throughout time while infiltration is occurring. For simplicity, the soil moisture m_o is assumed constant with respect to depth in the zone of aeration. (See Fig. 3.4).

Also it is assumed that before the upper soil profile is saturated no water enters the groundwater storage. After the upper soil profile is saturated, all infiltrated water enters groundwater storage.

The moisture content prior to the saturation of the upper soil profile is determined by the following equations:

$$m_o^c(t + \Delta t) = m_o^c(t) + \frac{f_i^c(t)\Delta t}{\eta_a} \quad (3.41)$$

for areas under canopy and

$$m_o^o(t + \Delta t) = m_o^o(t) + \frac{f_i^o(t)\Delta t}{\eta_a} \quad (3.42)$$

for areas without trees. Here η_a is the depth of the aeration zone.

After all the soil in the zone of aeration is saturated

$$m_o^c(t + \Delta t) = m_s \quad (3.43)$$

and

$$m_o^o(t + \Delta t) = m_s \quad (3.44)$$

For simplicity, the initial moisture contents for areas under canopy and for areas without trees are assumed to be the same. That is,

$$m_o^c(0) = m_o^o(0) = m_o(0) \quad (3.45)$$

in which $m_o(0)$ is the antecedent moisture content.

MEAN RAINFALL EXCESS RATE

From Eqs. 3.23, 3.37 and 3.38 the average rainfall excess rate for areas under canopy i_e^c is

$$i_e^c = i_n^c - f_m^c \quad (3.46)$$

$$\text{if } i_n^c > f_m^c$$

and

$$i_e^c = 0 \quad (3.47)$$

$$\text{if } i_n^e \leq f_m^c$$

Similarly, the average rainfall excess rate for areas without trees are

$$i_e^o = i_n^o - f_m^o \quad (3.48)$$

$$\text{if } i_n^o \geq f_m^o$$

and

$$i_e^o = 0 \quad (3.49)$$

$$\text{if } i_n^o < f_m^o$$

Usually, it is not practical to route water in the areas under canopy and in the areas without trees separately because these two types of areas are interconnected. Here, a weighting procedure is used to obtain an overall mean rainfall excess \bar{i}_e . It is

$$\bar{i}_e = D_c i_e^c + (1 - D_c) i_e^o \quad (3.50)$$

in which D_c is the canopy cover density.

4. WATER ROUTING

Runoff from a watershed, either in the form of overland flow or in the form of channel flow, is described by the equations of mass continuity and momentum and by equations representing the laws of resistance. The governing equations employed in the water routing procedure are described below.

CONTINUITY EQUATION FOR WATER

The equation of continuity for water flow in the x-direction is

$$\frac{\partial Q}{\partial x} + \frac{\partial A}{\partial t} = q_\ell \quad (4.1)$$

in which Q is the discharge, x is the downslope distance, and q_ℓ is the lateral inflow rate per unit length of channel.

The lateral inflow rate q_ℓ for overland flow units is the mean rainfall excess rate which is determined by Eq. 3.50. For channel flow, the lateral inflows are the resultant overland flow water discharges which enter the channel system.

MOMENTUM EQUATION

If the gradients due to local and convective accelerations are very small, and if the water surface slope is assumed equal to the bed slope, the momentum equation is

$$S_o \approx S_f = f' \frac{Q^2}{8gRA^2} \quad (4.2)$$

in which S_o is the bed slope, S_f is the friction slope, f' is the overall Darcy-Weisbach friction factor, g is the gravitational acceleration, and R is the hydraulic radius.

Equation 4.2 is called the approximate momentum equation for the kinematic-wave representation of runoff. By definition the hydraulic radius is

$$R = \frac{A}{P} \quad (4.3)$$

in which P is the wetted perimeter and usually can be represented as a power function of flow area A . (See Chapter 2).

RESISTANCE EQUATIONS

In a natural watershed, the form resistance due to the ground cover is a very important component of the resistance to flow. The dependence of flow resistance on the ground cover becomes further complicated depending on whether the ground cover is submerged or not.

The ground cover is rarely submerged in overland flow units. Therefore, in overland flow units, we consider the resistance as that caused by flow *through* ground cover. In channel flow units, the probability of submerging the ground cover is apparently large. The resistance is then considered as the resistance caused by flow through the ground cover and flow over the ground cover simultaneously. Therefore, separate resistance equations are developed for overland flow and for channel flow. The approach of Li and Shen (1973) is used to establish the variation of flow resistance.

Overland flow resistance

Assume that the factors describing resistance to flow are independent and the probability that the ground cover is submerged is practically zero. Then referring to Fig. 4.1, the force balance for uniform flow over a rectangular area with length L and width W is

$$\text{Downslope water weight component} = \text{Grain resistance} + \text{Form resistance due to ground cover}$$

That is,

$$\begin{aligned} \gamma y S_o (LW - A_g) &= \frac{1}{8} f \rho V^2 (LW - A_g) \\ &+ \frac{1}{2} C_d \rho V^2 \frac{A_g}{\ell_o} y \end{aligned} \quad (4.4)$$

in which γ is the specific weight of water, y is the flow depth, A_g is the area with ground cover within area LW , f is the Darcy-Weisbach friction factor for grain resistance only, ρ is the density of water, V is the mean velocity of water flow, C_d is the drag coefficient, and ℓ_o is the average length of overland-flow ground cover in the direction of flow.

The area with ground cover A_g is related to the total area LW by the expression

$$A_g = D_g LW \quad (4.5)$$

The one-dimensional form of Eq. 4.2 is

$$S_o = f' \frac{V^2}{8gy} \quad (4.6)$$

By substituting Eqs. 4.5 and 4.6 into Eq. 4.4 and rearranging, one obtains

$$f' = f + 4 \frac{C_d}{\ell_o} \frac{D_g}{1-D_g} y \quad (4.7)$$

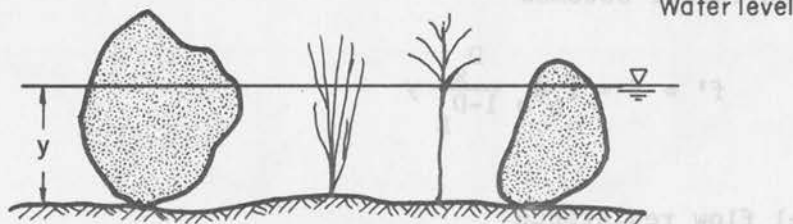
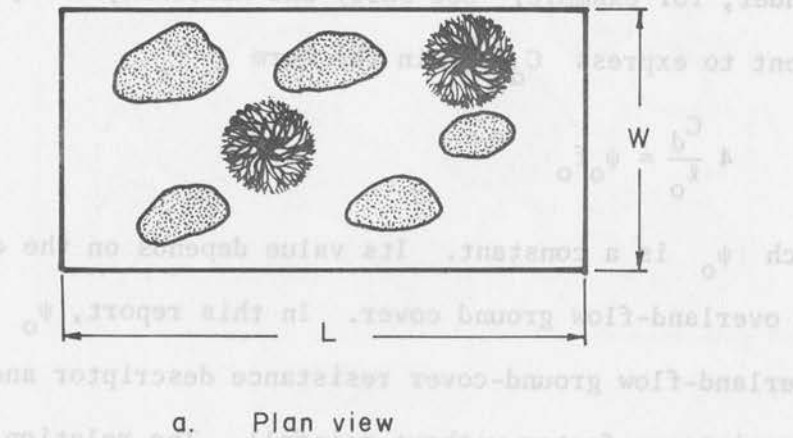


Fig. 4.1 Resistance to flow in overland flow units results from ground cover as well as from the soil

The grain resistance factor f is a function of flow Reynolds number and rainfall intensity. The functions are described later in this chapter.

The drag coefficient C_d is usually a function of the "obstacle" Reynolds number (the cylinder Reynolds number if the "obstacle" is a cylinder, for example. See Daily and Harleman, 1966, p. 380.) It is expedient to express C_d/ℓ_o in the form

$$4 \frac{C_d}{\ell_o} = \psi_o f_o \quad (4.8)$$

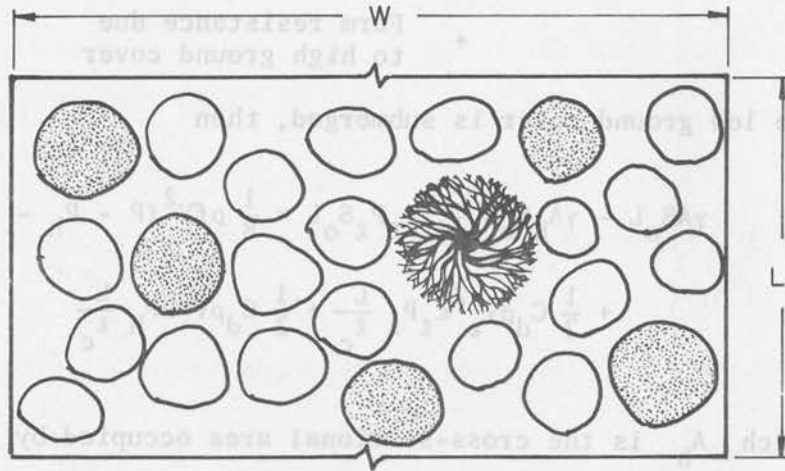
in which ψ_o is a constant. Its value depends on the characteristics of the overland-flow ground cover. In this report, ψ_o is defined as the overland-flow ground-cover resistance descriptor and f_o is the grain resistance factor without rainfall. The relation between f_o and f is developed later in this chapter.

By substituting Eq. 4.8 into Eq. 4.7, the expression for the friction factor becomes

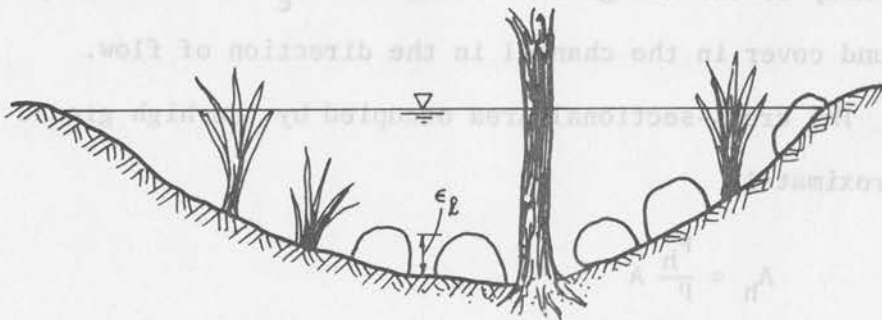
$$f' = f + f_o \psi_o \frac{D_g}{1-D_g} y \quad (4.9)$$

Channel flow resistance

As shown in Fig. 4.2, the ground cover in channels can be divided roughly into high ground cover (large rocks or trees) and low ground cover (smaller rocks and grass). The probability that the high ground cover is submerged during a storm is very small but the low ground cover is frequently submerged. Again, the factors for describing flow resistance are assumed to be independent. Then, the force balance for



a. Plan view



b. Elevation view

Fig. 4.2 Resistance to flow in channel flow units

uniform flow in a channel reach with length L and wetted perimeter P is

$$\begin{aligned} \text{Downslope component of water weight} &= \text{Grain resistance} + \text{Form resistance due to low ground cover} \\ &+ \text{Form resistance due to high ground cover} \end{aligned}$$

If the low ground cover is submerged, then

$$\begin{aligned} \gamma A S_o L - \gamma A_h S_o L - \gamma \epsilon_\ell P_\ell S_o L &\approx \frac{1}{8} \rho f V^2 (P - P_h - P_\ell) L \\ &+ \frac{1}{2} C_d \rho V_\epsilon^2 \epsilon_\ell P_\ell \frac{L}{\ell_c} + \frac{1}{2} C_d \rho V^2 R P_h \frac{L}{\ell_c} \end{aligned} \quad (4.10)$$

in which A_h is the cross-sectional area occupied by the high ground cover, ϵ_ℓ is the average height of the low ground cover. P_ℓ and P_h are respectively the average wetted perimeter occupied by the low ground cover and the high ground cover, V_ϵ is the mean flow velocity in the vicinity of the low ground cover, and ℓ_c is the average length of ground cover in the channel in the direction of flow.

The cross-sectional area occupied by the high ground cover is approximately

$$A_h \approx \frac{P_h}{P} A \quad (4.11)$$

The value of V_ϵ can be estimated by a linear approximation or

$$V_\epsilon = \frac{\epsilon_\ell}{R} V \quad (4.12)$$

Substituting Eqs. 4.11 and 4.12 into Eq. 4.10 and rearranging, one obtains

$$\gamma A S_o \left(1 - \frac{P_h}{P} - \frac{\epsilon_\ell}{R} - \frac{P_\ell}{P} \right) = \frac{1}{8} \rho f V^2 (P - P_h - P_\ell) + \frac{1}{2} \frac{C_d}{\ell_c} \rho V^2 \frac{\epsilon_\ell^3}{R^2} P_\ell + \frac{1}{2} \frac{C_d}{\ell_c} \rho V^2 R P_h \quad (4.13)$$

One alternative form of Eq. 4.2 is

$$S_o = f' \frac{V^2 P}{8gA} \quad (4.14)$$

From Eqs. 4.13 and 4.14,

$$f' \left(1 - \frac{P_h}{P} - \frac{\epsilon_\ell}{R} \frac{P_\ell}{P} \right) = f \left(1 - \frac{P_h}{P} - \frac{P_\ell}{P} \right) + 4 \frac{C_d}{\ell_c} \frac{\epsilon_\ell^3}{R^2} \frac{P_\ell}{P} + 4 \frac{C_d}{\ell_c} R \frac{P_h}{P} \quad (4.15)$$

The channel-flow ground cover density C_g is

$$C_g = \frac{P_h + P_\ell}{P} \quad (4.16)$$

Let λ be the ratio of high ground cover density to total ground cover density. Then

$$\frac{P_h}{P} = \lambda C_g \quad (4.17)$$

Now, it is assumed that

$$4 \frac{C_d}{\ell_c} = \psi_c f_o \quad (4.18)$$

in which ψ_c is the channel ground-cover resistance descriptor, the value of which depends on the characteristics of the channel ground cover. Since ℓ_c is usually larger than ℓ_o , it is anticipated that the value of ψ_c is less than that of ψ_o .

The substitution of Eqs. 4.16, 4.17, and 4.18 into Eq. 4.15 gives

$$f' = \frac{f(1-C_g) + f_o \psi_c C_g \left[(1-\lambda) \frac{\epsilon_\ell^3}{R^2} + \lambda R \right]}{1 - \lambda C_g - \frac{\epsilon_\ell}{R} (1-\gamma) C_g} \quad (4.19)$$

for $R > \epsilon_\ell$

If the low ground cover is not submerged (i.e., $R \leq \epsilon_\ell$), the flow resistance equation is obtained by substituting R in place of ϵ_ℓ in Eq. 4.19 so that

$$f' = f + f_o \psi_c \frac{C_g}{1-C_g} R \quad (4.20)$$

for $R \leq \epsilon_\ell$

Grain resistance factor

The Darcy-Weisbach friction factor for channel flow or overland flow on rigid boundaries is a function of the roughness of the boundary, the depth of flow, the rainfall intensity and the flow Reynolds number. By definition, the flow Reynolds number is

$$N_r = \frac{QR}{\nu A} \quad (4.21)$$

in which ν is the kinematic viscosity of water.

Herein, the grain resistance is defined as the skin resistance acting on the particles forming the bed of the channel or overland flow unit. The grain resistance does not include bed-form resistance. It is assumed that the information on friction factors for rigid boundaries can be applied in establishing grain resistance factors. That is, the grain resistance factor is estimated from the friction

factor versus Reynolds number versus relative roughness relation given in fluid mechanics textbooks. (For example, Daily and Harleman, 1966, p. 276 or Chow, 1959, p. 11.)

The effect of rainfall on flow resistance is a major factor in shallow flows. The impact of raindrops in the flow causes energy losses in addition to those caused by the boundary roughness. In shallow flows, this impact loss is an important percentage of the total loss. Shen and Li (1973) have experimentally determined an equation for estimating the friction factors for flows with raindrop impact. Their findings have been incorporated into this routing model to take care of raindrop impact effects.

The equations to estimate the grain resistance with and without rainfall are given below.

For $N_r \leq 900$

$$f = \frac{K_1}{N_r} = \frac{K_o + K_r \bar{i}^{0.41}}{N_r} \quad (4.22)$$

and

$$f_o = \frac{K_o}{N_r} \quad (4.23)$$

in which K_1 is a parameter describing grain resistance with rainfall for the flow Reynolds number N_r indicated, K_o is a constant representing grain resistance without rainfall, K_r is a number describing the added friction resulting from rainfall, and \bar{i} is the average rainfall intensity.

For overland flow units

$$\bar{i} = (1-D_c)(1-D_g)i \quad (4.24)$$

and for channel units

$$\bar{i} = (1-D_c)(1-C_g)i \quad (4.25)$$

For $2,000 \leq N_r \leq 25,000$, the friction factor is given by the

Blasius form of the resistance equation which is

$$f = f_o = \frac{K_2}{N_r^{0.25}} \quad (4.26)$$

in which K_2 is a constant depending on the size of bed material.

For $N_r \geq 100,000$, the friction factor is generally independent of N_r , or

$$f = f_o = K_3 \quad (4.27)$$

in which K_3 is a constant representing grain resistance for the specified flow Reynolds number range.

In the transition ranges, the friction factor is estimated by linear interpolation.

For $900 < N_r < 2,000$

$$f = \frac{K_1 900 (1.25 \ln \frac{K_1}{K_2} - 7.14)}{N_r (1.25 \ln \frac{K_1}{K_2} - 6.14)} \quad (4.28)$$

and for $25,000 < N_r < 100,000$

$$f = \frac{K_3 100,000 (0.72 \ln \frac{K_2}{K_3} - 1.83)}{N_r (0.72 \ln \frac{K_2}{K_3} - 1.83)} \quad (4.29)$$

Overall resistance factor

By combining the information collected in the previous part of this chapter, the following equations for the overall resistance factor in natural watersheds are obtained.

For $N_r \leq 900$

$$f' = \frac{K_1'}{N_r} = \frac{K_0 \psi + K_r \bar{i}^{0.41}}{N_r} \quad (4.30)$$

For $2,000 \leq N_r \leq 25,000$

$$f' = \frac{K_2'}{N_r^{0.25}} = \frac{\psi K_2}{N_r^{0.25}} \quad (4.31)$$

For $N_r \geq 100,000$

$$f' = \frac{K_3'}{N_r^{0.0}} = \psi K_3 \quad (4.32)$$

For $900 < N_r < 2,000$

$$f' = \frac{K_1' 900 (1.25 \ln \frac{K_1'}{K_2'} - 7.14)}{N_r (1.25 \ln \frac{K_1'}{K_2'} - 6.14)} \quad (4.33)$$

And for $25,000 < N_r < 100,000$

$$f' = \frac{K_3' 100,000 (0.72 \ln \frac{K_2'}{K_3'} - 1.83)}{N_r (0.72 \ln \frac{K_2'}{K_3'} - 1.83)} \quad (4.34)$$

in which K_1' , K_2' and K_3' are constants representing the overall friction factor for the specified flow Reynolds number, and ψ is a constant which depends on the characteristics of the flow unit. The values of ψ are as follows.

In overland flow units,

$$\psi = 1 + \psi_o \frac{D}{1-D} \frac{g}{y} \quad (4.35)$$

and in channel units,

$$\psi = \frac{1 - C_g + \psi C_g [(1-\lambda) \frac{\epsilon_\ell^3}{R^2} + \lambda R]}{1 - \lambda C_g - \frac{\epsilon_\ell}{R} (1 - \lambda) C_g} \quad (4.36)$$

for $R > \epsilon_\ell$ and

$$\psi = 1 + \psi_c \frac{C_g}{1-C_g} R \quad (4.37)$$

for $R \leq \epsilon_\ell$

In summary, the general form of the resistance equation is

$$f' = \frac{a_2}{b_2 N_r} \quad (4.38)$$

in which a_2 and b_2 are functions of the rainfall intensity, the boundary roughness, the ground cover density, the canopy cover density, the depth of flow, and the flow Reynolds number.

DISCHARGE AND FLOW AREA RELATION

In general, the flow cross-sectional area can be expressed as a power function of discharge or

$$A = \alpha Q^\beta \quad (4.39)$$

in which α and β are coefficients whose values depend on the shape and roughness of the channel.

The values of α and β can be determined by first substituting Eqs. 2.1, 4.3, 4.21, and 4.38 into Eq. 4.2 and then comparing with Eq. 4.39. The solutions are

$$\alpha = \left[\frac{a_2^v b_2^{(1+b_2)} a_1}{8gS_o} \right] \left(\frac{1}{3-b_1-b_1b_2} \right) \quad (4.40)$$

and

$$\beta = \frac{2-b_2}{3-b_1-b_1b_2} \quad (4.41)$$

For overland flow units or for very wide channel flow, the wetted perimeter is constant so that $b_1 = 0$ and $\beta = \frac{2-b_2}{3}$.

NUMERICAL SCHEME

The problem of water routing is a matter of solving Eqs. 4.1 and 4.39 simultaneously. The analytical solutions of these two equations are available for the case of constant rainfall and constant channel roughness. At the present time, numerical solutions are necessary for the case of time-variant inflows. Herein, a nonlinear scheme with an iterative procedure is used to obtain solutions to the more complex cases of time-variant inflows and varying roughness. A linear scheme is also used to obtain the initial estimate for the nonlinear scheme.

Nonlinear scheme

The finite-difference forms of Eq. 4.1 can be represented as (see Fig. 4.3)

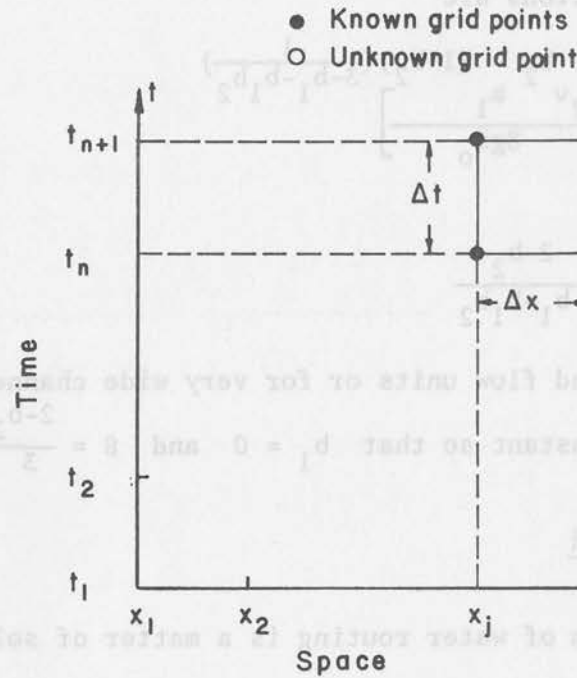


Fig. 4.3 Rectangular network in the x - t plane

$$\frac{Q_{j+1}^{n+1} - Q_j^{n+1}}{\Delta x} + \frac{A_{j+1}^{n+1} - A_j^{n+1}}{\Delta t} = q_{\ell, j+1}^{n+1} \quad (4.42)$$

in which Q_j^n is the quantity Q at grid point $x = j\Delta x$, $t = n\Delta t$, Δx is the space increment and Δt is the time increment.

The unknowns in Eq. 4.42 are Q_{j+1}^{n+1} and A_{j+1}^{n+1} , but the discharge bears a definite relation with the flow area as indicated by Eq. 4.39. With two equations, the values of the two unknowns can be obtained.

Either Q or A can be selected as the independent variable in the numerical procedure. According to the custom in backwater computations, the depth of flow (equivalent to A above) is chosen as the independent variable (see Henderson, 1966 for example); but Q is a better choice for the following reason. By taking the logarithm of both sides of Eq. 4.39, one obtains

$$\ln A = \ln \alpha + \beta \ln Q \quad (4.43)$$

The corresponding differential equation is

$$\frac{dA}{A} = \beta \frac{dQ}{Q} \quad (4.44)$$

Generally, β is less than 1.0 and has a value of one-third for Reynolds number less than 900. Consequently, if one computes discharge incorrectly, the relative error in the flow area is smaller than the relative error in the discharge. On the other hand, the error in the discharge estimation is magnified if the numerical computations are performed on the flow area. Therefore, the discharge is the better selection for the unknown in numerical computations. From the physical viewpoint, it is more appropriate to consider routing unit volumes of water rather than areas of flow.

From Eq. 4.39

$$A_{j+1}^{n+1} = \alpha(Q_{j+1}^{n+1})^\beta \quad (4.45)$$

Recall that α and β are functions of the flow Reynolds number and the hydraulic depth or depth of flow. Approximate values of the flow Reynolds number and hydraulic depth are necessary to carry the computations further. They are estimated as follows.

$$\bar{Q} = \frac{Q_{j+1}^n + Q_j^{n+1}}{2} \quad (4.46)$$

and

$$\bar{A} = \frac{A_{j+1}^n + A_j^{n+1}}{2} \quad (4.47)$$

in which \bar{Q} and \bar{A} are the approximate flow discharge and cross-sectional area of flow.

Using Eqs. 2.1, 4.3, and 4.21 one obtains.

$$\bar{P} = a_1 \bar{A}^{b_1} \quad (4.48)$$

$$\bar{R} = \frac{\bar{A}}{\bar{P}} \quad (4.49)$$

and

$$\bar{N}_r = \frac{\bar{Q} \bar{R}}{\nu \bar{A}} \quad (4.50)$$

in which \bar{P} , \bar{R} , and \bar{N}_r are respectively approximate wetted perimeter, hydraulic radius, and flow Reynolds number.

The substitution of Eq. 4.45 in Eq. 4.42 yields

$$\frac{\Delta t}{\Delta x} Q_{j+1}^{n+1} + \alpha(Q_{j+1}^{n+1})^\beta = \frac{\Delta t}{\Delta x} Q_j^{n+1} + A_{j+1}^n + \Delta t q_{\ell, j+1}^{n+1} \quad (4.51)$$

The right side of Eq. 4.51 contains known quantities and is denoted by Ω ; i.e.,

$$\Omega = \frac{\Delta t}{\Delta x} Q_j^{n+1} + A_{j+1}^n + \Delta t q_{j+1}^{n+1} \quad (4.52)$$

Let $r = Q_{j+1}^{n+1}$ and $\theta = \frac{\Delta t}{\Delta x}$ so that the left side of Eq. 4.51 can be expressed as

$$f(r) = \theta r + \alpha r^\beta \quad (4.53)$$

The solution to Eq. 4.51 is therefore the solution r^* which satisfies the condition

$$f(r^*) = \theta r^* + \alpha r^{*\beta} = \Omega \quad (4.54)$$

Equation 4.54 is nonlinear in r^* . An approximate solution to this nonlinear equation is easily obtained by the following iterative scheme.

Let r^k be the value of r at k -th iteration. The Taylor Series expansion of the function $f(r)$ around r^k is

$$\begin{aligned} f(r) = & f(r^k) + (r-r^k)f'(r^k) + \frac{1}{2} (r-r^k)^2 f''(r^k) \\ & + \frac{1}{6} (r-r^k)^3 f'''(r^k) + \dots \end{aligned} \quad (4.55)$$

in which $f'(r^k)$ and $f''(r^k)$ are values of the first and second derivatives of the function at r^k . Dropping the terms higher than third order, one obtains

$$f(r) \approx f(r^k) + (r-r^k) f'(r^k) + \frac{1}{2} (r-r^k)^2 f''(r^k) \quad (4.56)$$

The purpose of iteration is to force $f(r^{k+1})$ to approach the value of Ω , or

$$\Omega \approx f(r^k) + (r^{k+1} - r^k) f'(r^k) + \frac{1}{2} (r^{k+1} - r^k)^2 f''(r^k) \quad (4.57)$$

The solution of Eq. 4.57 is

$$r^{k+1} = r^k - \frac{f'(r^k)}{f''(r^k)} \pm \sqrt{\left(\frac{f'(r^k)}{f''(r^k)}\right)^2 - \frac{2(f(r^k) - \Omega)}{f''(r^k)}} \quad (4.58)$$

in which

$$f(r^k) = \theta r^k + \alpha (r^k)^\beta \quad (4.59)$$

$$f'(r^k) = \theta + \alpha \beta (r^k)^{\beta-1} \quad (4.60)$$

and

$$f''(r^k) = \alpha \beta (\beta-1) (r^k)^{\beta-2} \quad (4.61)$$

There are two solutions to Eq. 4.58. It is advisable to choose the solution which gives the smaller value of $|f(r^{k+1}) - \Omega|$. The above iteration is continued until the absolute error $|f(r^{k+1}) - \Omega|$ is less than a preassigned tolerance ϵ ; i.e., the termination criterion is

$$|f(r^{k+1}) - \Omega| \leq \epsilon \quad (4.62)$$

An appropriate value for ϵ is 0.01Ω . However, it may be changed according to the purpose of individual problems.

The scheme represented by Eq. 4.42 has been proven to be unconditionally stable and can be used with a wide range of time increment to space increment ratio without loss of significant accuracy. (See Li, 1974). However, the initial guess, r^0 , is the key to the speed of

convergence to the correct numerical solution. The best way of determining r^0 is to use a linear scheme.

Linear scheme

The term $\frac{\partial A}{\partial t}$ in Eq. 4.1 can be expressed as

$$\frac{\partial A}{\partial t} = \frac{\partial A}{\partial Q} \frac{\partial Q}{\partial t} \quad (4.63)$$

Also, from Eq. 4.39

$$\frac{\partial A}{\partial Q} = \alpha \beta Q^{\beta-1} \quad (4.64)$$

The substitution of Eqs. 4.63 and 4.64 into Eq. 4.1 yields

$$\frac{\partial Q}{\partial x} + \alpha \beta Q^{\beta-1} \frac{\partial Q}{\partial t} = q_l \quad (4.65)$$

The finite-difference form of Eq. 4.65 is given by the expression

$$\frac{Q_{j+1}^{n+1} - Q_j^{n+1}}{\Delta x} + \alpha \beta \left(\frac{Q_{j+1}^n + Q_j^{n+1}}{2} \right)^{\beta-1} \frac{Q_{j+1}^{n+1} - Q_{j+1}^n}{\Delta t} = q_{l,j+1}^{n+1} \quad (4.66)$$

so that

$$r^0 = Q_{j+1}^{n+1} = \frac{\theta Q_j^{n+1} + \alpha \beta Q_{j+1}^n \left(\frac{Q_{j+1}^n + Q_j^{n+1}}{2} \right)^{\beta-1} + \Delta t q_{l,j+1}^{n+1}}{\theta + \alpha \beta \left(\frac{Q_{j+1}^n + Q_j^{n+1}}{2} \right)^{\beta-1}} \quad (4.67)$$

Equation 4.67 provides the best initial estimate of r^0 for the nonlinear scheme. However, Eq. 4.67 is not applicable if both Q_{j+1}^n and Q_j^{n+1} are zero. When both Q_{j+1}^n and Q_j^{n+1} are zero, use $\beta = 1$ in Eq. 4.54 and then

$$r^0 = \frac{\Omega}{\theta + \alpha} \quad (4.68)$$

5. SEDIMENT ROUTING

CONTINUITY FOR SEDIMENT

The equation of continuity for sediment can be expressed as

$$\frac{\partial G_s}{\partial x} + \frac{\partial CA}{\partial t} + \frac{\partial Pz}{\partial t} = g_s \quad (5.1)$$

in which

$$C = \frac{G_s}{Q} \quad (5.2)$$

and G_s is the total sediment transport rate by volume, C is the sediment concentration by volume, z is the net depth of loose soil, P is the wetted perimeter, and g_s is the lateral sediment inflow.

Sediment load can further be divided into two main categories; 1. bed-material load and 2. wash load. Wash load is defined herein as the sediment load with particle sizes smaller than 0.062 mm. The remaining sediment load is bed-material load. Then, the continuity equation (Eq. 5.1) can be divided into two parts,

$$\frac{\partial G_b}{\partial x} + \frac{\partial C_b A}{\partial t} + \frac{\partial Pz_b}{\partial t} = g_b \quad (5.3)$$

and

$$\frac{\partial G_w}{\partial x} + \frac{\partial C_w A}{\partial t} + \frac{\partial Pz_w}{\partial t} = g_w \quad (5.4)$$

in which G_b and G_w are respectively the bed-material load and the wash load transport rates, C_b and C_w are respectively the concentrations of suspended bed-material load and of suspended wash load, z_b and z_w are respectively depths of loose soil for the bed-material load size

and wash load size, and g_b and g_w are respectively the lateral inflow rate of bed-material load and wash load. By definition

$$G_s = G_b + G_w \quad (5.5)$$

$$C_b = \frac{G_b}{Q} \quad (5.6)$$

$$C_w = \frac{G_w}{Q} \quad (5.7)$$

$$C = C_b + C_w \quad (5.8)$$

and

$$z = z_b + z_w \quad (5.9)$$

SEDIMENT TRANSPORT EQUATIONS

The sediment transport equation is used to determine the sediment transporting capacity of a specific flow condition. Different transport capacities can be expected for different sediment sizes. For either sediment size, the transporting rate includes the bed-load transport rate and the suspended load transport rate. The following equations are adopted in this study to determine either bed-material load transporting capacity or wash load transporting capacity.

The Meyer-Peter-Muller equation is a simple and commonly used bed-load transport equation (see USBR, 1960). It is

$$q_b = \frac{8}{\sqrt{\rho}(\gamma_s - \gamma)} (\tau_o - \tau_c)^{1.5} \quad (5.10)$$

in which

$$\tau_c = 0.047(\gamma_s - \gamma)d_s \quad (5.11)$$

Here q_b , is the bed-load transport rate in volume per unit width τ_o is the boundary shear stress acting on the grain, τ_c is the critical tractive force, γ_s is the specific weight of sediment, and d_s is the size of sediment.

The flow discharge Q and flow area A are determined in time and space by the water routing procedure described in Chapter 4. The corresponding value of τ_o is computed as follows.

The mean flow velocity is

$$V = Q/A \quad (5.12)$$

Then, the boundary shear stress acting on the grain is

$$\tau_o = \frac{1}{8} \rho f V^2 \quad (5.13)$$

in which f is the Darcy-Weisbach friction factor due to grain resistance.

In a natural watershed the average bed-load transport rate is

$$q_b = \frac{8}{\sqrt{\rho}(\gamma_s - \gamma)} (1 - D_g) (\tau_o - \tau_c)^{1.5} \quad (5.14)$$

for overland flow units and

$$q_b = \frac{8}{\sqrt{\rho}(\gamma_s - \gamma)} (1 - C_g) (\tau_o - \tau_c)^{1.5} \quad (5.15)$$

for channel flow units because there is no sediment yield from areas covered by rocks etc.

The sediment concentration profile which relates the sediment concentration with depth above the bed (See Einstein, 1950) can be written

$$\frac{C_\xi}{C_a} = \left(\frac{R - \xi}{\xi} \frac{a}{R - a} \right)^w \quad (5.16)$$

in which C_ξ is the sediment concentration at the distance ξ from the bed, C_a is the known concentration at a distance "a" above the bed, and w is a parameter defined as

$$w = \frac{v_s}{0.4U_*} \quad (5.17)$$

Here v_s is the settling velocity of the sediment particles and U_* is the shear velocity of the flow defined as

$$U_* = \left(\frac{\tau_*}{\rho} \right)^{1/2} \quad (5.18)$$

Note that

$$\tau_* = \frac{1}{8} f' \rho V^2 (1 - D_g) \quad (5.19)$$

for overland flow units,

$$\tau_* = \frac{1}{8} f' \rho V^2 \left[1 - \lambda C_g - \frac{\epsilon_\ell}{R} (1 - \lambda) C_g \right] \quad (5.20)$$

for channel flow units with $R > \epsilon_\ell$ and

$$\tau_* = \frac{1}{8} f' \rho V^2 (1 - C_g) \quad (5.21)$$

for channel flow units with $R \leq \epsilon_\ell$. The term τ_* is the effective overall resistance force, and f' is overall resistance factor which is given in Chapter 4.

A logarithmic velocity profile is commonly adopted to describe the velocity distribution in turbulent flows. For simplicity, a logarithmic velocity profile is assumed in this study. The equation is

$$\frac{u_\xi}{U_*} = B + 2.5 \ln \left(\frac{\xi}{\eta_s} \right) \quad (5.22)$$

in which u_ξ is the point mean velocity at the distance ξ from the bed, B is a constant dependent on roughness, and η_s is the roughness height.

The integral of suspended load above the "a" level in the flow is obtained by combining Eqs. 5.16 and 5.22 or

$$q_s = \int_a^R u_\xi C_\xi d\xi$$

$$= C_a U_* \int_a^R [B + 2.5 \ln(\frac{\xi}{\eta_s})] (\frac{R-\xi}{\xi} \frac{a}{R-a})^w d\xi \quad (5.23)$$

Let

$$\sigma = \frac{\xi}{R} \quad (5.24)$$

and

$$G = \frac{a}{R} \quad (5.25)$$

Then one obtains

$$q_s = C_a U_* a \frac{G^{w-1}}{(1-G)^w} \{ [B + 2.5 \ln(\frac{R}{\eta_s})] \int_G^1 (\frac{1-\sigma}{\sigma})^w d\sigma$$

$$+ 2.5 \int_G^1 \ln \sigma (\frac{1-\sigma}{\sigma})^w d\sigma \} \quad (5.26)$$

According to Einstein (1950), the concentration near the "bed layer" C_a is related to the bed-load transport rate q_b by the expression

$$q_b = 11.6 C_a U_* a \quad (5.27)$$

in which "a" is now defined as the thickness of the bed layer which is twice the size of sediment.

The average flow velocity V is defined by the equation

$$V = \frac{\int_0^R u_\xi d\xi}{\int_0^R d\xi} \quad (5.28)$$

Using Eq. 5.22

$$\frac{V}{U_*} = B + 2.5 \ln\left(\frac{R}{\eta_s}\right) - 2.5 \quad (5.29)$$

Einstein (1950) defined the two integrals in Eq. 5.26 as

$$J_1 = \int_G^1 \left(\frac{1-\sigma}{\sigma}\right)^w d\sigma \quad (5.30)$$

and

$$J_2 = \int_G^1 \left(\frac{1-\sigma}{\sigma}\right)^w \ln \sigma d\sigma \quad (5.31)$$

The integrals J_1 and J_2 cannot be integrated in closed form for most values of w so a numerical integration is necessary. An efficient numerical method of determining J_1 and J_2 was developed by Li (1974) and is adopted in this study.

The substitution of Eqs. 5.27, 5.29, 5.30 and 5.31 into Eq. 5.26 yields

$$q_s = \frac{q_b}{11.6} \frac{G^{w-1}}{(1-G)^w} \left[\left(\frac{V}{U_*} + 2.5\right) J_1 + 2.5 J_2 \right] \quad (5.32)$$

When the total load per unit width is

$$q_t = q_b + q_s \quad (5.33)$$

and the sediment transporting capacity of the section G_c is

$$G_c = Pq_t \quad (5.34)$$

EQUATIONS FOR SEDIMENT SUPPLY

The sediment supply rate is a main factor in determining the sediment transport rate in a watershed system. The sediment supply depends on the initial depth of loose soil left from previous storms, the amount of soil detachment by raindrop impact, and the amount of soil detachment by overland flow erosion and channel erosion.

Soil detachment by raindrop impact

The potential rate of soil detachment by raindrops impact is assumed to be

$$D_i = a_3 i^{b_3} \left(1 - \frac{z}{z_m}\right) \quad (5.35)$$

if $z \leq z_m$ and

$$D_i = 0 \quad (5.36)$$

if $z > z_m$

Here, D_i is the potential rate of soil detachment (in units of depth) per unit time, a_3 and b_3 are coefficients depending on soil erodibility and z_m is the equivalent maximum penetration depth of raindrop impact on the soil layer. Expressions for the equivalent maximum penetration depth are

$$z_m = (1 - D_g) D_p \quad (5.37)$$

for overland flow units and

$$z_m = (1 - C_g) D_p \quad (5.38)$$

for the channel flow units. Here D_p is the maximum depth to which a raindrop can penetrate the soil layer.

The soil detachment rate under the canopy or ground cover is zero and the rate is expected to be negligible for the higher Reynolds number flow. Therefore, it is assumed that the actual supply rate of loose soil by raindrop impact \bar{D}_i is as follows. For overland flow units

$$\bar{D}_i = (1 - D_c)(1 - D_g) D_i \quad (5.39)$$

if $N_r \leq 900$ and

$$\bar{D}_i = 0 \quad (5.40)$$

if $N_r > 900$.

For channel units

$$\bar{D}_i = (1 - D_c)(1 - C_g) D_i \quad (5.41)$$

if $N_r \leq 900$ and

$$\bar{D}_i = 0 \quad (5.42)$$

if $N_r > 900$.

Then, the new amounts of loose soil available for transport at time $t + \Delta t$ are

$$z_b(t + \Delta t) = z_b(t) + F_b \bar{D}_i \Delta t \quad (5.43)$$

and

$$z_w(t + \Delta t) = z_w(t) + F_w \bar{D}_i \Delta t \quad (5.44)$$

in which $z_b(t)$ and $z_w(t)$ are respectively the amounts of loose bed-load soil and wash load soil available at time t , and F_b and F_w are respectively the percent of bed-material load size and the percent of wash load size in a typical soil sample.

Soil detachment by surface runoff

The amount of soil detachment by surface runoff in overland flow units or in channel flow units is determined by examining the sediment transporting capacity and the available amount of loose soil. It is assumed that because of the armoring effect of larger size sediments, wash load soils are not detached unless some bed-material has been detached by flowing water. Thus, soil erosion of bed material is the main concern in this process. By substituting the bed-material load transporting capacity G_c given by Eq. 5.34 into bed-material load transport rate G_b given by Eq. 5.3, the potential change in loose soil storage for bed-material load size Δz_b^P is determined. Then

$$\Delta z_b^P = \frac{\partial z_b}{\partial t} \Delta t \quad (5.45)$$

If $\Delta z_b^P \geq -z_b$, the loose soil storage is enough for transport and no detachment of soil is expected. Soil is detached if $\Delta z_b^P < -z_b$ and the amount of detachment is assumed to be

$$D_b = -D_f(\Delta z_b^P + z_b) \quad (5.46)$$

in which D_b is the amount of detached bed-material soil, and D_f is a constant defined as "detachment coefficient" with values between 0.0 and 1.0 depending on the soil erodibility. For large rivers, the sediment in the riverbed is always loose, and the value of D_f is unity.

The new amounts of loose soil available for at time $t + \Delta t$ are then

$$z_b(t+\Delta t) = z_b(t) + D_b \quad (5.47)$$

and

$$z_w(t+\Delta t) = z_w(t) + D_b F_w/F_b \quad (5.48)$$

NUMERICAL PROCEDURE FOR SEDIMENT ROUTING

The following numerical procedure for sediment routing is used to couple the equations governing sediment motion with the water routing procedure described in Chapter 4.

Bed-material load routing

The bed-material transport capacity is determined with Eq. 5.34 for a given bed-material load size, and for the flow conditions obtained by routing the excess rainfall. The potential bed-material load concentration is then

$$C_b^P = \frac{G_c(\text{bed-material load})}{Q} \quad (5.49)$$

Using the same finite-difference approximation as that in the water routing procedure (See Fig. 4.3), the potential change in loose soil storage for bed-material size sediment is determined by utilizing Eqs. 5.3 and 5.49. That is,

$$\Delta z_b^P = \frac{1}{P} [(G_{bj}^{n+1} - C_b^P Q_{j+1}^{n+1})\theta - C_b^P A_{j+1}^{n+1} + C_{bj+1}^n A_{j+1}^n + g_{bj+1}^{n+1} \Delta t] \quad (5.50)$$

If Δz_b^P is positive, the bed is aggrading, and if negative, the bed is degrading.

The bed-material load transport rate is dependent on both the availability of bed-material load and the transporting capacity of the flow. If $\Delta z_b^P \geq -z_b$, the availability is greater than the transporting capacity. Thus, the bed-material load transport rate is equal to its transporting capacity or

$$C_{b,j+1}^{n+1} = C_b^P \quad (5.51)$$

and the actual change in z_b is

$$\Delta z_b = \Delta z_b^P \quad (5.52)$$

If $\Delta z_b^P < -z_b$, the availability of bed-material load is less than the transporting capacity. Under this condition, soil detachment by surface runoff occurs, and the amount of soil detachment is determined by Eq. 5.46. The bed-material load transport rate is limited to the availability of soil given by Eq. 5.47. The bed-material load concentration is therefore,

$$C_{b,j+1}^{n+1} = \frac{Pz_b + g_{b,j+1}^{n+1} \Delta t + C_{b,j+1}^n A_{j+1}^n + G_{b,j}^{n+1} \theta}{A_{j+1}^{n+1} + Q_{j+1}^{n+1} \theta} \quad (5.53)$$

and

$$\Delta z_b = -z_b \quad (5.54)$$

The bed-material load transport rate $G_{b,j+1}^{n+1}$ is determined by Eq. 5.6 or

$$G_{b,j+1}^{n+1} = C_{b,j+1}^{n+1} Q \quad (5.55)$$

Wash load routing

The wash load transport rate is usually determined by the availability of soil unless flow discharges are very small. The potential wash load concentration C_w^P is given by the expression

$$C_w^P = \frac{G_c (\text{wash load})}{Q} \quad (5.56)$$

The potential change in loose soil storage for the wash load size is

$$\Delta z_w^P = \frac{1}{P} [(G_{w,j}^{n+1} - C_w^P Q_{j+1}^{n+1})\theta - C_w^P A_{j+1}^{n+1} + C_{w,j+1}^n A_{j+1}^n + g_{w,j+1}^{n+1} \Delta t] \quad (5.57)$$

If $\Delta z_w^P \geq -z_w$, the wash load availability is greater than the transporting capacity of the flow. Therefore, the wash load transport rate is equal to the transporting capacity or

$$C_{w,j+1}^{n+1} = C_w^P \quad (5.58)$$

and the actual change in z_w is

$$\Delta z_w = \Delta z_w^P \quad (5.59)$$

If $\Delta z_w^P < -z_w$, the wash load transporting capacity is greater than the availability of wash load. This is the usual case. Under this condition, the wash load transport rate is limited to its availability or

$$C_{w,j+1}^{n+1} = \frac{P z_w + g_{w,j+1}^{n+1} \Delta t + C_{w,j+1}^n A_{j+1}^n + G_{w,j}^{n+1} \theta}{A_{j+1}^{n+1} + Q_{j+1}^{n+1} \theta} \quad (5.60)$$

and

$$\Delta z_w = -z_w \quad (5.61)$$

The wash load transport rate is then determined by Eq. 5.7 and

$$G_{wj+1}^{n+1} = C_{wj+1}^{n+1} Q \quad (5.62)$$

Degradation or aggradation

The amount of degradation or aggradation is evaluated by considering changes in loose soil storage. Degradation or aggradation may cause changes in bed slope and in ground cover. However, such changes in overland flow units are usually not significant in natural watersheds. In mountainous channels as in the Beaver Creek Watersheds streambeds are composed of large boulders. These streambeds are rather stable and changes in bed slope due to degradation or aggradation are usually not significant and may be neglected in the flow routing computation.

Changes in channel ground cover play a very important role in sediment routing. Therefore, in this study, the processes of degradation and aggradation and changes in channel ground cover are taken into account in the manner shown below.

The mean elevation change of a channel reach is given by the expression

$$\Delta Z_{j+1}^{n+1} = \Delta z_b / (1 - \epsilon_b) + \Delta z_w / (1 - \epsilon_w) \quad (5.63)$$

in which ΔZ is the mean elevation change, and ϵ_b and ϵ_w are respectively the porosities of the bed-material and wash load sediments.

The effective height of the low ground cover in the channel is

$$\bar{\epsilon} = \epsilon_l (1 - C_g) \quad (5.64)$$

If ΔZ is greater or equal to $\bar{\epsilon}$, the loose soil deposit fills up the space in the low ground cover and reduces the low ground cover density to zero. In addition, the average height of low ground cover becomes zero and the drag resistance due to low ground cover no longer exists. When $\Delta Z \geq \bar{\epsilon}$, the parameters describing the low ground cover (See Chapter 4) for the next time step, are modified so that,

$$\epsilon_{\ell}(t+\Delta t) = 0 \quad (5.65)$$

and

$$\lambda(t+\Delta t) = 1 \quad (5.66)$$

If ΔZ is negative ($\Delta Z < 0$) the bed is degrading and the height of low ground cover is increased. Then the drag resistance due to low ground cover may be increased. The change in low ground cover height is $\Delta Z/\bar{\epsilon}$ so the modified height of low ground cover to be used in the resistance equations is

$$\epsilon_{\ell}(t+\Delta t) = \epsilon_{\ell}(t) \left(1 - \frac{\Delta Z}{\bar{\epsilon}}\right) \quad (5.67)$$

If ΔZ is between 0.0 and $\bar{\epsilon}$, decreases in low ground cover density and height of low ground cover are expected to reduce the drag resistance. The modified low ground cover parameters are

$$\epsilon_{\ell}(t+\Delta t) = \epsilon_{\ell}(t) \left(1 - \frac{\Delta Z}{\bar{\epsilon}}\right) \quad (5.68)$$

$$C_g(t+\Delta t) = \{\lambda(t) + [1-\lambda(t)] \left(1 - \frac{\Delta Z}{\bar{\epsilon}}\right)\} C_g(t) \quad (5.69)$$

and

$$\lambda(t+\Delta t) = \frac{\lambda(t)}{\lambda(t) + [1-\lambda(t)][1 - \frac{\Delta Z}{\bar{z}}]} \quad (5.70)$$

(5.65)

$$e_1(t+\Delta t) = 0$$

and

(5.66)

$$\lambda(t+\Delta t) = 1$$

If ΔZ is negative ($\Delta Z < 0$) the bed is degrading and the height of low ground cover is increased. Then the drag resistance due to low ground cover may be increased. The change in low ground cover height is $\Delta Z/\bar{z}$ so the modified height of low ground cover to be used in the resistance equation is

(5.67)

$$e_1(t+\Delta t) = e_1(t) \left(1 - \frac{\Delta Z}{\bar{z}}\right)$$

If ΔZ is between 0.0 and \bar{z} , decreases in low ground cover density and height of low ground cover are expected to reduce the drag resistance. The modified low ground cover parameters are

(5.68)

$$e_1(t+\Delta t) = e_1(t) \left(1 - \frac{\Delta Z}{\bar{z}}\right)$$

(5.69)

$$e_2(t+\Delta t) = (e_2(t) + [1-\lambda(t)] \left(1 - \frac{\Delta Z}{\bar{z}}\right)) C(t)$$

6. MODEL APPLICATION AND VERIFICATION

A computer program based on the mathematical formulations presented above was developed to simulate water and sediment outflow hydrographs of small watersheds. A listing of this computer program is given in the Appendix.

Five runoff events in Watershed 1 and one runoff event in Watershed 17 were used to test the applicability of the proposed mathematical model.

Watershed 1 is a small drainage catchment with an area of 313.6 acres and has been clear-cut. The five storm events in Watershed 1 used in this study area occurred on November 22, 1965, November 24, 1965, November 25, 1965, September 6, 1967, and September 5, 1970. The latter is known as the "Labor Day" storm.

Watershed 17 has an area of 287.4 acres. The only storm available for testing is the "Labor Day" storm of September 5, 1970.

The data required to run the numerical model and for parameter calibration were obtained from the Rocky Mountain Forest and Range Experiment Station, Flagstaff, Arizona and from the field surveys made by Colorado State University.

The details of input data, test results, and applications to predict watershed treatment effects are given below.

INPUT DATA

Three types of data are required. They are the basin characteristics data, the storm characteristics data, and the antecedent conditions

(see Fig. 1.1). The basin characteristics data include the watershed geometry, soil data, vegetation and ground cover data, flow resistance parameters and sediment routing parameters. These data are assumed to be time-invariant unless some treatments are imposed on the watershed.

The storm characteristics data are rainfall records, aerial distribution of rainfall and the mean evaporation rate. The antecedent conditions include initial interception storage content, antecedent moisture content, and initial loose soil storage. The storm characteristics data and antecedent conditions change from storm to storm.

Basin characteristics data

Geometry data. The geometric segmentation of Watershed 1 and Watershed 17 are shown respectively in Figs. 6.1 and 6.2 and a typical wetted perimeter versus flow area is given in Fig. 2.2.

Because the data on vegetation, ground cover, and soil properties are not available on the basis of small overland flow units, large overland flow units are grouped from the small ones according to the procedure presented in Chapter 2 (page 9). In this treatment, water is routed from overland flow units to channels and to the watershed outlet. The overland flow units in the following analysis are large overland flow units.

Watershed 1 is composed of 12 overland flow units, 6 channel units, and 1 road unit. The road unit is superposed because it has the potential for producing a large amount of sediment because there is no ground nor canopy cover.

Watershed 17 is decomposed into 16 overland flow units, 8 channel flow units and 3 road units.

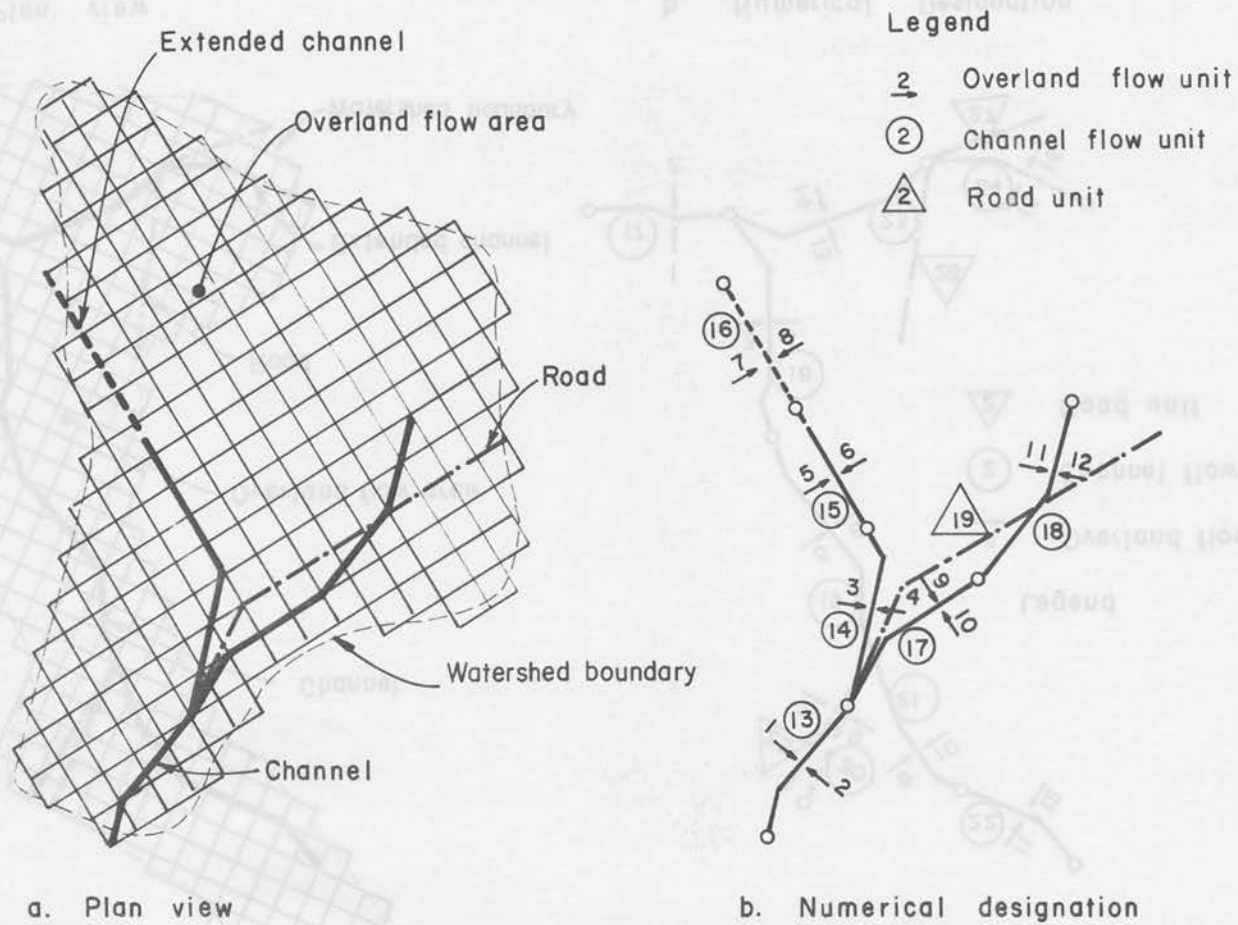


Fig. 6.1 Geometric segmentation of Watershed 1

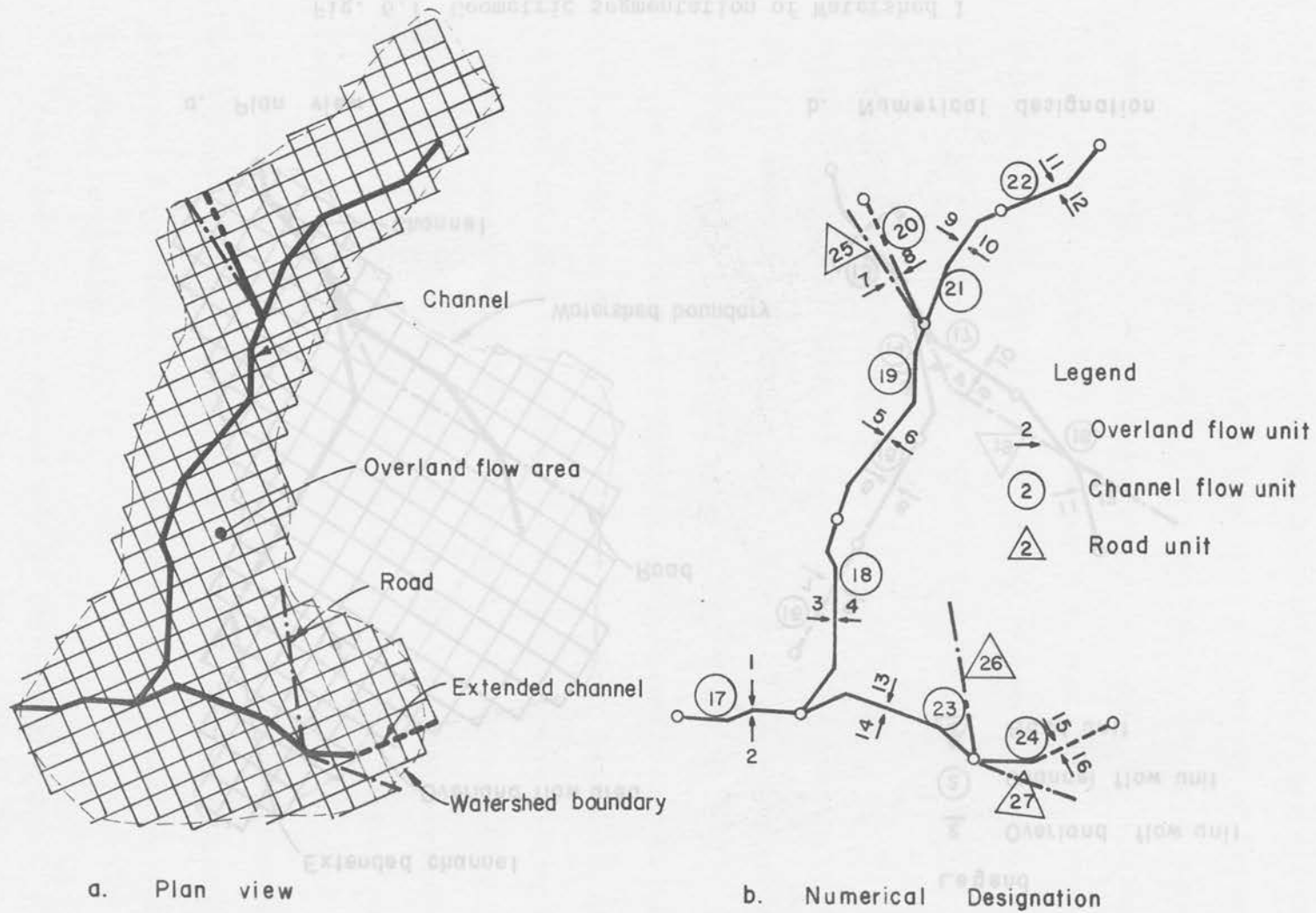


Fig. 6.2 Geometric segmentation of Watershed 17

Table 6.1 Geometry of Watershed 1

Index	Length ft	Slope	Wetted Perimeter versus flow area relation		Type
			a_1	b_1	
1	1440	0.0931	1.	0.	O.F.
2	288	0.0743	1.	0.	O.F.
3	730	0.1156	1.	0.	O.F.
4	327	0.1158	1.	0.	O.F.
5	264	0.1395	1.	0.	O.F.
6	858	0.1164	1.	0.	O.F.
7	198	0.0764	1.	0.	O.F.
8	726	0.1209	1.	0.	O.F.
9	1120	0.0986	1.	0.	O.F.
10	240	0.0762	1.	0.	O.F.
11	3280	0.0919	1.	0.	O.F.
12	551	0.1200	1.	0.	O.F.
13	1210	0.0389	5.363	0.552	C.F.
14	1380	0.0636	4.494	0.671	C.F.
15	1060	0.1193	4.494	0.671	C.F.
16	1060	0.0843	5.998	0.615	C.F.
17	1380	0.0506	6.249	0.555	C.F.
18	1580	0.0525	7.036	0.623	C.F.
19	3170	0.0514	15.	0.	R.D.

Notes: O.F. means overland flow unit
C.F. means channel flow unit
R.D. means a road unit

Table 6.2 Geometry of Watershed 17

Index	Length ft	Slope	Wetted Perimeter versus flow area relations		Type
			a_1	b_1	
1	439	0.0702	1.	0.	O.F.
2	731	0.0973	1.	0.	O.F.
3	471	0.0865	1.	0.	O.F.
4	910	0.0639	1.	0.	O.F.
5	440	0.0852	1.	0.	O.F.
6	503	0.0546	1.	0.	O.F.
7	467	0.0463	1.	0.	O.F.
8	700	0.0776	1.	0.	O.F.
9	412	0.1102	1.	0.	O.F.
10	247	0.0745	1.	0.	O.F.
11	879	0.1141	1.	0.	O.F.
12	382	0.0844	1.	0.	O.F.
13	659	0.0993	1.	0.	O.F.
14	890	0.0851	1.	0.	O.F.
15	442	0.0791	1.	0.	O.F.
16	320	0.0849	1.	0.	O.F.
17	1090	0.0219	8.940	0.532	C.F.
18	1820	0.0203	10.132	0.448	C.F.
19	1910	0.0393	6.684	0.556	C.F.
20	1200	0.0358	7.338	0.629	C.F.
21	1210	0.0643	7.866	0.619	C.F.
22	1050	0.0945	6.986	0.409	C.F.
23	1470	0.0251	6.836	0.548	C.F.
24	1470	0.0306	6.986	0.409	C.F.
25	1400	0.0400	15.	0.	R.D.
26	1350	0.0310	15.	0.	R.D.
27	1300	0.0324	15.	0.	R.D.

Notes: O.F. means overland flow unit
C.F. means channel flow unit
R.D. means a road unit

Tables 6.1 and 6.2 provide summaries of the geometry for each segment in the watersheds. The parameters a_1 and b_1 given in Tables 6.1 and 6.2 describe the wetted perimeter versus flow area and were estimated from the channel survey data. The values of b_1 for overland flow and road units are 0.0. The average width of road is approximately 15 ft making $a_1 = 15$ for the road unit.

Table 6.3 and Table 6.4 give the computation sequence for Watershed 1 and Watershed 17 respectively. The computation sequence is established by the logics of gravity flow and flow continuity requirements. The computational order (Column 2) is the order for the computation of flow routing in the segment identified in Column 1 and shown in Figs. 6.1 and 6.2. The numbers in Column 3 indicate the upstream inflow segments to the segment in Column 1 and the numbers in Column 4 are the lateral inflow segments. The symbol "0" is used to indicate there are no upstream inflow segments or lateral inflow segments.

Soil data. Williams et al. (1967) reported the soil survey on the Beaver Creek Area. This report is the main source of soil data required in the model input. The soil type in Watershed 1 is predominantly Springerville, a very stony clay. There are several soil types in Watershed 17 including Broliar silt loam, Broliar stony clay, and Siesta stony silt loams.

Engineering properties of all these soils are very similar. The saturated hydraulic conductivity k_s is approximately 0.05 inches per hour, the estimated depth of the aeration zone η_a is 36 inches, the average water storage capacity is 18 inches, and the moisture content at saturation m_s is approximately 0.5.

Table 6.3 Computational Sequence for Watershed 1

Index (1)	Computational order (2)	Upstream inflow Segments (3)			Lateral inflow Segments (4)	
1	1	0	0	0	0	0
2	2	0	0	0	0	0
3	3	0	0	0	0	0
4	4	0	0	0	0	0
5	5	0	0	0	0	0
6	6	0	0	0	0	0
7	7	0	0	0	0	0
8	8	0	0	0	0	0
9	9	0	0	0	0	0
10	10	0	0	0	0	0
11	11	0	0	0	0	0
12	12	0	0	0	0	0
13	19	14	17	19	1	2
14	18	15	0	0	3	4
15	16	16	0	0	5	6
16	14	0	0	0	7	8
17	17	18	0	0	9	10
18	15	0	0	0	11	12
19	13	0	0	0	0	0

Table 6.4 Computational Sequence for Watershed 17

Index (1)	Computational order (2)	Upstream inflow Segments (3)			Lateral inflow Segments (4)	
1	1	0	0	0	0	0
2	2	0	0	0	0	0
3	3	0	0	0	0	0
4	4	0	0	0	0	0
5	5	0	0	0	0	0
6	6	0	0	0	0	0
7	7	0	0	0	0	0
8	8	0	0	0	0	0
9	9	0	0	0	0	0
10	10	0	0	0	0	0
11	11	0	0	0	0	0
12	12	0	0	0	0	0
13	13	0	0	0	0	0
14	14	0	0	0	0	0
15	15	0	0	0	0	0
16	16	0	0	0	0	0
17	27	18	23	0	1	2
18	26	19	0	0	3	4
19	25	20	21	25	5	6
20	20	0	0	0	7	8
21	23	22	0	0	9	10
22	21	0	0	0	11	12
23	24	24	26	27	13	14
24	22	0	0	0	15	16
25	17	0	0	0	0	0
26	18	0	0	0	0	0
27	19	0	0	0	0	0

According to Linsley et al. (1958, p. 126) the moisture content at the wilting point m_2 is approximately 0.15 and the magnitude of the capillary potential at the wilting point P_w is about 15 atmospheres (approximately 6100 inches of water head) for a typical clay or silt loam soil. These values were adopted in the analysis.

Samples of Watershed 12 bed-material load taken on November 23, 1970 indicate that the mean bed-material load size is 1.0 mm. Pipette size analysis of Watershed 1 wash load samples taken on August 4, 1964 show that the mean wash load size is 0.011 mm. The fractions of wash load size and bed-material size, as determined by Williams et al., are approximately 0.5.

Vegetation and ground cover data. The vegetation and ground cover data were determined from ground surveys and aerial photographs.

The canopy cover density D_c in Watershed 1 is 0.0 (clear-cut treatment) and a value of 0.1 was estimated for Watershed 17.

In Watershed 1, ground cover densities were estimated to be 0.65 in overland flow areas and 0.85 in channels. The average height of the low ground cover is approximately 0.25 ft and the ratio of high ground cover density to total ground cover density was assumed to be 0.3 (thirty percent of ground cover in the channel is never submerged by the flow). No ground cover data were readily available for Watershed 17 so the values for Watershed 1 were used in Watershed 17.

The interception storage capacity of the ground cover per unit area V_g was assumed to be 0.1, a value estimated from Zinke's (1965) report. According to Penman (1965), the ratio of evaporating surface to the horizontal projected area for ground cover S_g is on the order of 10 for grasses and on the order of 5 for agricultural crops. In this

study, S_g was assumed to be 5.0. According to Zinke (1965) the maximum measured interception storage for forest lands is around 0.36 in. In this study, the ratio of interception storage capacity of a tree canopy to that of ground cover per unit area r_v was assumed to be 2.0. This value implies that the interception storage volume under a canopy is 0.27 inch.

Flow resistance parameters. The flow resistance parameters are K_o , K_r , K_2 , K_3 , ψ_o and ψ_c (See Chapter 4). The values K_o and K_2 for flow in rough channels (given by Chow, 1959, p. 11) are 45 and 0.45 respectively. As reported by Shen and Li (1973), the coefficient K_r is 27 for raindrops with terminal velocities. The average Darcy-Weisbach friction factor for a plane bed (grain resistance only) for flows with a large Reynolds number was measured as 0.03 by Simons and Richardson (1966, p. 17). Thus, the parameter K_3 was assumed to be 0.03 in this study.

The Manning's roughness coefficient n for mountain streams with cobbles and large boulders in the streambed is normally about 0.05 and has a maximum value of 0.07 (Chow, 1959, p. 113). The streams in Watershed 1 and Watershed 17 belong to this category. Assuming that the maximum roughness occurs at high flow with a hydraulic radius of approximately 3 feet (estimated from measured flood stage), the value of channel-flow ground-cover resistance descriptor was estimated as follows.

Comparing the Darcy-Weisbach equation with Manning's equation one obtains

$$f' = \frac{8gn^2}{2.22 R^{1/3}} \quad (6.1)$$

For high Reynolds number flow, Eq. 4.19 can be rewritten as

$$\psi_c = \frac{f' \{1 - \lambda C_g - \frac{\epsilon_l}{R} (1 - \lambda) C_g\} - K_3 (1 - C_g)}{K_3 C_g \{ (1 - \lambda) \frac{\epsilon_l^3}{R^2} + \lambda R \}} \quad (6.2)$$

With $n = 0.07$ and $R = 3$, the value of ψ_c is 11.7 according to Eqs. 6.1 and 6.2. Thus, ψ_c was assumed to be 11.0 in the analysis.

If R is equal to 0.25 (the height of the low ground cover), Manning's n is approximately 0.05, the normal value for mountain streams.

As mentioned in Chapter 4, the overland flow ground cover resistance descriptor ψ_o is greater than ψ_c ; i.e., $\psi_o > 11.0$. Due to insufficient information on resistance to overland flow, the value of ψ_o was estimated by a calibration procedure which is presented later in this chapter.

Sediment routing parameters. The equations describing sediment transporting capacity (both bed material and wash load) are given in Chapter 5. From considerations of raindrop impact energy, the maximum penetration depth of raindrop impact on the soil layer was assumed to be 0.10 ft. The values a_3 and b_3 in Eq. 5.35 which describe the potential soil detachment rate by raindrop impact are not precisely known. However, the value of b_3 was assumed to be 0.4, the value given by Shen and Li (1973) in their equation for estimating the added friction factor due to raindrop impact. The value of a_3 is dependent on the soil erodibility and is related to wash-load sediment yield. The value of a_3 was estimated by the calibration procedure.

The value of the detachment coefficient D_f controlling the amount of soil detachment by surface runoff is between 0.0 and 1.0. The value is dependent on the soil erodibility and was estimated by the calibration procedure.

Storm characteristics data

The rainfall intensities for storms on September 5, 1970 and September 6, 1967 on Watershed 1 and on September 5, 1970 on Watershed 17 were derived from records of the accumulation of precipitation over a five-minute interval. For storms on November 22, 1965, November 24, 1965 and November 25, 1965 on Watershed 1, the intensities were determined on a thirty-minute interval.

The aerial distribution of rainfall intensity was not available because there is only one recording raingage in each watershed. It was assumed that the rainfall intensity was uniform over the entire area of the watershed.

The evaporation rates during storms are usually very small because the air is nearly saturated with moisture. Thus, the mean evaporation rate E for all storms was considered negligible.

Antecedent conditions

The precipitation records immediately preceding the storms indicate that vegetation and ground cover were dry prior to storms. For simplicity, the initial interception storage content, I_s was assumed zero in all cases.

Because of the large water-storage capacity of soil in both watersheds and due to presence of a soil moisture supply prior to storms, it was estimated that the antecedent moisture content $m_o(0)$ was greater than the field capacity of the soil (0.4 for clay or silt loam). The proper values of $m_o(0)$ for different storms must be estimated by the calibration method with the constraint that

$$0.4 \leq m_o(0) \leq 0.5.$$

Data on the initial loose soil storages were not available. Three storms occurred in succession in Watershed 1 in 1965. The initial loose soil storages for these storms on November 24 and 25 were assumed those left from the storms on November 22 and November 24 respectively. For the other storms, the initial loose soil storage were assumed zero because these storms were preceded by very small storms without runoff.

Summary

The input data required for this simulation model are:

1. *Geometry data* - including slope length, bed slope, and wetted perimeter versus flow area relations.
2. *Soil data* - including the saturated hydraulic conductivity, depth of aeration, moisture contents at the wilting point and at the saturation, magnitude of the capillary potential at the wilting point, mean bed-material size, mean wash load size, and particle size distribution.
3. *Vegetation and ground cover data* - including canopy cover density, ground cover density in overland flow units and in channel units, the average height of low ground cover and the ratio of high ground cover density to total ground cover density in channels, the interception storage capacity of ground cover, ratio of evaporating surface to the horizontal projected area for ground cover, and ratio of the interception storage capacity of a tree canopy to the interception storage capacity of ground cover.
4. *Flow resistance parameters* - including constants describing grain resistance for different Reynolds numbers, the constant representing added roughness due to raindrop impact, and values for the overland flow ground-cover resistance descriptor, and channel-flow ground-cover resistance descriptor.
5. *Sediment routing parameters* - including parameters describing the sediment transporting capacity, maximum penetration depth of raindrop impact, parameters describing the potential soil detachment rate and the detachment coefficient of soil by surface runoff (soil erodibility).
6. *Storm characteristics* - including rainfall intensity, aerial distribution of rainfall intensity, and mean evaporation rate.
7. *Antecedent conditions* - including the initial interception storage content, antecedent soil moisture content, and initial loose soil storage.

MODEL CALIBRATION

The values of the four unknown coefficients ψ_0 , a_3 , D_f and $m_0(0)$ have been obtained by model calibration. As described in the previous sections the range of values of these four unknowns are:

$$\psi_0 \geq 11.0 \quad (6.3)$$

$$a_3 \geq 0.0 \quad (6.4)$$

$$0.0 \leq D_f \leq 1.0 \quad (6.5)$$

and

$$0.4 \leq m_0(0) \leq 0.5 \quad (6.6)$$

Only the value of $m_0(0)$ is different for each storm.

From a physical point of view, the value of $m_0(0)$ controls the water balance between rainfall input and streamflow output. The parameter ψ_0 determines the peak flow, the time to peak flow and the shape of the hydrograph. Both parameters a_3 and D_f describe the soil erodibility, which in turn, control sediment yield (bed-material load and wash load). Parameter a_3 is more related to wash load.

In order to simplify the calibration procedure, separate calibrations for water balance, water routing and sediment routing were made. The storm on September 5, 1970 on Watershed 17 was used to calibrate the parameters for water and sediment routing because more information is available for that storm than the others. The steps of calibration are as follows:

1. Estimated $m_0(0)$ by adjusting the estimated volume of rainfall excess to be nearly equal to the total volume of the measured runoff. This adjustment is made by trial and error.

2. With the value of $m_o(0)$ estimated in Step 1, adjust the value of ψ_o to obtain the correct value of the peak flow. Then check if the time to peak flow and the shape of hydrograph are satisfactory in comparison with the measured hydrograph. If not select another value of $m_o(0)$ and repeat Steps 1 and 2 until a satisfactory answer is obtained. The calibration on water balance and water routing is completed at this step.
3. Assume a_3 is zero and adjust the value of D_f to make the computed bed-material load equal to the measured bed-material load.
4. Adjust the value of a_3 to obtain the correct wash load, and check if the bed-material load is still correct. If the bed-material load is not correct, repeat Steps 1, 2 and 3 until a satisfactory answer is found.

As mentioned earlier, parameters ψ_o , a_3 , and D_f are independent of storms. The assumption is made herein that the values of ψ_o , a_3 , and D_f are the same for both Watershed 1 and Watershed 17. Then the only unknown parameter for Watershed 1 is the antecedent moisture content $m_o(0)$ which is different for different storms. The procedure to estimate $m_o(0)$ is simply to adjust its value until a satisfactory water yield is obtained. When the water balance model for simulating the water budget during interstorm periods becomes available, the value of $m_o(0)$ can be estimated with that model.

The estimated values of ψ_o , a_3 and D_f are: $\psi_o = 120$, $a_3 = 0.00001$ and $D_f = 0.1$. The antecedent moisture contents for all storms are given in Table 6.5.

The performance of the model is very much dependent on the results of model calibration. A more systematic and reliable method for estimating model parameters is needed for practical applications of the model.

Table 6.5 Antecedent moisture contents

<u>Storm</u>	<u>Antecedent moisture content, $m_o(0)$</u>
Watershed 17	
September 5, 1970	0.470
Watershed 1	
September 5, 1970	0.445
September 6, 1967	0.443
November 22, 1965	0.427
November 24, 1965	0.490
November 25, 1965	0.488

TEST RESULTS

In the numerical computations, the time increment Δt of 5 min was chosen for the Labor Day storm on Watersheds 1 and 17 and the September 6, 1967 storm on Watershed 1. For the other storms a 30-min time increment was used.

Five space increments for each segment were chosen for all storms. The space increments were between 48 ft and 656.6 ft making the ratio of time increment to space increment in the range of 0.46 to 37.5 sec/ft.

Comparisons of the simulated and measured results

When measured data were available, comparisons of the simulated and the measured results were made. The available measured data were water hydrographs and water yields from all storms. The wash load data were available only for the Labor Day storm on Watershed 17 and the September 6, 1967 storm on Watershed 1. Bed-material load data were available for the Labor Day storm on both watersheds. No measured sediment hydrographs were available for comparison.

The comparisons of the simulated and the measured water hydrographs for all storms used in the analysis are given in Figs. 6.3, 6.4, 6.5, 6.6, 6.7 and 6.8. The agreement between the measured water hydrographs and the simulated water hydrographs is, in the most part, satisfactory. Other comparisons on water yield, peak water flow, time to peak water flow, and sediment yield are given respectively in Figs. 6.9, 6.10, 6.11 and 6.12.

In order to assess the agreement between measured and simulated results the following errors were computed:

1. The percentage error in the total volume of surface runoff, designated E_v .
2. The relative mean absolute error in water hydrograph, designated E_a .
3. The percentage error in the magnitude of the peak water flow, designated E_p .
4. The percentage error in the time to peak water discharge, designated E_t .
5. The percentage error in the total bed-material load, designated E_b .
6. The percentage error in the total wash load, designated E_w .

In equation form the errors are respectively

$$E_v = 100 \left\{ 1 - \frac{\sum_{t=1}^N Q(t) \Delta t}{\sum_{t=1}^N Q_m(t) \Delta t} \right\} \quad (6.7)$$

$$E_a = \frac{100}{N} \sum_{t=1}^N \frac{|Q(t) - Q_m(t)|}{Q_{mp}} \quad (6.8)$$

$$E_p = 100 \left(1 - \frac{Q_{op}}{Q_{mp}} \right) \quad (6.9)$$

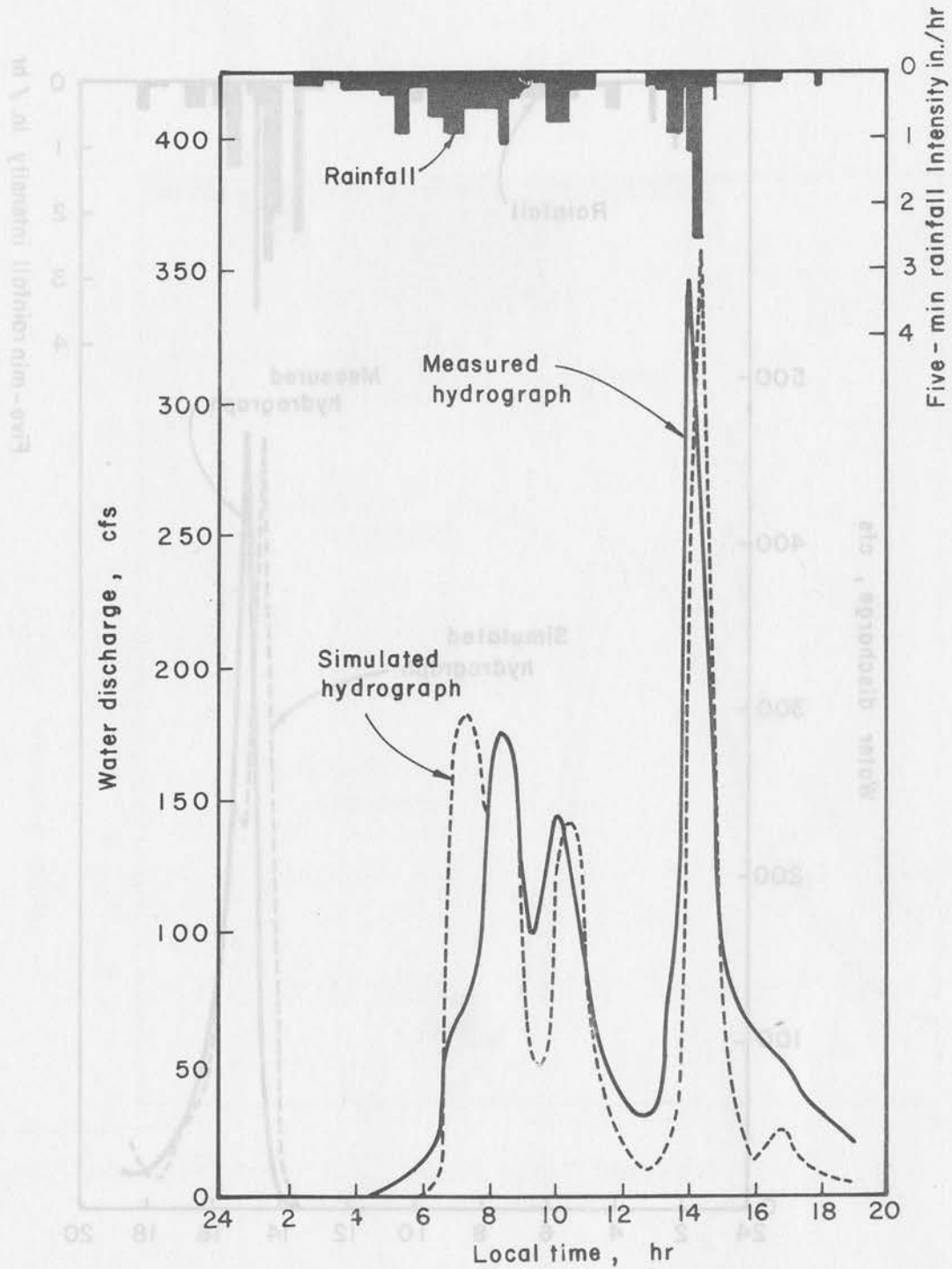


Fig. 6.3 Water hydrograph from Watershed 17 for the September 5, 1970 storm

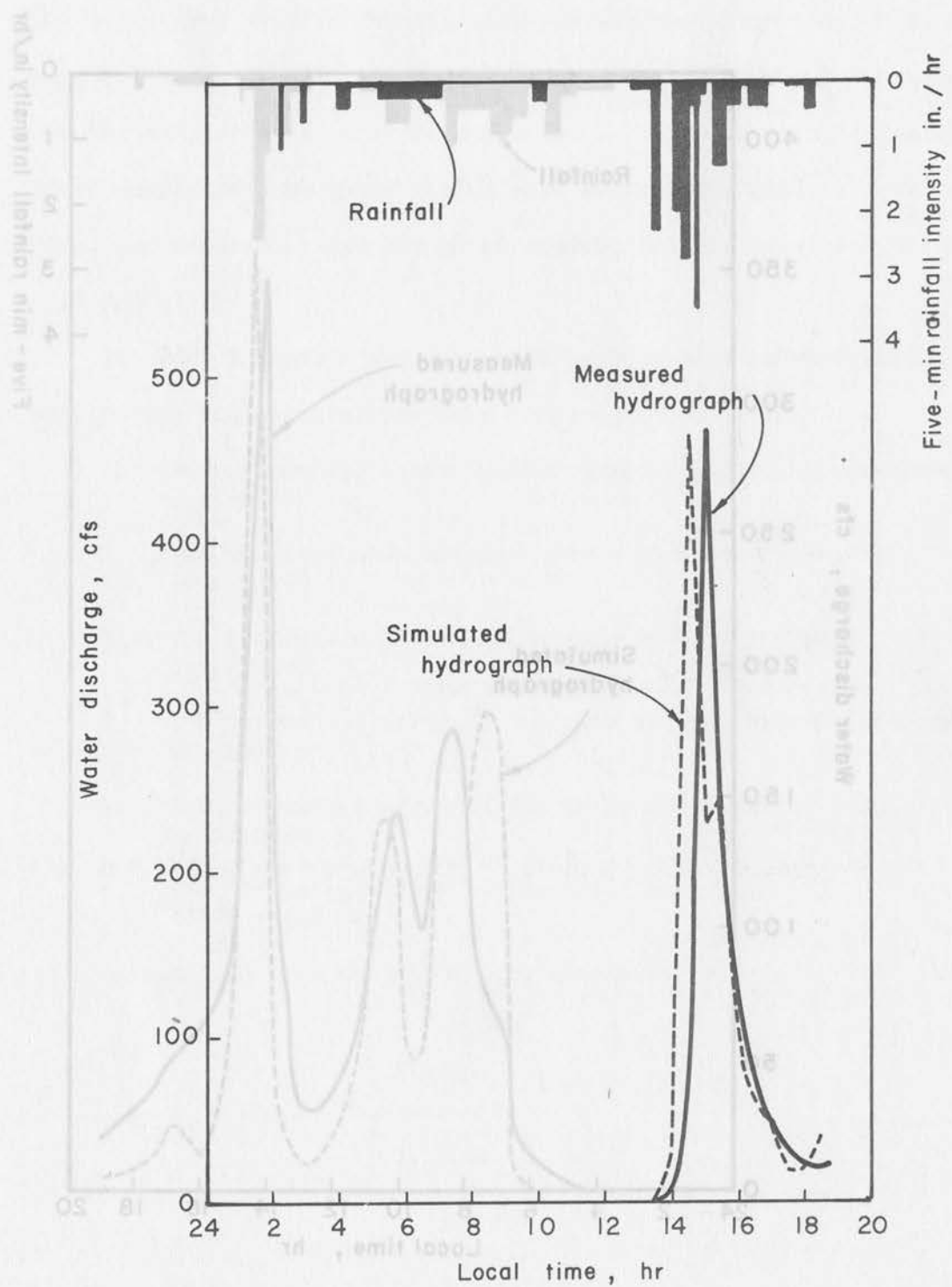


Fig. 6.4 Water hydrograph from Watershed 1 for the September 5, 1970 storm

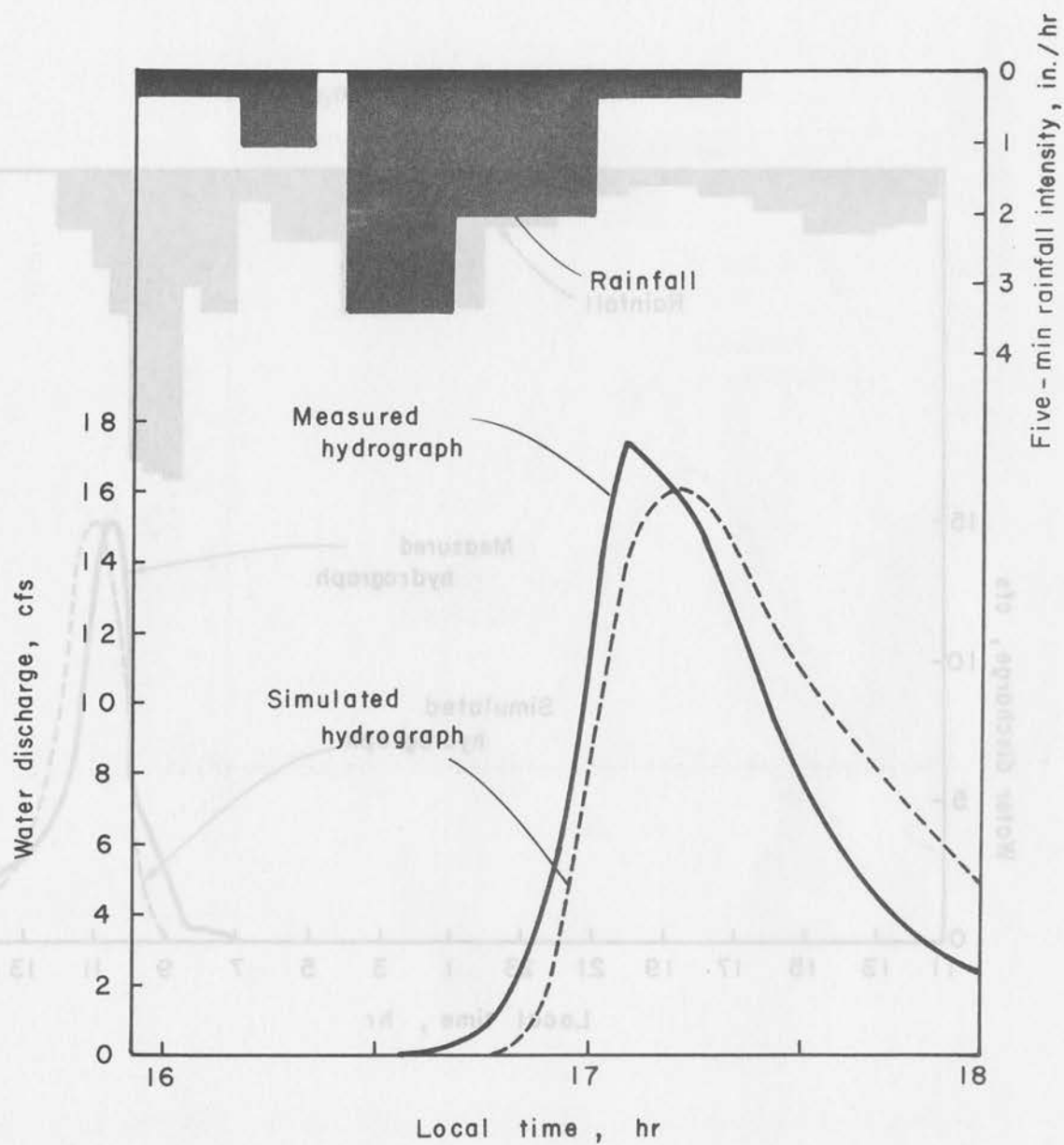


Fig. 6.5 Water hydrograph from Watershed 1 for the September 6, 1967 storm

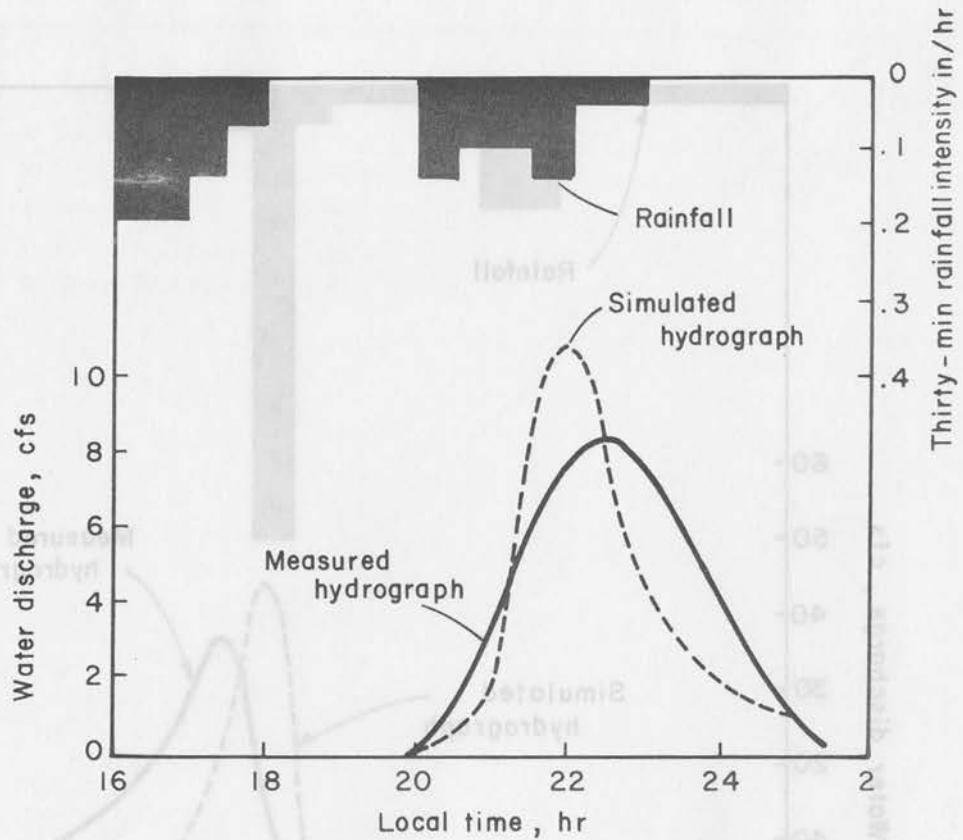


Fig. 6.7 Water hydrograph from Watershed 1 for the November 24, 1965 storm

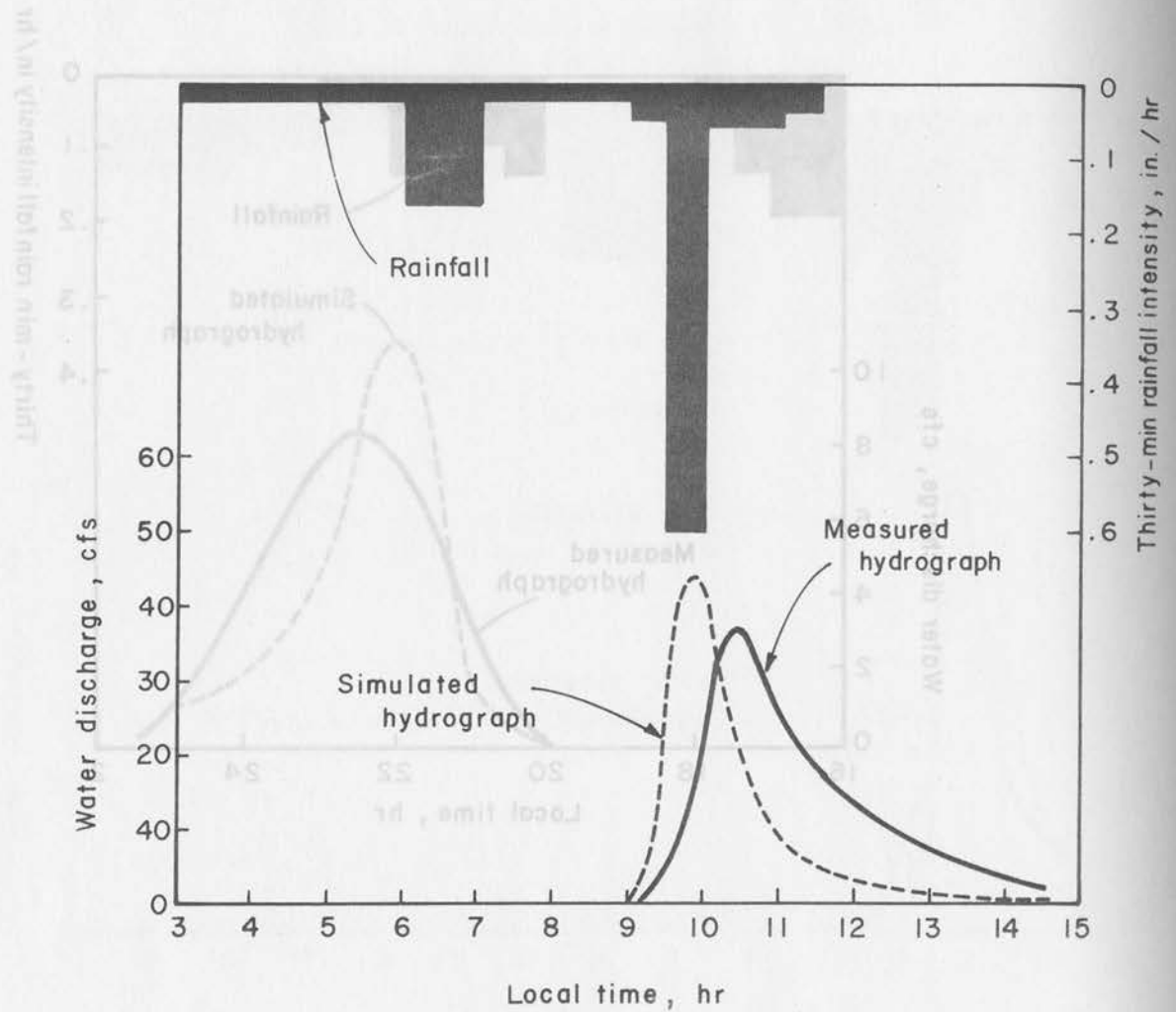


Fig. 6.8 Water hydrograph from Watershed 1 for the November 25, 1965 storm

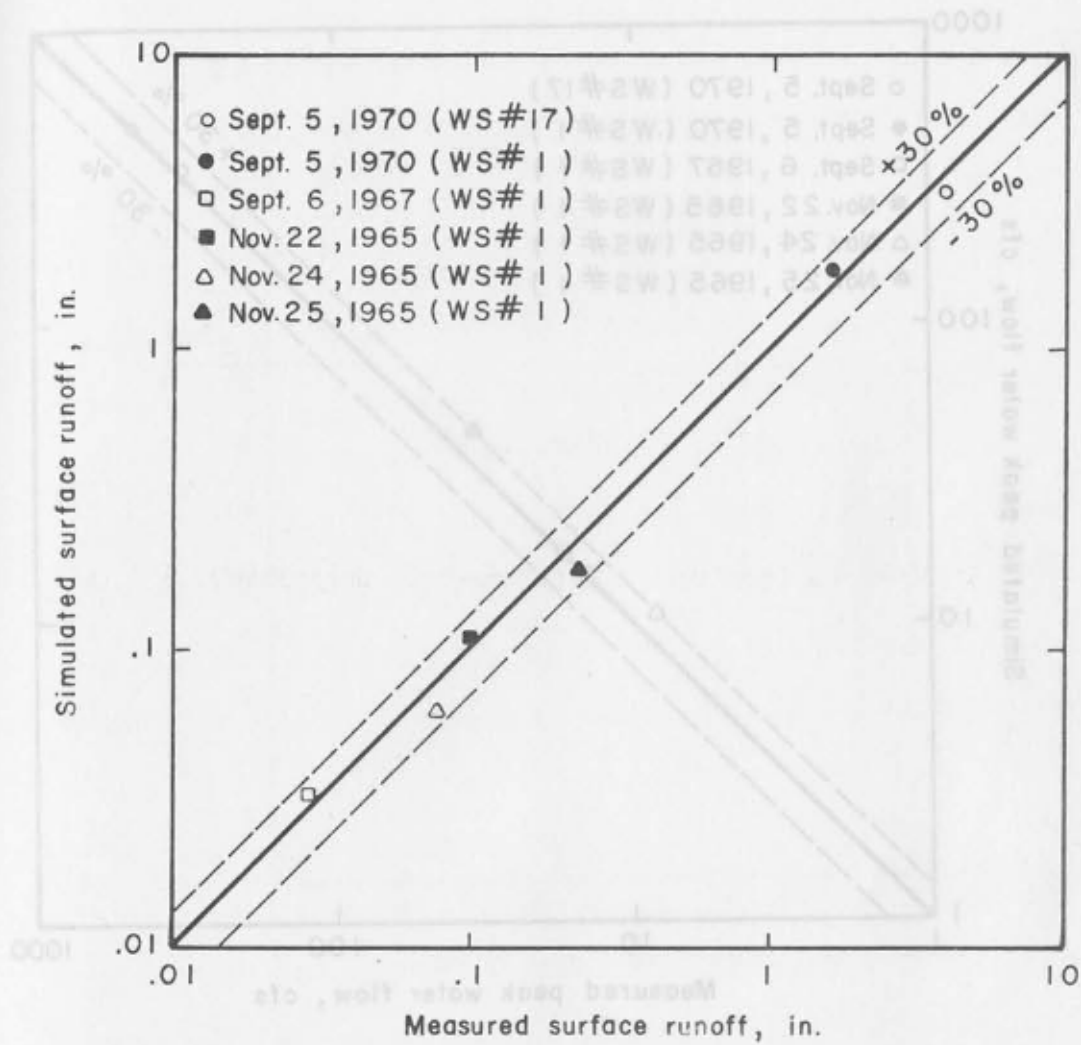


Fig. 6.9 Comparison of measured and simulated water yield

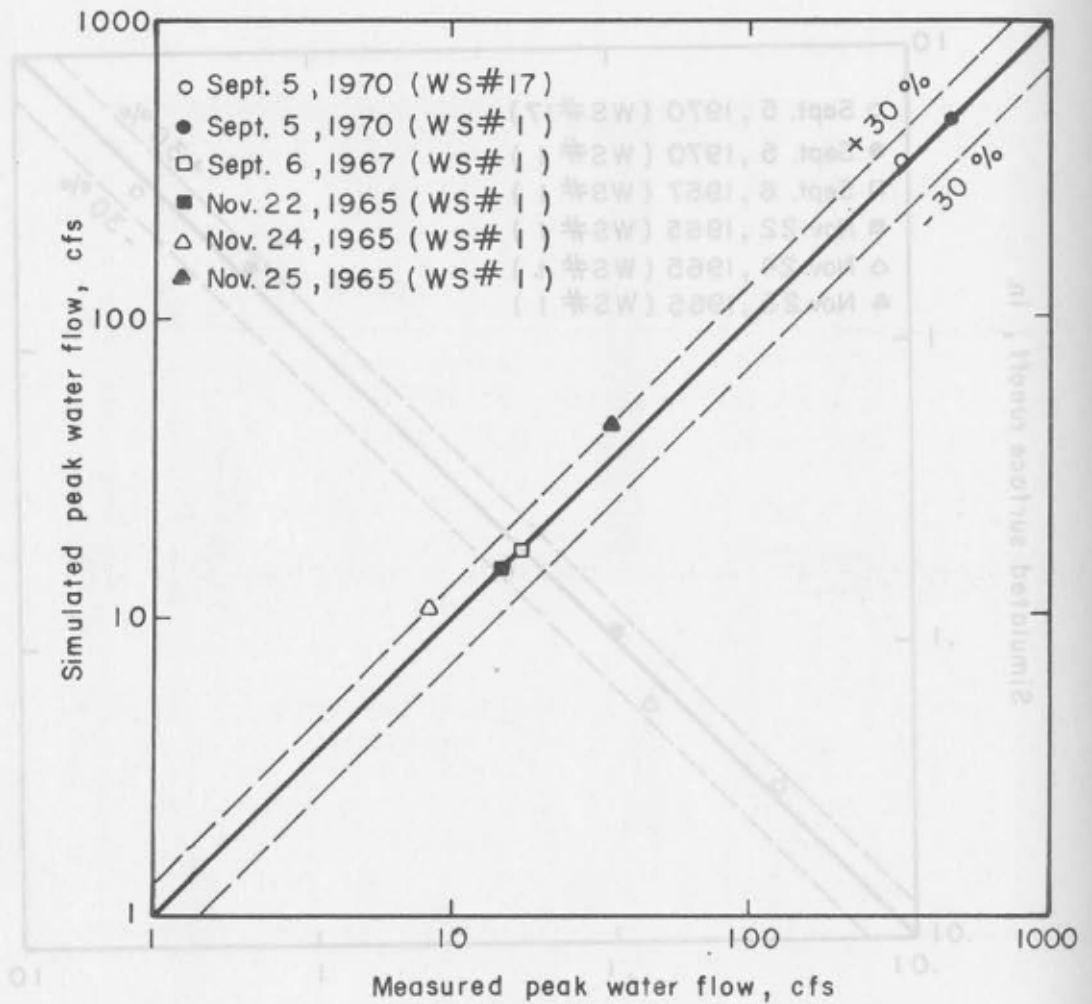


Fig. 6.10 Comparison of measured and simulated peak water flows

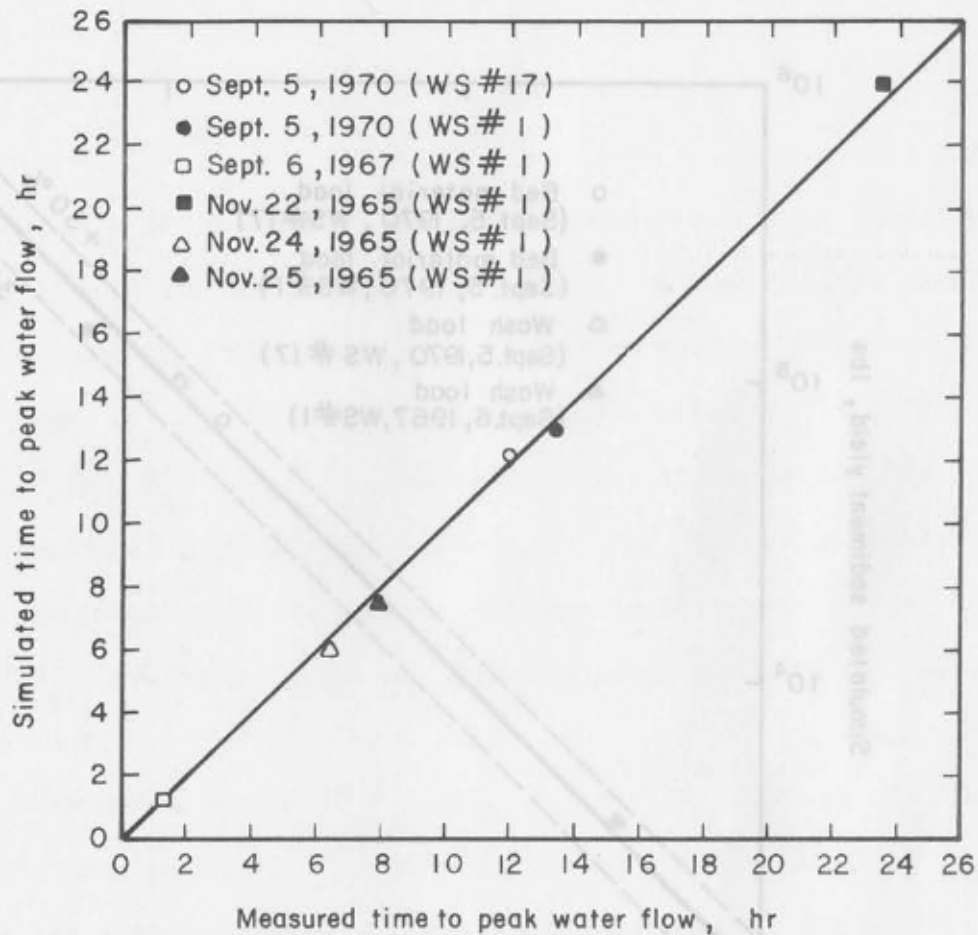


Fig. 6.11 Comparison of measured and simulated time to peak water flow

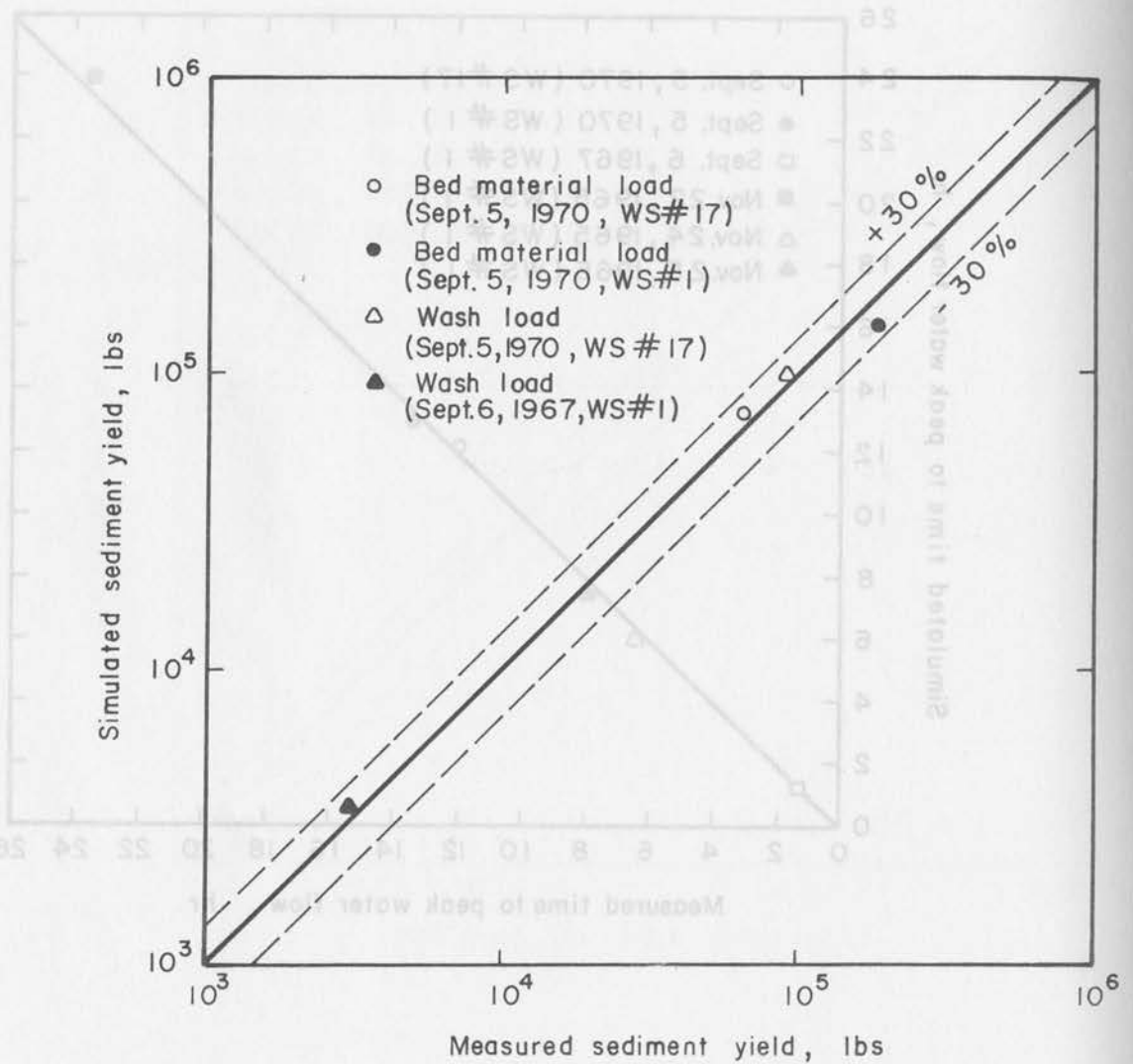


Fig. 6.12 Comparison of measured and simulated sediment yields

$$E_t = 100 \left(1 - \frac{t_{op}}{t_{mp}} \right) \quad (6.10)$$

$$E_b = 100 \left\{ 1 - \frac{\sum_{t=1}^N G_b(t) \Delta t}{G_{mb}} \right\} \quad (6.11)$$

and

$$E_w = 100 \left\{ 1 - \frac{\sum_{t=1}^N G_w(t) \Delta t}{G_{mw}} \right\} \quad (6.12)$$

in which N is the number of time increments extending from the beginning to the end of the runoff event, $Q(t)$ and $Q_m(t)$ are respectively the simulated and the measured surface runoff at time t ,

Q_{op} and Q_{mp} are respectively the simulated and the measured peak water flow, t_{op} and t_{mp} are respectively the simulated and the measured time to peak water flow, $G_b(t)$ and $G_w(t)$ are respectively the simulated bed-material load and wash load at time t , and G_{mb} and G_{mw} are respectively the measured total bed-material and total wash load.

The values of E_v , E_a , E_p , E_t , E_b and E_w for the six runoff events used in this study are given in Table 6.6. These errors indicate that the water and sediment routing model simulated the shape, volume, peak flow, and time to peak flow of the six water hydrographs, and the sediment yield from Watershed 1 and Watershed 17 within approximately 30 percent.

Discussion of test results

The applicability of the Colorado State University water and sediment routing model is demonstrated by comparing simulated and measured water and sediment yields from Watersheds 1 and 17.

Table 6.6 Errors in Simulation

Storm	Measured surface runoff, in.	Percent error					
		E_v	E_a	E_p	E_t	E_b	E_w
<u>Watershed 17</u>							
Sept 5, 1970	3.98	-14.6	+8.0	+11.4	+2.1	+14.7	+6.0
<u>Watershed 1</u>							
Sept 5, 1970	1.64	+12.9	+4.1	-0.2	-3.1	-22.0	-
Sept 6, 1967	0.03	+7.2	+9.4	-7.7	+6.7	-	+10.7
Nov 22, 1965	0.11	+1.3	+3.7	-0.4	+2.1	-	-
Nov 24, 1965	0.08	-23.7	+15.2	+31.0	-7.7	-	-
Nov 25, 1965	0.24	-23.2	+14.7	+23.6	-6.3	-	-

Note: The blanks denoted by "-" indicate no measured data were available

Satisfactory results were obtained for different size storms in a watershed by using only one set of model parameters. This verifies that the model can be used to synthesize missing data and to predict the response of watersheds to various types of watershed management practices. Also, it has been demonstrated that the model could be used to estimate flood flows from ungaged watersheds.

The transferability of the model is one of the main advantages of this physical process simulation model over the conventional models such as the Unit Hydrograph and Universal Soil loss equation. For example, the Labor Day (September 5, 1970) storm produced approximately 2.2 times the surface runoff in Watershed 17 than in Watershed 1, but only about 0.4 times the yield of sediment. There was more surface runoff and less sediment yield in Watershed 17 because it is longer and narrower and its average slope is less than in Watershed 1.

The following examples are presented to further demonstrate the applicability of the water and sediment routing.

An example of the computed infiltration rate during a storm is given in Fig. 6.13. The computed infiltration rate decreases as time increases, a trend similar to most field measurements.

Figure 6.14 shows degradation and aggradation in a channel system. The amounts of degradation and aggradation in this mountainous channel are very small and their effects on channel slope can be neglected without consequence.

The computed sediment hydrographs for the large Labor Day storm (September 5, 1970) and for a small storm (November 22, 1965) on Watershed 1 are given in Figs. 6.15 and 6.16 respectively. The shapes of sediment and water hydrographs are similar for the large storm but different for the small storm. For the small storm tested, the peak of the sediment hydrograph occurs earlier than that of the water hydrograph because the sediment supply rate is greater in the early stage of surface runoff. This effect is not significant for a larger storm.

A test on the effect of a sequence of storms on sediment yield in Watershed 1 was made and the results are shown in Fig. 6.17. The five storms used have the same size as the storm of September 6, 1967, but the initial loose soil storages are different. In the sequence, the initial loose soil storages are those left from the previous storm. Figure 6.17 shows that the bed-material load increases and the wash load decreases with each succeeding storm. This is because the availability of bed-material load increases and the availability of wash load decreases with each succeeding storm.

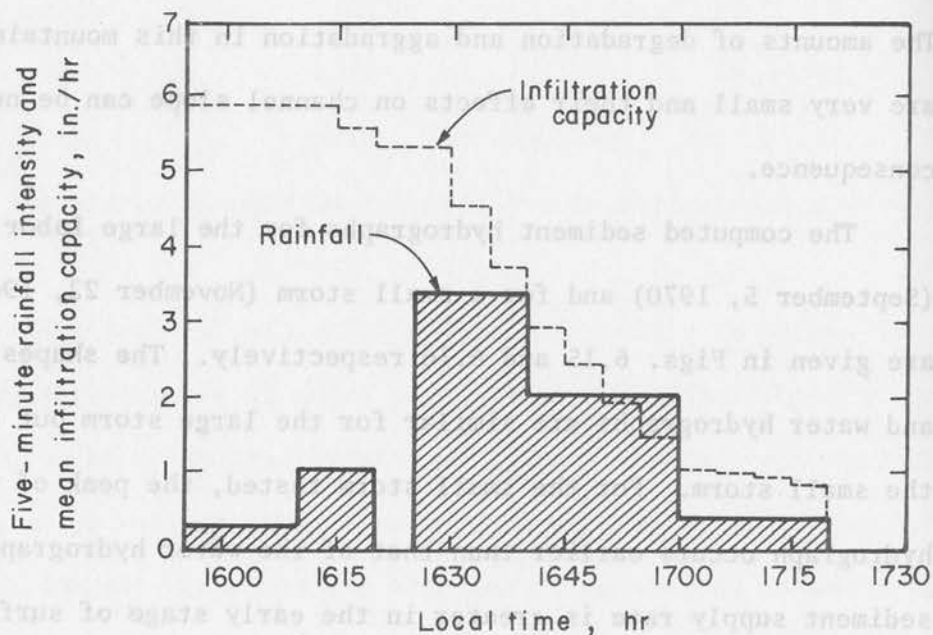


Fig. 6.13 Computed infiltration capacity in Watershed 1 during the September 6, 1967 storm

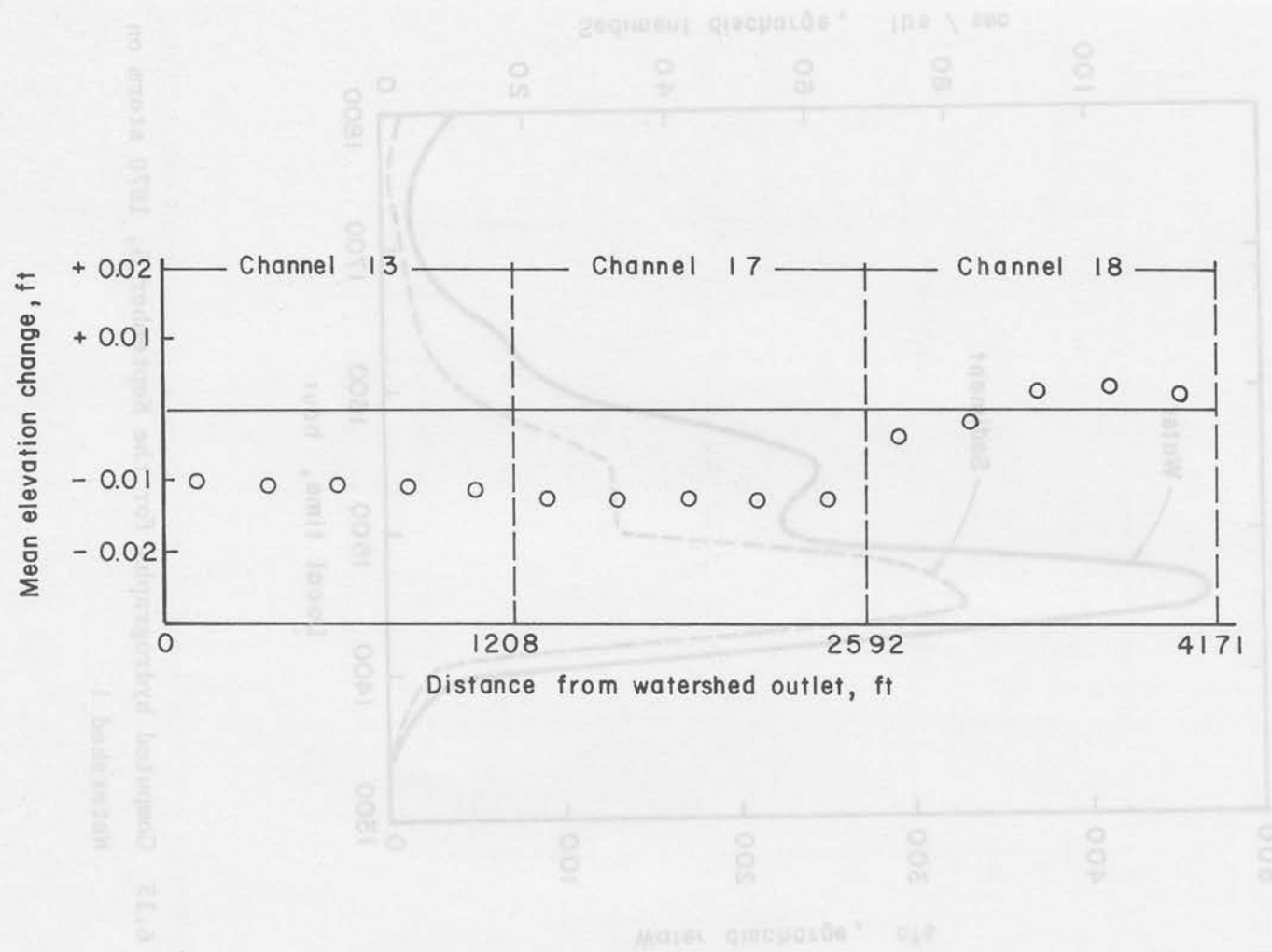


Fig. 6.14 Aggradation and degradation of channels in Watershed 1 during the September 5, 1970 storm

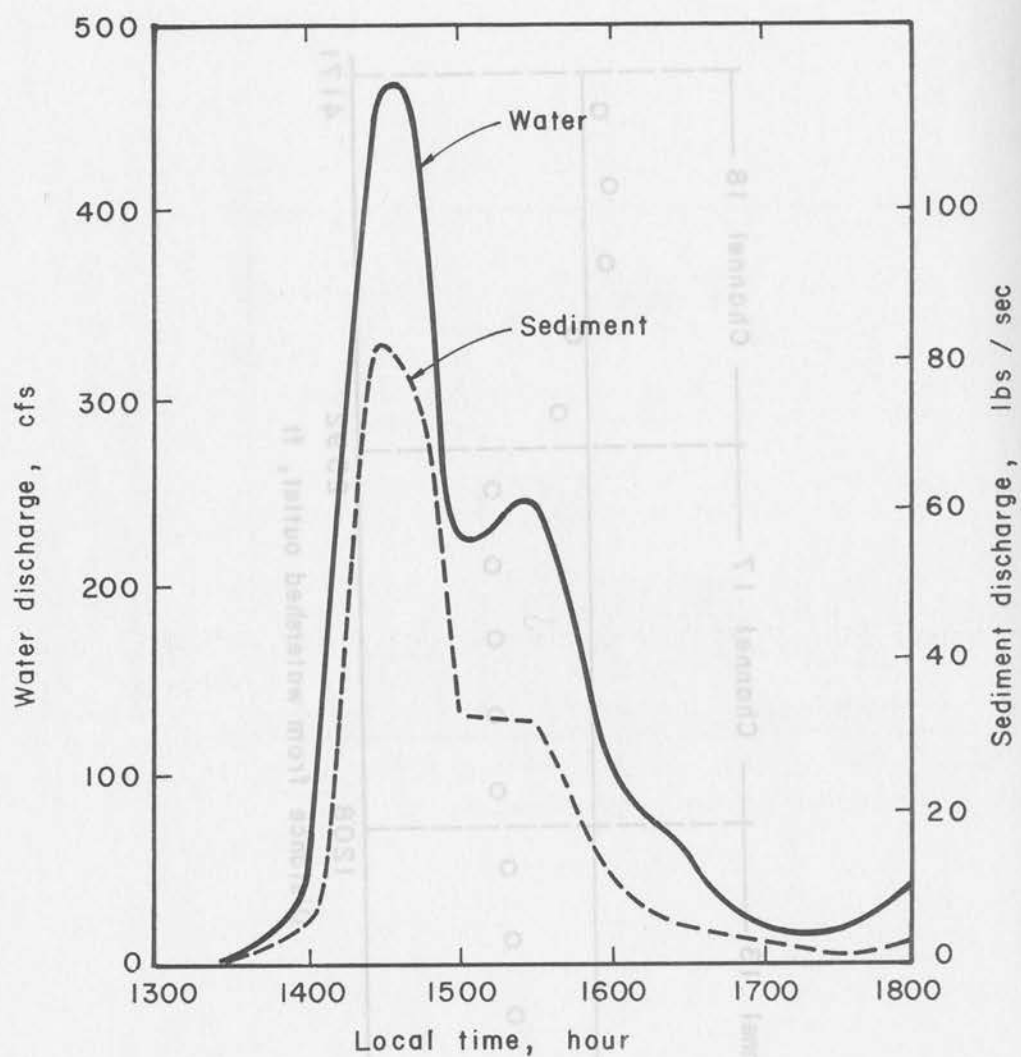


Fig. 6.15 Computed hydrographs for the September 5, 1970 storm on Watershed 1

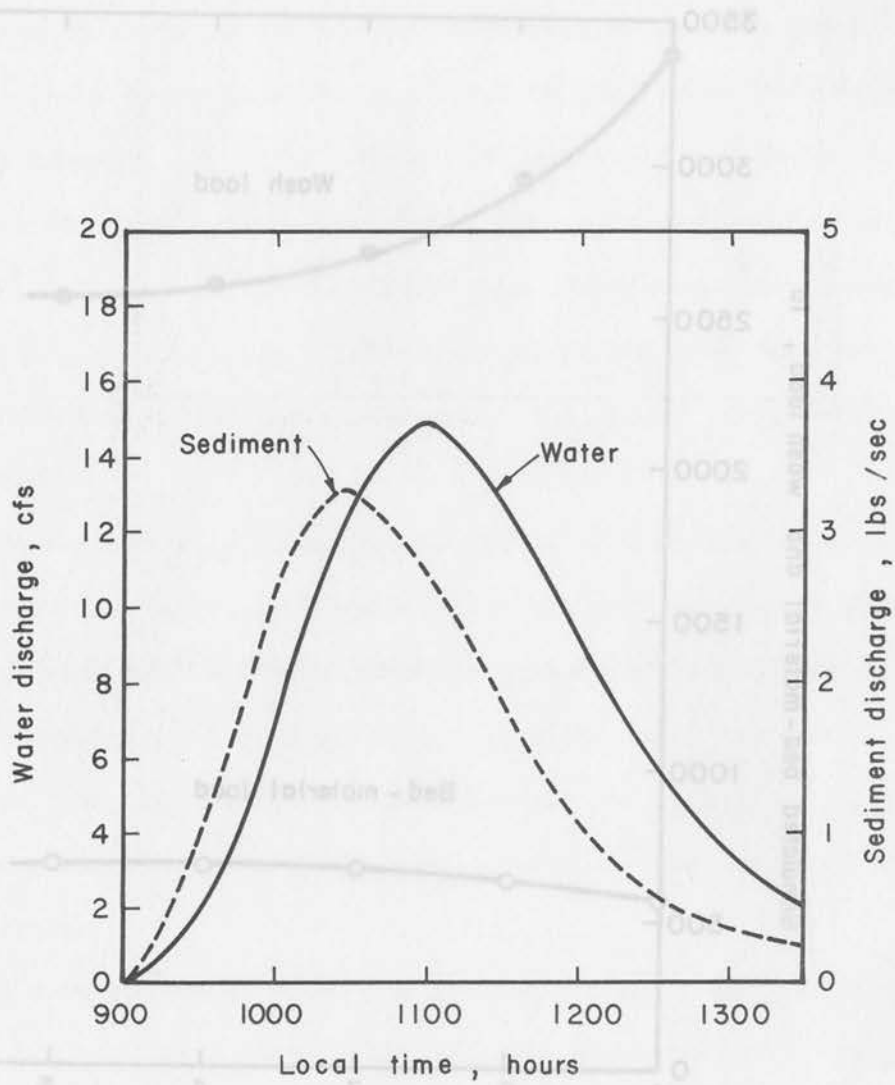


Fig. 6.16 Computed hydrographs for the November 22, 1965 storm on Watershed 1

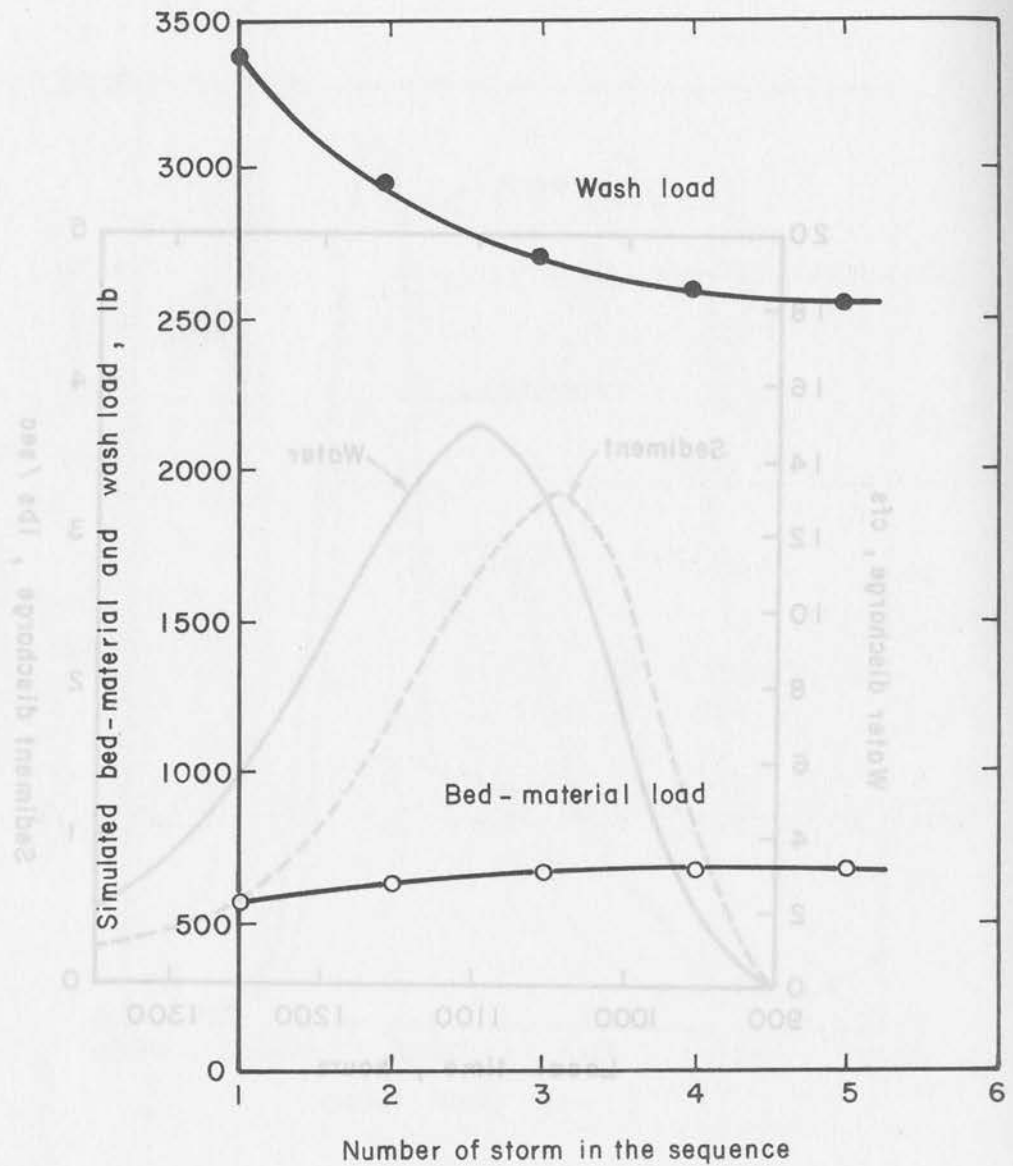


Fig. 6.17 Sediment yields from a sequence of storms over Watershed 1

Applications to predict watershed treatment effects

The vegetation treatment effects on water and sediment yields are estimated by changing the canopy cover density and the ground cover density in overland flow units. Based on the storms of September 5, 1970 and September 6, 1967, the effects of vegetation treatment on the water and sediment yields from Watershed 1 have been evaluated. As shown in Figs. 6.18 and 6.19, for a constant and undisturbed ground cover of 65 percent, water yield, sediment yield and the peak flow rates from these two storms are increased as the canopy cover density is decreased.

The reduction in interception caused by removing the vegetation results in the increase of excess rainfall and loose soil detachment. These effects are much more pronounced in Watershed 1 for the smaller size of storm than for large storms like the Labor Day storm.

The time to peak flow is shortened as the canopy cover is decreased for the small storm but there is no change in time to peak flow for the large storm.

If a watershed is clear cut and the forest litter, tree mulch, rocks, etc. are also removed in different degrees, or if the ground cover is seriously destroyed by a burning treatment, the associated response can be estimated by changing the ground cover density in overland flow units. The changes in water and sediment yields in Watershed 1 for the storms of September 5, 1970 and September 6, 1967 are shown in Figs. 6.20 and 6.21. As the ground cover is decreased, the total surface runoff and peak water flow are increased moderately, the sediment yield and peak sediment flow are increased greatly and the time to peak flow shortened slightly. The effect on water yield is

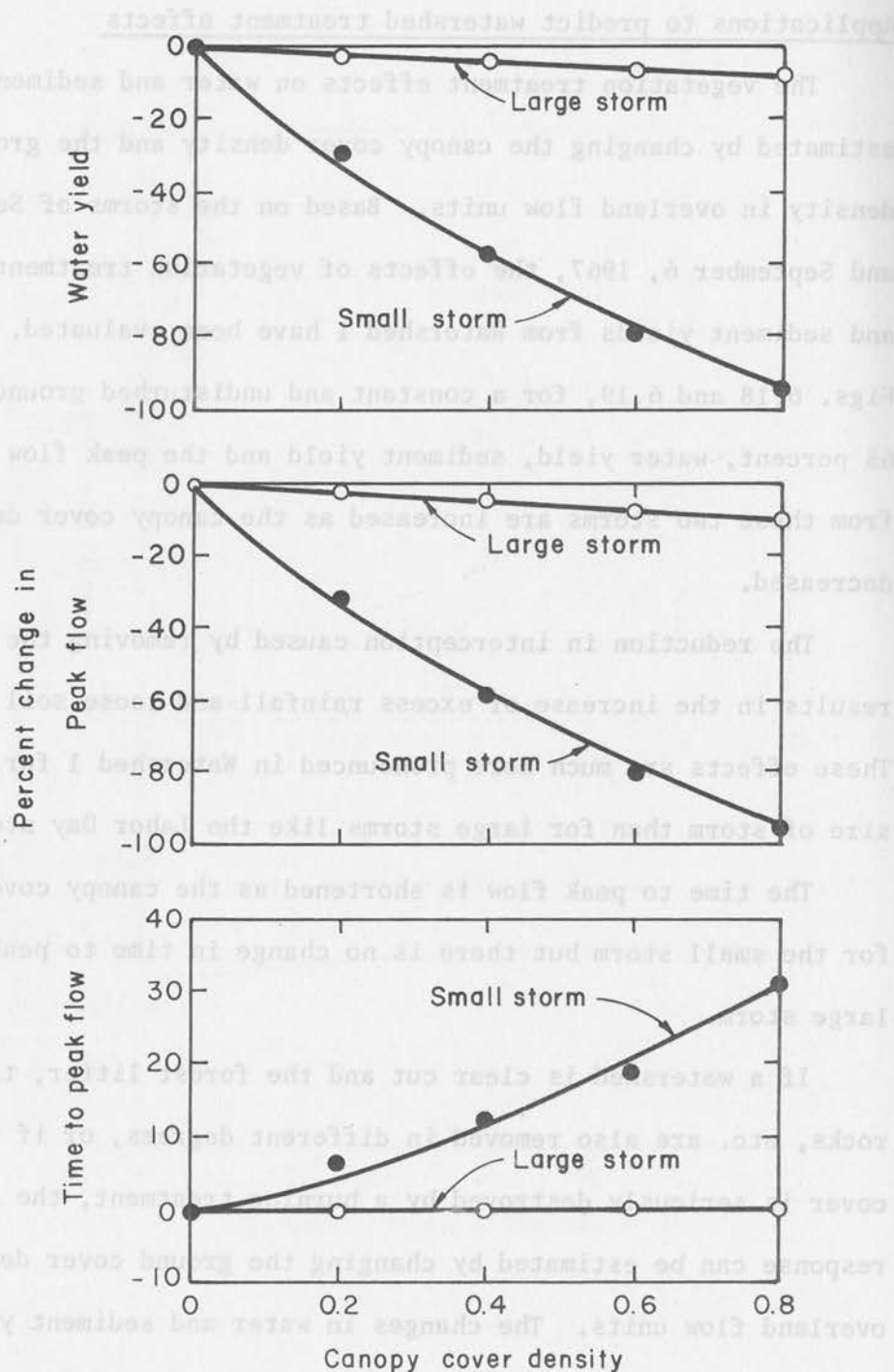


Fig. 6.18 Effect of Canopy Cover Density on the Water Hydrograph from

Watershed 1

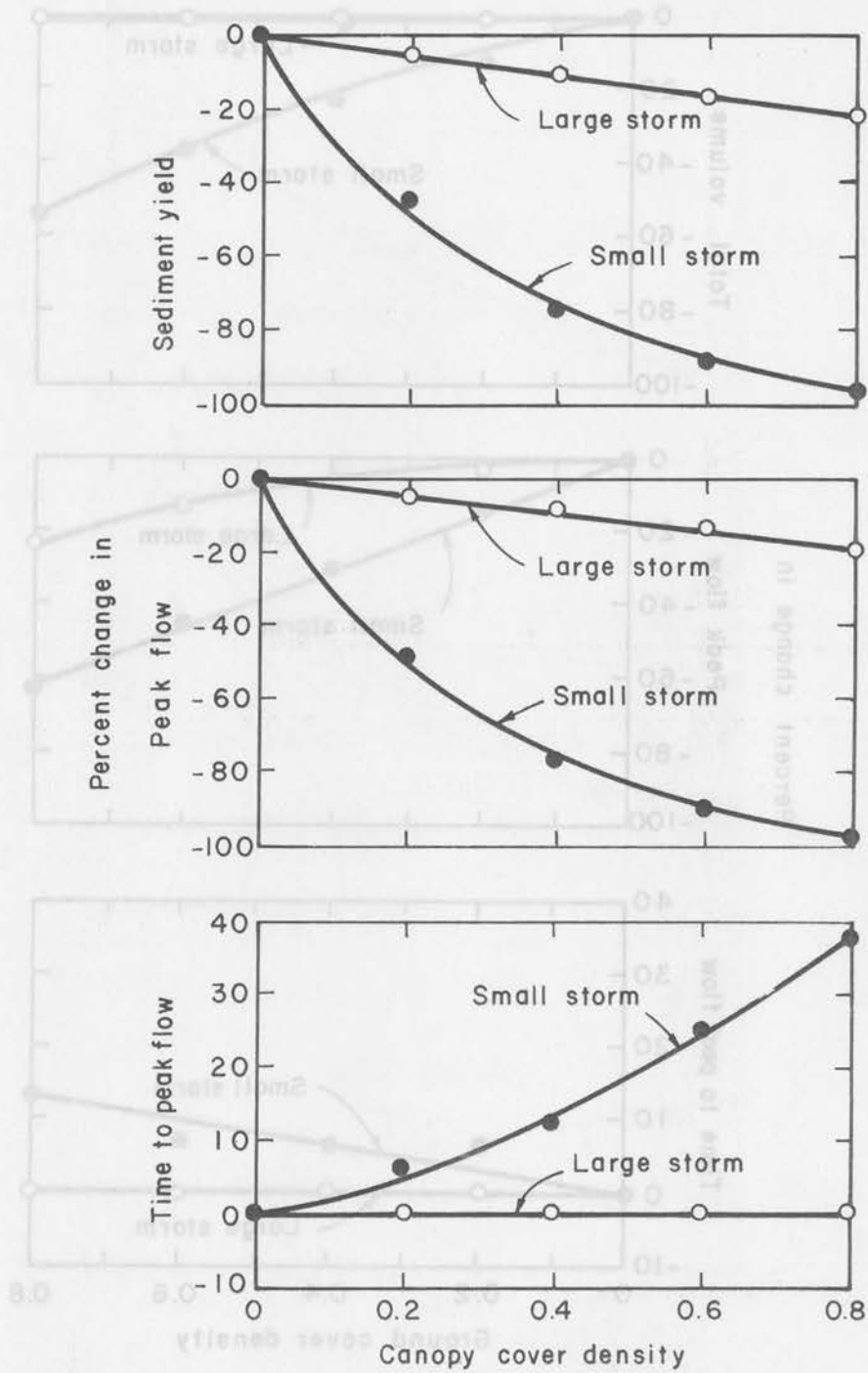


Fig. 6.19 Effect of Canopy Cover Density on the Sediment Hydrograph from Watershed 1

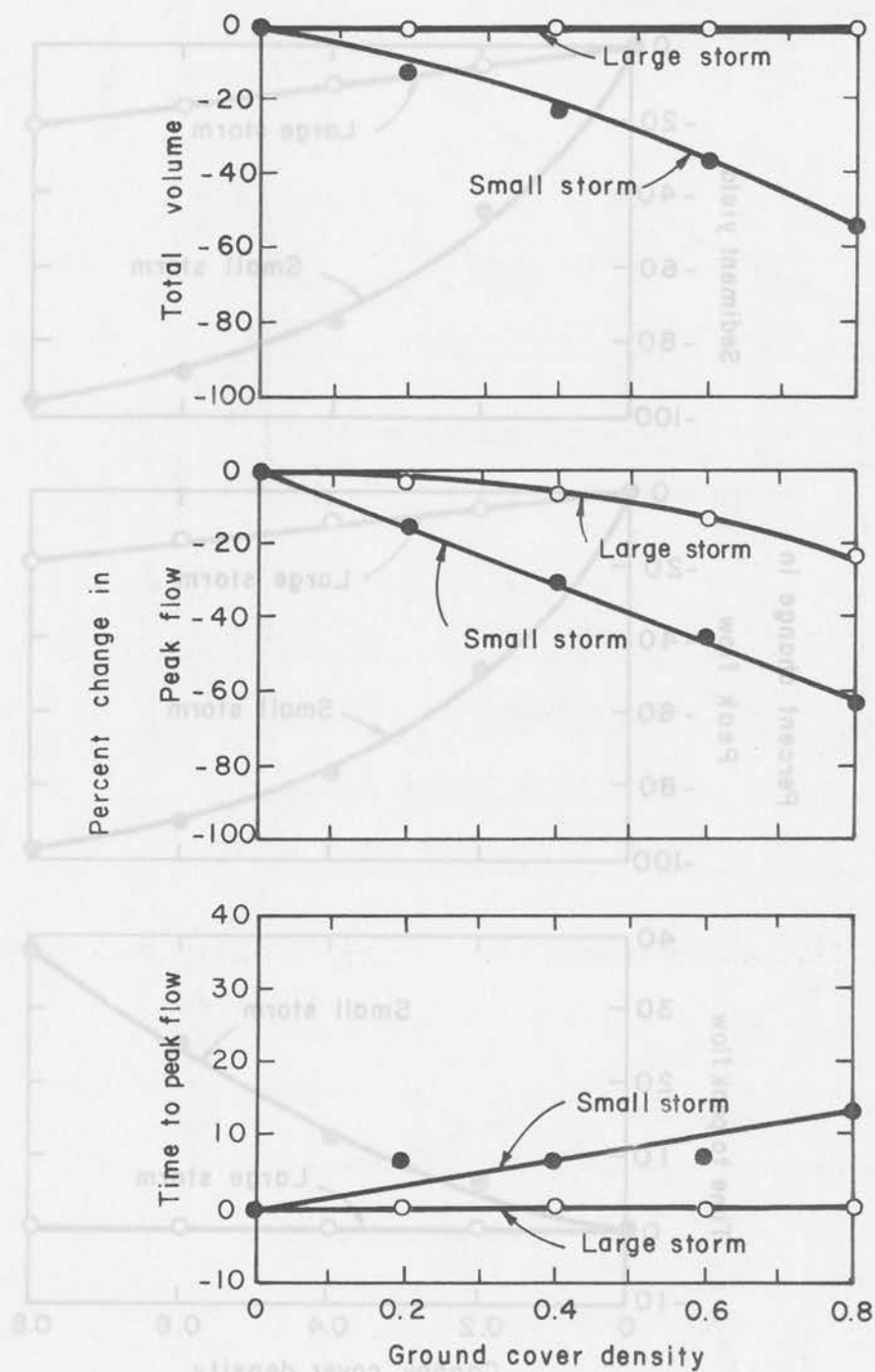


Fig. 6.20 Effect of ground cover density on the water hydrograph from Watershed 1

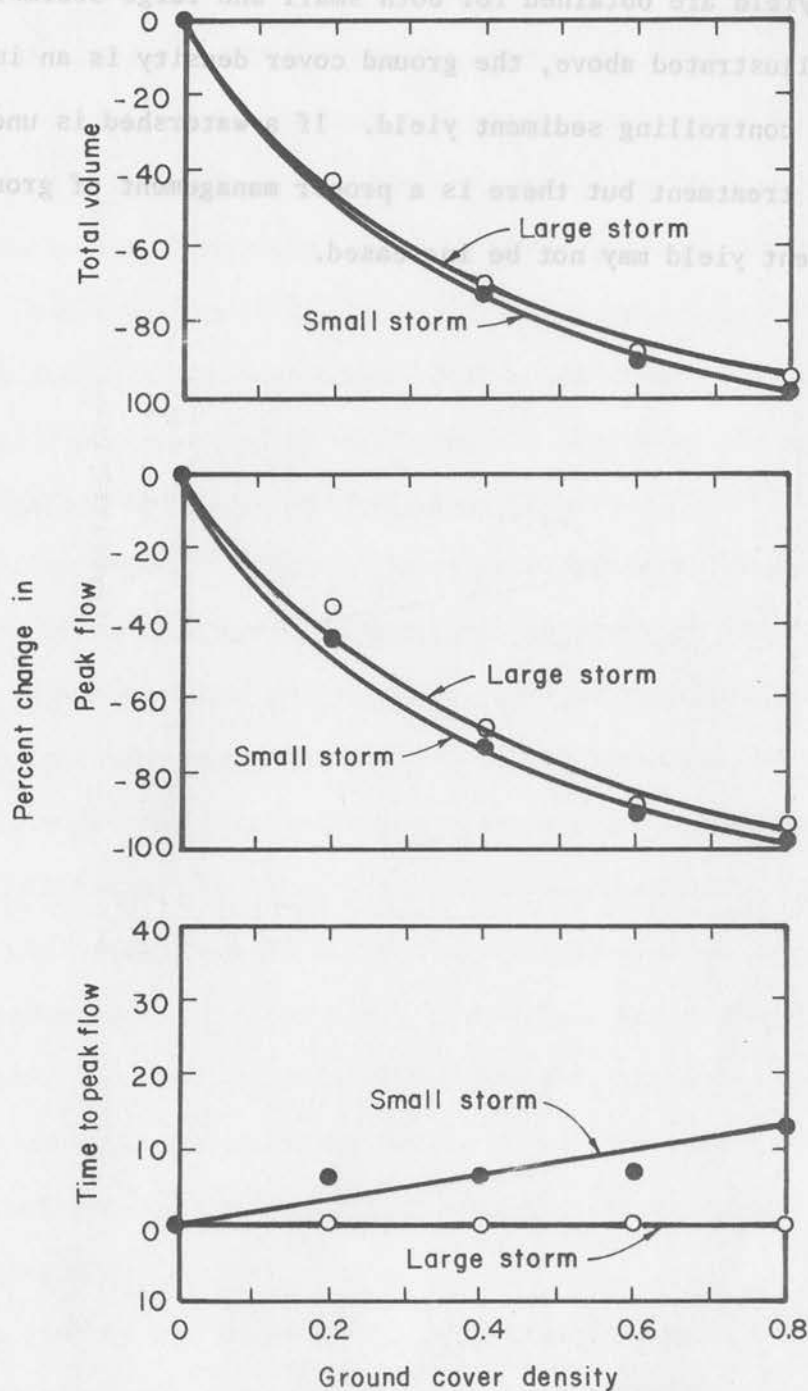


Fig. 6.21 Effect of ground cover density on the sediment yield from Watershed 1

more pronounced for a smaller storm but nearly the same effects on sediment yield are obtained for both small and large storms.

As illustrated above, the ground cover density is an important factor in controlling sediment yield. If a watershed is under the clear cut treatment but there is a proper management of ground cover, the sediment yield may not be increased.

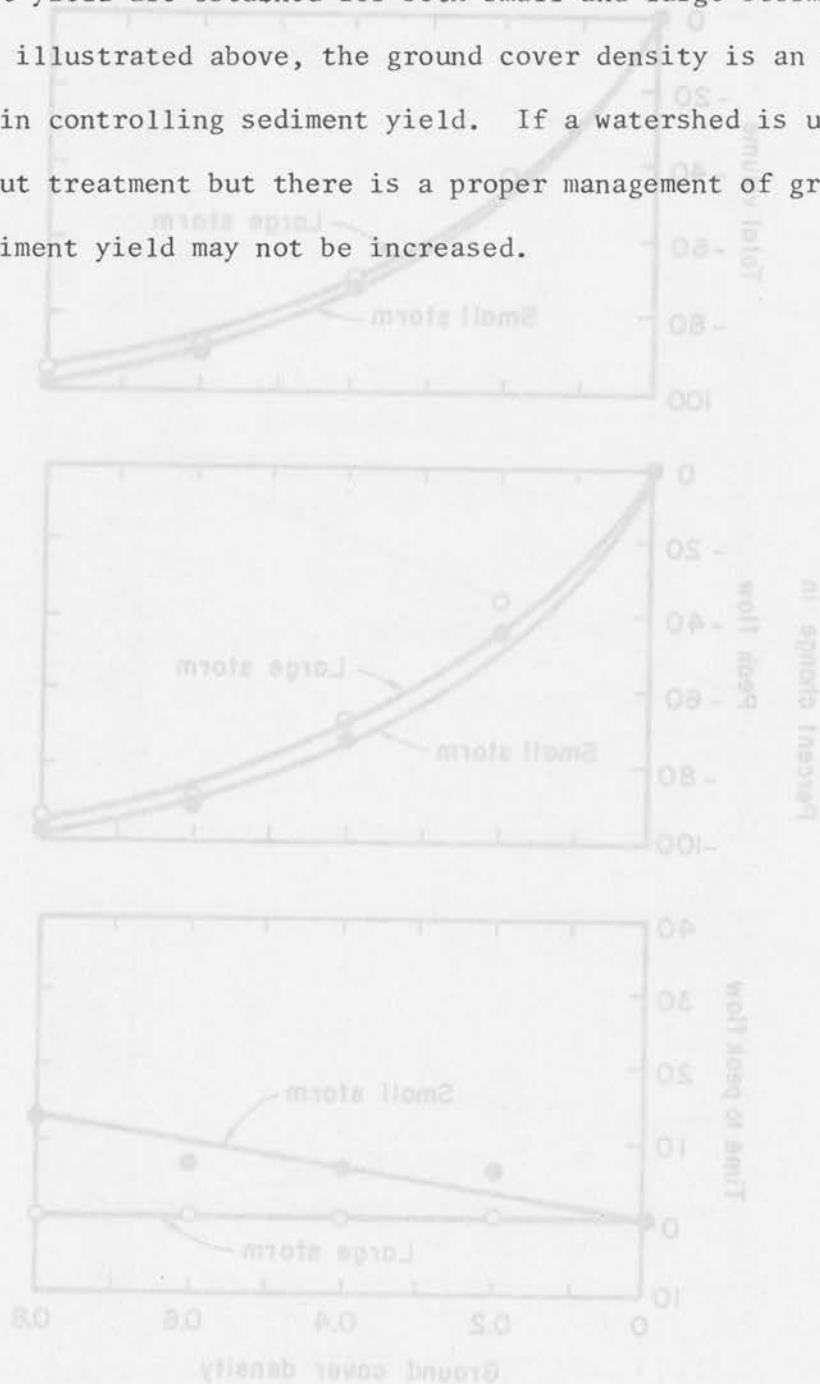


Fig. 6-21 Effect of ground cover density on the sediment yield from Watershed 1

7. SUMMARY

A mathematical model simulating water and sediment hydrographs from small watersheds has been developed. This model is designed to simulate the response of the basin to individual storms. The model includes a water balance on the single storm basis, loose soil detachment by raindrop impact and by moving water, and water and sediment routing features for both overland flow and channel systems. The flow routing is accomplished by employing the nonlinear kinematic-wave approximation developed in this study.

Unlike the conventional approach to parametric modeling of watershed response, this model is based on the physical processes governing the mechanics of water and sediment flow and requires less calibration than any existing water or sediment models known to the writers.

The model has been validated with data from Watershed 1 and Watershed 17 in the Beaver Creek drainage of north-central Arizona. With the model, the shape, peak flow and time to peak flow of water and sediment hydrographs along with the total water yield and sediment yield were simulated. In addition, this model has the capability to predict the effects on water and sediment yields of various land and resource management practices and can be used to estimate the water and sediment yields from ungaged watersheds.

In view of the mathematical approximations made in formulating this water and sediment routing model, the applicability of the model at present is limited to the following situations:

1. The streams within the watershed are ephemeral, and the movement of subsurface flow and ground water flow are negligible.

2. The kinematic-wave approximation for flow routing is valid; i.e., the gradients due to local and convective accelerations are negligible and the water surface slope is nearly equal to the bed slope.
3. The water yield simulation is on the single storm basis.
4. The stream channel geometry is stable; that is, erosion and deposition of channel bank material is negligible.

When a water balance model for simulating the water budget during interstorm periods is incorporated, long-term water and sediment yields can be estimated with this model.

Test results show that there are satisfactory agreements between the simulated and the measured peak water flow; time to peak water flow, water yield and sediment yield for different size storms in two watersheds using only one set of model parameters. This verifies that the model can be used to synthesize missing data and to predict the response of watersheds to various types of watershed management practices. Also, it has been demonstrated that the model could be used to estimate flood flows from ungaged watersheds.

In view of the mathematical approximations made in formulating this water and sediment routing model, the applicability of the model at present is limited to the following situations:

1. The streams within the watershed are ephemeral, and the movement of subsurface flow and ground water flow are negligible.

8. FUTURE WORK

The preparation of this report and the completion of the model testing described herein is considered, by joint agreement, suffice to meet the principal objective of the contract between the Forest and Range Experiment Station and Colorado State University. With these obligations completed we would then consider arranging a new contract to continue with the development and refinement of the water and sediment routing techniques.

PLANNED WORK

As a consequence of the October Meeting (October 2, 1974) at Flagstaff, and as a result of a high level of interest in the water and sediment model, the following plans for future Colorado State University participation in the Beaver Creek Pilot Project were devised.

1. Colorado State University would apply the water and sediment routing model to other watersheds and would further verify the utility of the model. It was suggested that the Rocky Mountain Forest and Range Experiment Station personnel would contact the Agricultural Research Service and obtain water and sediment discharge data from the Walnut Gulch Watershed near Tombstone, Arizona. If these data are adequate, it would be worthwhile to apply the water and sediment routing model on the Walnut Gulch Watershed to further demonstrate the utility of the method.
2. Colorado State University would help in defining the required instrumentation needed in the Thomas Creek and Woods Canyon Watersheds so as to have adequate data to check the acceptability of the Colorado State University water and sediment routing model.
3. In a joint effort, the Rocky Mountain Forest and Range Experiment Station and Colorado State University would incorporate the general water balance model developed by J. Rogers with the CSU water and sediment routing model.

4. For convenience in application, Colorado State University would document all of the water and sediment routing components of the model.
5. The infiltration component was not included in the current project. The infiltration model presented in this report is crude and preliminary, a refined infiltration model along with the subsurface routing component would be developed by Colorado State University (which will be developed under agreement 16-518-CA of Eisenhower Consortium for Western Environmental Forestry Research).
6. The procedure to segment a watershed into overland flow units and channel units is the key to watershed modeling. Colorado State University would develop and document a computer program for segmentation of a watershed.
7. The model performance is very much dependent on the model parameters. Colorado State University would develop and document a reliable and systematic procedure for model calibration.

OTHER CONSIDERATIONS

In addition to the planned work, some other future studies are recommended:

1. In order to make the present model more suitable for management operations, some simplifications may be required. Possibly, we could transfer the information obtained from the physical simulation model into a simple transfer-function type model such as the instantaneous unit hydrograph for water routing. Some other application strategy may be required to regionalize the model parameters.
2. The extension of the water and sediment routing technique to accommodate routing of dissolved solids and contaminated bed materials.
3. In order to assess the quality of an ecosystem, the integration of techniques for water, sediment, and other pollutant routings is necessary to predict the instream flow regime and to estimate the impact on aquatic and riparian systems by various land management activities.
4. The study of the effect of ground freezing and thawing on the detachment and transport of sediment may be necessary to accommodate snow-melting events.

5. A study to develop model components that would extend the technique to accommodate unstable channels by predicting channel bank erosion and deposition.
6. The long-term response of a watershed to various management practices is dependent not only on the practices but also on the type and sequence of storm events. For example, the increase in water yield from Watershed 1 is much greater for small storms than for large storms. Consequently, we must speak of averages and probabilities when discussing the long-term response of a watershed to any one treatment. The development and addition of a stochastic component to the present model would greatly enhance the usefulness of the model.

Hewlett, J. B. and W. L. Hunter, 1958, "An Outline of Forest Hydrology," University of Georgia Press, Athens, Georgia.

Horton, R. E., 1919, "Rainfall Interception," Mon. Weather Rev. 47, 603-23.

Li, R. M., 1974, "Mathematical Modeling of Response from Small Watershed," Ph.D. Dissertation, Department of Civil Engineering, Colorado State University, Fort Collins, Colorado, 212 p.

Li, R. M. and H. W. Shen, 1973, "Effect of Tail Vegetation on Flow and Sediment," Journal of the Hydraulics Division, ASCE, Vol. 99, No. HY 5, pp. 703-814, May.

Linsley, R. K., Jr., M. A. Kohler and J. L. H. Paulhus, 1958, "Hydrology for Engineers," McGraw-Hill, New York.

Pennman, H. L., 1965, "Discussion of 'Mathematical Theory of Interception' by R. E. Isenhardt," International Symposium on Forest Hydrology, edited by W. E. Sopper and H. W. Lull, p. 136, September.

Shen, H. W. and R. M. Li, 1973, "Rainfall Effect on Sheet Flow Over Smooth Surface," Journal of Hydraulics Division, ASCE, Vol. 99, No. HY 5, pp. 771-783, May.

Simons, D. B. and E. V. Richardson, 1966, "Resistance to Flow in Alluvial Channels," ASCE, professional paper 452-4.

USBR, 1960, "Investigation of Meyer-Peter, Miller Bedload Formulas," Sedimentation Section, Hydrology Branch, Division of Project Investigations, U.S. Department of the Interior, Bureau of Reclamation, June.

Williams, J. A. and Anderson, T. C., 1967, "Soil Survey of Beaver Creek Area, Arizona," U.S. Department of Agriculture, Forest Service and Soil Conservation Service in cooperation with Arizona Agricultural Experiment Station, April.

REFERENCES

- Chow, V. T., 1959, "Open Channel Hydraulics," McGraw-Hill Book Co., New York.
- Daily, J. W. and D. R. F. Harleman, 1966, "Fluid Dynamics," Addison-Wesley, Massachusetts.
- Einstein, H. A., 1950, "The Bed Load Function for Sediment Transportation in Open Channel Flows," USDA, Tech. Bulletin, No. 1026.
- Henderson, F. M., 1966, "Open Channel Flow," Macmillan, New York.
- Hewlett, J. D. and W. L. Nutter, 1969, "An Outline of Forest Hydrology," University of Georgia Press, Athens, Georgia.
- Horton, R. E., 1919, "Rainfall Interception," Mon. Weather Rev. 47, 603-23.
- Li, R. M., 1974, "Mathematical Modeling of Response from Small Watershed," Ph.D. Dissertation, Department of Civil Engineering, Colorado State University, Fort Collins, Colorado, 212 p.
- Li, R. M. and H. W. Shen, 1973, "Effect of Tall Vegetation on Flow and Sediment," Journal of the Hydraulics Division, ASCE, Vol. 99, No. HY 5, pp. 793-814, May.
- Linsley, R. K., Jr., M. A. Kohler and J. L. H. Paulhus, 1958, "Hydrology for Engineers," McGraw-Hill, New York.
- Penman, H. L., 1965, "Discussion of 'Mathematical Theory of Interception' by R. E. Leonard," International Symposium on Forest Hydrology, edited by W. E. Sopper and H. W. Lull, p. 136, September.
- Shen, H. W. and R. M. Li, 1973, "Rainfall Effect on Sheet Flow Over Smooth Surface," Journal of Hydraulics Division, ASCE, Vol. 99, No. HY 5, pp. 771-792, May.
- Simons, D. B. and E. V. Richardson, 1966, "Resistance to Flow in Alluvial Channels," USGS, professional paper 422-J.
- USBR, 1960, "Investigation of Meyer-Peter, Muller Bedload Formulas," Sedimentation Section, Hydrology Branch, Division of Project Investigations, U.S. Department of the Interior, Bureau of Reclamation, June.
- Williams, J. A. and Anderson, T. C., 1967, "Soil Survey of Beaver Creek Area, Arizona," U.S. Department of Agriculture, Forest Service and Soil Conservation Service in cooperation with Arizona Agricultural Experiment Station, April.

- Zahner, R., 1965, "Refinement in Empirical Functions for Realistic Soil-Moisture Regimes Under Forest Cover," International Symposium on Forest Hydrology, edited by W. E. Sopper and H. W. Lull, pp. 261-274, September.
- Zinke, P. J., 1965, "Forest Interception Studies in the United States," International Symposium on Forest Hydrology, edited by W. E. Sopper and H. W. Lull, pp. 137-161, September.

APPENDIX

COMPUTER PROGRAM LISTING

Salmon, R., 1962, "Refinement in Empirical Functions for Realistic Soil-Moisture Regimes Under Forest Cover," International Symposium on Forest Hydrology, edited by W. E. Sopper and H. W. Lull, pp. 261-274, September.

Slake, P. J., 1962, "Forest Interception Studies in the United States," International Symposium on Forest Hydrology, edited by W. E. Sopper and H. W. Lull, pp. 157-161, September.

APPENDIX

COMPUTER PROGRAM LISTING

LIST OF FORTRAN LABELS

The input and output variables of the model are summarized as follows.

<u>Fortran label</u>	<u>Definition</u>	<u>Symbol in the text</u>
ADF	Detachment coefficient of runoff	D_f
AGB, AWP, BEX	Parameter describing sediment transporting capacity (Eq. 5.10)	
AIM	Coefficient in raindrop soil detachment equation	a_3
AMC	Antecedent moisture content	$m_o(0)$
BIM	Exponent in raindrop soil detachment equation	b_3
CB	Concentration of suspended bed material load	C_b
CGC	Channel-flow ground cover density	C_g
CND	Canopy cover density	D_c
CPER	Coefficient in P vs. A relation	a_1
CPW	Magnitude of capillary potential head at wilting point	P_w
CW	Concentration of wash load	C_w
DR	Rainfall rate or intensity	i
DT	Time increment in computation	Δt
EPER	Exponent in P vs. A relation	b_4
EIA	Depth of the aeration zone	η_a
EVP	Mean evaporation rate from the interception storage	E
DMB, DMW	Mean sediment size (bed material and wash load size)	ds
FK1	Constant representing grain resistance without rainfall for $N_r \leq 900$	K_o

LIST OF FORTRAN LABELS - Continued

<u>Fortran label</u>	<u>Definition</u>	<u>Symbol in the text</u>
FK2	Constant describing grain resistance for $2,000 \leq N_r \leq 25,000$	K_2
FK3	Constant describing grain resistance for $N_r \geq 100,000$	K_3
GBOUT	Bed-material load transport rate	G_b
GCD	Overland flow ground cover density	D_g
GMNX	Maximum depth to which a raindrop can penetrate the soil layer	D_p
GWOUT	Wash load transport rate	G_w
HIR	Ratio of high ground cover density to total ground cover density	λ
HLR	Average height of the low ground cover	ϵ_l
ICONS	Numerical control for sediment supply determination	
ICONW	Numerical control for computation	
ILAT	Lateral inflow segment	
ISEG	Computational sequence	
ITCOM	Total number of time increment for computation	
ITMAX	Total number of time increment at the end of a storm	
IUP	Upstream inflow segment	
NCH	Number of channel flow segments	
NDX	Number of space increment	
NOV	Number of overland flow segments	
NRD	Number of road segments	
NSGG	Total number of segments	

LIST OF FORTRAN LABELS - Continued

<u>Fortran label</u>	<u>Definition</u>	<u>Symbol in the text</u>
NSTOM	Number of storm for computation	
PB	Percent of bed-material load size in a typical soil sample	F_b
PERM	Saturated hydraulic conductivity	k_s
PW	Percent of wash-load size in a typical soil sample	F_w
QDEF	Difference in surface runoff (discharge) estimation	
AMES	Measured surface runoff	
QOUT	Water discharge	Q
SB	Depth of loose soil for bed material load size	z_b
SEG	Alphabetical or numerical identification of segments	
SLEN	Length of an overland flow plot, or channel length	L
SLOP	Bed slope	S_o
SM	Soil moisture content at saturation	m_s
SNU	Kinematic viscosity of water	ν
SPG	Ratio of the evaporation surface to the horizontal projected area for a typical ground cover	S_g
STORM	Alphabetical or numerical identification of a storm	
SW	Depth of loose soil for wash load size	z_w
TITLE	Alphabetical or numerical identification of the problem	
VIN	Initial interception storage content, defined as the ratio of the initial interception storage capacity to the total interception storage capacity	I_s

LIST OF PORTKIN LABELS - CONCL

<u>Fortran label</u>	<u>Definition</u>	<u>Symbol in the text</u>
VOG	Interception storage capacity of the ground cover per unit area of ground cover	V_g
VOR	Ratio of V_c to V_g	r_v
WP	Soil moisture content at wilting point	m_w
XIC	Channel ground-cover resistance descriptor	ψ_c
XIO	Overland flow ground-cover resistance descriptor	ψ_o
ZE	Net depth of loose soil	z
ZD	Depth of loose soil for bed material load size	z_d
ZSC	Alphabetical or numerical identification of segments	z_{sc}
L	Length of an overland flow plot, or channel length	SLEN
SLOP	Bed slope	SLOP
SM	Soil moisture content at saturation	SM
SNV	Kinematic viscosity of water	SNV
SPC	Ratio of the evaporation surface to the horizontal projected area for a typical ground cover	SPC
STORM	Alphabetical or numerical identification of a storm	STORM
SW	Depth of loose soil for wash load size	SW
TITLE	Alphabetical or numerical identification of the problem	TITLE
VIN	Initial interception storage constant, defined as the ratio of the initial interception storage capacity to the total interception storage capacity	VIN

PROGRAM WASED (INPUT,OUTPUT)

PROGRAM WASED (INPUT,OUTPUT)

C THIS IS A RAINFALL-RUNOFF-SEDIMENT MODEL
 C THIS PROGRAM IS DESIGNED TO SIMULATE WATER AND SEDIMENT HYDROGRAPH
 C FROM SMALL WATERSHEDS
 C NOTATIONS FOR THE MODEL INPUT
 C TITLE = ALPHABETICAL OR NUMERICAL IDENTIFICATION OF THE PROBLEM
 C NOV = NUMBER OF OVERLAND FLOW SEGMENTS
 C NCH = NUMBER OF CHANNEL FLOW SEGMENTS
 C NRD = NUMBER OF ROAD SEGMENTS
 C NSEG = TOTAL NUMBER OF SEGMENTS
 C NDX = NUMBER OF SPACE INCREMENTS
 C NSTOM = NUMBER OF STORM FOR COMPUTATION
 C DT = TIME INCREMENT FOR NUMERICAL COMPUTATION IN MINUTES
 C SNU = KINEMATIC VISCOSITY OF WATER IN SQUARE FEET PER SECOND *E5
 C ARFA = TOTAL AREA OF THE WATERSHED IN ACRES
 C SFG = ALPHABETICAL OR NUMERICAL IDENTIFICATION OF SEGMENTS
 C SLEN = LENGTH OF AN OVERLAND FLOW PLOT OR A CHANNEL REACH IN FEET
 C SLOPE = BED SLOPE
 C CPER,EPER = PARAMETERS DESCRIBING P-A RELATIONS
 C ISEG = COMPUTATIONAL SEQUENCE
 C IUP = UPSTREAM INFLOW SEGMENT
 C ILAT = LATERAL INFLOW SEGMENT
 C PERM = SATURATED HYDRAULIC CONDUCTIVITY IN INCHES PER HOUR
 C SM = MOISTURE CONTENT AT SATURATION
 C WP = MOISTURE CONTENT AT WILTING POINT
 C CPW = CAPILLARY POTENTIAL HEAD AT WILTING POINT IN INCHES
 C DMR = MEAN DIAMETER OF RED MATERIAL LOAD IN MILLIMETERS
 C DMW = MEAN DIAMETER OF WASH LOAD IN MILLIMETERS
 C PH = PERCENT OF RED MATERIAL LOAD SIZE IN SOIL SAMPLE
 C PW = PERCENT OF WASH LOAD SIZE IN SOIL SAMPLE
 C ETA = DEPTH OF THE ZONE OF AERATION IN INCHES
 C CND = CANOPY COVER DENSITY
 C GCD = GROUND COVER DENSITY IN OVERLAND FLOW AREAS
 C CGC = GROUND COVER DENSITY IN CHANNELS
 C VOG = INTERCEPTION STORAGE CAPACITY FOR THE TYPICAL GROUND COVER
 C IN INCHES
 C SRG = RATIO OF THE EVAPORATING SURFACE TO THE PROJECTED AREA
 C VOR = RATIO OF THE INTERCEPTION STORAGE CAPACITY OF A TYPICAL
 C CANOPY COVER TO THAT OF THE GROUND COVER
 C HLR = HEIGHT OF THE LOW GROUND COVER IN CHANNELS (FEET)
 C HIR = RATIO OF HIGH GROUND COVER DENSITY TO TOTAL GROUND COVER
 C DENSITY IN CHANNELS
 C FK1,FK2,FK3 = CONSTANTS DESCRIBING DARCY-WEISBACH FRICTION FACTOR
 C DUE TO GRAIN RESISTANCE ONLY
 C XIO = GROUND COVER RESISTANCE DESCRIPTOR FOR OVERLAND FLOW
 C XIC = GROUND COVER RESISTANCE DESCRIPTOR FOR CHANNEL FLOW
 C AIM,RIM,GMAX = PARAMETERS DESCRIBING SOIL DETACHMENT BY RAINDROP
 C IMPACT
 C AGR,AWP,PEX = PARAMETERS DESCRIBING SEDIMENT TRANSPORTING CAPACITY
 C ADF = DETACHMENT COEFFICIENT FOR SURFACE-RUNOFF EROSION
 C STORM = ALPHABETICAL OR NUMERICAL IDENTIFICATION OF STORMS
 C ITMAX = TOTAL NUMBER OF TIME INCREMENT AT THE END OF A STORM
 C ITCOM = TOTAL NUMBER OF TIME INCREMENT FOR COMPUTATION
 C ICONW = NUMERICAL CONTROL FOR COMPUTATION
 C ICONW = 0. WATER YIELD IS DISCONTINUOUS FROM PREVIOUS STORM
 C ICONW = 1. MOISTURE CONTENT IS CONTINUOUS FROM PREVIOUS STORM
 C ICONW = 2. WATER YIELD AND SEDIMENT YIELD ARE CONTINUOUS FROM
 C PREVIOUS STORM
 C ICONS = NUMERICAL CONTROL FOR SEDIMENT SUPPLY DETERMINATION
 C ICONS = 0. SEDIMENT SUPPLY IS DISCONTINUOUS FROM PREVIOUS STORM
 C ICONS = 1. SEDIMENT SUPPLY IS CONTINUOUS FROM PREVIOUS STORM
 C EVP = MEAN EVAPORATION RATE IN INCHES PER HOUR
 C VIN = INITIAL INTERCEPTION STORAGE CONTENT
 C AMC = ANTECEDENT MOISTURE CONTENT
 C DR = RAINFALL INPUT IN INCHES PER TIME INCREMENT
 C QMES = MEASURED SURFACE RUNOFF IN CUBIC FEET PER SECOND

PPOGRAM WASFD (INPUT,OUTPUT)

```

C
  DIMENSION QOUT(300), GROUT(300), GWOUT(300), CB(300), CW(300), SEG
  1(100)
  DIMENSION TITLF(10), GTOT(300), QMES(300), QDEF(300)
  COMMON /INO/ NSEG,NOV,NTQ,NDX,DT,DTS,DTN,IT,FPS,IMAX,ITMAX
  COMMON /FLO/ Q(100),A(100,10),DR(300),FR(300),EVP,VIN,AMC,CMC
  COMMON /SEQ/ ISEG(100),IUP(100,3),ILAT(100,2),OP(100,10)
  COMMON /GEO/ SLEN(100),SLOPE(100),CPER(100),EPER(100)
  COMMON /REF/ PERM,SM,WP,CPW,ETA,CND,GCD,CGC,VOG,SRG,VOR
  COMMON /FRC/ QN,AN,SNU,SLP,FK1,FK2,FK3,ALP,BET,CPR,EPR,ARF,CRF,GRF
  1,ERF,WHT,CHG,CLG,ELG,XIC,XIO
  COMMON /SED/ GR(100),GW(100),RR(100,10),RW(100,10),SB(100,10),SW(1
  100,10),ZE(100,10),SMR,SMW,CGB,CWL,AIM,RIM,GMAX,AGB,AWP,BEX,ADF,PR,
  2PW,PORR,PORW,FVR,FVW,HLR,ZSM
  IMAX=50
  EPS=0.1
C
C   INPUT AND OUTPUT TITLE
C
  READ 300, TITLE
  PRINT 310, TITLE
C
C   INPUT AND OUTPUT GENERAL INFORMATION
C
  READ 320, NOV,NCH,NRD,NDX,NSTOM,DT,SNU,AREA
  NTO=NOV-NCH
  NSEG=NTQ+NRD
  PRINT 330, NSEG,NDX,NSTOM,DT,SNU,AREA
C
C   INPUT AND OUTPUT BASIN CHARACTERISTICS DATA
C   INPUT AND OUTPUT GEOMETRY DATA
C
  READ 340, (SEG(I),SLEN(I),SLOPE(I),CPER(I),EPER(I),I=1,NSEG)
  PRINT 350, (SEG(I),SLEN(I),SLOPE(I),CPER(I),EPER(I),I=1,NSEG)
C
C   INPUT AND OUTPUT COMPUTATION SEQUENCE
C
  READ 360, (ISEG(I),(IUP(I,J),J=1,3),(ILAT(I,J),J=1,2),I=1,NSEG)
  PRINT 370, (ISEG(I),(IUP(I,J),J=1,3),(ILAT(I,J),J=1,2),I=1,NSEG)
C
C   INPUT AND OUTPUT SOIL DATA
C
  READ 200, PERM,SM,WP,CPW,ETA,DMB,DMW,PR
  PRINT 390, PERM,SM,WP,CPW,ETA,DMR,DMW,PR
  PW=1.-PR
C
C   INPUT AND OUTPUT VEGETATION AND GROUND CHARACTERISTICS DATA
C
  READ 380, CND,GCD,CGC,VOG,SRG,VOR,HLR,HIR
  PRINT 400, CND,GCD,CGC,VOG,SRG,VOR,HLR,HIR
C
C   INPUT AND OUTPUT FLOW RESISTANCE PARAMETERS
C
  READ 410, FK1,FK2,FK3,XIC,XIO
  PRINT 420, FK1,FK2,FK3,XIC,XIO
C
C   INPUT AND OUTPUT SEDIMENT ROUTING PARAMETERS
C
  READ 210, AIM,RIM,AGB,AWP,BEX,ADF,GMAX
  PRINT 220, AIM,RIM,AGB,AWP,BEX,ADF,GMAX
C
C   ESTABLISH SOME INVARIANT INFORMATION
C
  AIM=AIM/100000.
  IOUT=ISEG(NSEG)
  SNU=SNU/100000.
  DT=DT/60.
  DTS=DT*3600.
  DTN=DTS*FLOAT(NDX)

```


PROGRAM WASED (INPUT,OUTPUT)

```

FACT=12.*3600./(43560.*AREA)
PORR=1.-0.245-0.0864/(0.1*DMR)**0.21
PORW=1.-0.245-0.0864/(0.1*DMW)**0.21
DMR=DMR/304.8
DMW=DMW/304.8
CGR=4.84*DMR
CWL=4.84*DMW
FVW=53.13*DMW*DMW/SNU
FVR=(SQRT(36.064*DMR**3+36.*SNU**2))-6.*SNU)/DMR
SMR=2.*DMR
SMW=2.*DMW
CHG=HIF*CGC
CLG=CGC-CHG
ZSM=HLP*(1.-CGC)
CMC=WP
DO 190 L=1,NSTOM

```

```

C
C INPUT AND OUTPUT STORM CHARACTERISTICS DATA
C
  READ 430, STORM,ITMAX,ITCOM,ICONW,ICONS,EVP,VIN,AMC
  IF (ICONW.EQ.0) GO TO 110
  AMC=CMC
110 PRINT 440, STORM,ITMAX,ITCOM,EVP,VIN,AMC

```

```

C
C INPUT AND OUTPUT RAINFALL RECORDS
C
  PRINT 450
  READ 460, (DR(I),I=1,ITMAX)
  DO 120 I=1,ITMAX
    DR(I)=DR(I)/DT
120 CONTINUE
  PRINT 470, (I,DR(I),I=1,ITMAX)

```

```

C
C INPUT MEASURED SURFACE RUNOFF
C
  READ 230, (QMES(I),I=1,ITCOM)
C
C RAINFALL EXCESS DETERMINATION
C
  CALL RAINEX (ITCOM)
C
C INITIALIZE ENTIRE WATERSHED
C

```

```

  IF (ICONW.EQ.2) GO TO 150
  DO 140 I=1,NSEG
    Q(I)=0.
    GR(I)=0.
    GW(I)=0.
    DO 130 J=1,NDX
      A(I,J)=0.
      QP(I,J)=0.
      RR(I,J)=0.
      RW(I,J)=0.
      IF (ICONS.EQ.1) GO TO 130
      SR(I,J)=0.
      SW(I,J)=0.
      ZE(I,J)=0.
130 CONTINUE
140 CONTINUE

```

```

C
C ROUTING FOR EACH TIME INCREMENT
C
150 SUMGB=0.
  SUMGW=0.
  SUMMR=0.
  SUMSR=0.
  STAND=0.
  ARERR=0.
  QPRE=0.
  GPRE=0.
  GWPRE=0.

```

PROGRAM WASED (INPUT,OUTPUT)

```

DO 180 IT=1,ITCOM
  CALL ROUT
  QCUR=Q(IOUT)
  GHCUR=GH(IOUT)*102.96
  GWCUR=GW(IOUT)*102.96
  QOUT(IT)=0.5*(QPRE+QCUR)
  GROUT(IT)=0.5*(GPRE+GHCUR)
  GWOUT(IT)=0.5*(GWPRE+GWCUR)
  GSUM=GROUT(IT)+GWOUT(IT)
  GTOT(IT)=GSUM
  IF (GSUM.LE.0.) GO TO 160
  RATIO=1000./(QOUT(IT)+GSUM/62.4)/62.4
  CB(IT)=GROUT(IT)*RATIO
  CW(IT)=GWOUT(IT)*RATIO
  GO TO 170
160  CB(IT)=0.
     CW(IT)=0.
170  SUMGR=SUMGR+GROUT(IT)
     SUMGW=SUMGW+GWOUT(IT)
     SUMMR=SUMMR+QMES(IT)
     SUMSR=SUMSR+QOUT(IT)
     QDEF(IT)=QOUT(IT)-QMES(IT)
     STAND=STAND+QDEF(IT)*QDEF(IT)
     ABERR=ABERR+ABS(QDEF(IT))
     QPRE=QCUR
     GPRE=GHCUR
     GWPRE=GWCUR
180  CONTINUE
     PRINT 240
     PRINT 250, ((I,J,ZE(I,J),SB(I,J),SW(I,J),J=1,NDX),I=1,NSEG)
C
C   DETERMINE AMOUNT OF DIRECT RUNOFF
C
     SUMMR=SUMMR*DT*FACT
     SUMSR=SUMSR*DT*FACT
     STAND=SQRT(STAND/FLOAT(ITCOM))
     ABERR=ABERR/FLOAT(ITCOM)
     VOERR=100.*(SUMSR/SUMMR-1.)
     PRINT 260, SUMMR,SUMSR,STAND,ABERR,VOERR
     SUMGR=SUMGR*DT*FACT
     SUMGW=SUMGW*DT*FACT
     PRINT 270, SUMGR,SUMGW,CMC
     PRINT 480
     PRINT 280, (I,QOUT(I),GROUT(I),GWOUT(I),CB(I),CW(I),GTOT(I),I=1
1       ,ITCOM)
     PRINT 290, (I,QOUT(I),QMES(I),QDEF(I),I=1,ITCOM)
190  CONTINUE
     STOP
C
200  FORMAT (8F10.4)
210  FORMAT (7F10.5)
220  FORMAT (46X,27HSEDIMENT ROUTING PARAMETERS//18X,7F12.5)
230  FORMAT (12F6.2)
240  FORMAT (/40X,49HDEGRADATION, AGGRADATION AND AVAILABILITY OF SOIL/
1)
250  FORMAT (35X,2I10,3F10.5)
260  FORMAT (/41X,27HAMOUNT OF MEASURED RUNOFF =,F10.5/41X,28HAMOUNT O
IF SIMULATED RUNOFF =,F10.5/45X,20HSTANDARD DEVIATION =,F10.5/45X,2
21HMEAN ABSOLUTE ERROR =,F10.5/41X,28HPERCENTAGE ERROR IN VOLUME =,
3F10.5)
270  FORMAT (/33X,39HAMOUNT OF SIMULATED BED MATERIAL LOAD =,F15.2//37
1X,31HAMOUNT OF SIMULATED WASH LOAD =,F15.2//42X,26HCURRENT MOISTUR
ZE CONTENT =,F10.5)
280  FORMAT (10X,I10,5X,F10.5,5X,F10.5,5X,F10.5,5X,F10.5,5X,F10.5,5X,F1
10.5)
290  FORMAT (25X,I10,5X,F10.5,5X,F10.5,5X,F10.5)
300  FORMAT (10A8)

```

OUTPUT)

occurred in over

OCCURRED IN OVERL

SEDIMENT POUTING

T.DTS.DTN.IT.FPS.I

T,DTS,DTN,IT,EPS,]

R(300) • ER(300) • EVF

3), ILAT(100,2), QP(

0) • CPER(100) • EPER(

CND • GCD • CGC • VOG • S

FK2, FK3, ALP, BET, CR

doi:10.1017/S0022292410000510

(100,10), RW(100,10)

WL, AIM, PIM, GMAX, AC

OF SEGMENT TO THE

ST SEGMENT TO THE

ST SEGMENT TO THE

ST SEGMENT TO THE

SUBROUTINE ROUT

```

      CIM=GMAX*(1.-GCD)
      EPA=1.-GCD
      GO TO 150
130  IF (K.GT.NTO) GO TO 140
      ITPF=2
      APF=DPF*(1.-CND)*(1.-CGC)
      DIM=RIM*(1.-CND)*(1.-CGC)
      CIM=GMAX*(1.-CGC)
      GO TO 150
140  ITYPE=3
      ARF=DRF
      DIM=RIM
      CIM=GMAX
      ERA=1.
150  SLP=SLOPE(K)
      CPR=CPR(K)
      EPR=EPR(K)
      DTX=DTN/SLN(K)
      AUP=0.
      QUP=0.
      GBUP=0.
      GWUP=0.
      GLAT=0.
      GBLAT=0.
      GWLAT=0.

C
C   DETERMINE THE UPSTREAM INFLOW RATE
C
      IF (IUP(K+1).EQ.0) GO TO 170
      DO 160 J=1,3
        IF (IUP(K,J).EQ.0) GO TO 170
        JJ=IUP(K,J)
        AUP=AUP+A(JJ,NDX)
        QUP=QUP+Q(JJ)
        GRUP=GRUP+GB(JJ)
        GWUP=GWUP+GW(JJ)
160  CONTINUE

C
C   DETERMINE THE LATEPAL INFLOW RATE
C
170  IF (ITYPE.EQ.2) GO TO 180
      QLAT=QLAT+CPR*EPRM/43200.
180  IF (ILAT(K+1).EQ.0) GO TO 200
      DO 190 J=1,2
        IF (ILAT(K,J).EQ.0) GO TO 200
        JJ=ILAT(K,J)
        QLAT=QLAT+Q(JJ)
        GBLAT=GBLAT+GB(JJ)
        GWLAT=GWLAT+GW(JJ)
190  CONTINUE

C
C   NONLINEAR SCHEME FOR WATER ROUTING
C
200  ALAT=QLAT*NTS
      RLAT=GBLAT*NTS
      WLAT=GWLAT*NTS
      DO 440 J=1,NDX
        RPER=CPR
        ATEM=A(K,J)
        RTEM=RR(K,J)
        WTEM=RW(K,J)
        ZTEM=ZE(K,J)
        ZH=SR(K,J)
        ZW=SW(K,J)
        ZSUM=ZB+ZW
        ASUM=ALAT+ATEM+DTX*QUP
        IF (ASUM.LE.1.0E-5) GO TO 410

C
C   SET UP A-Q RELATIONSHIP
C
      QPRE=QP(K,J)
      AN=0.5*(AUP+ATEM)

```

SUBROUTINE ROUT

```

      QN=0.5*(QUP+QPRE)
      QAVE=QN
      IF (QN.GT.1.0E-5) GO TO 210
      QN=1.0E-5
      AN=1.0E-5
210    IF (ITYPE.EQ.1.OR.ITYPE.EQ.3) GO TO 230
C
C    MODIFICATION OF PARAMETERS FOR LOW GROUND COVER
C
      IF (ZTEM.GT.ZSM) GO TO 220
      RATIO=1.-ZTEM/ZSM
      RHT=HLR*RATIO
      IF (RATIO.GT.1.) RATIO=1.
      ELG=CLG*RATIO
      ERA=1.-CHG-ELG
      GO TO 230
220    RHT=0.
      FLG=0.
      ERA=1.-CHG
C
C    DETERMINE THE COEFFICIENT AND THE EXPONENT IN A-Q RELATION
C
230    CALL FRICT (ITYPE)
      REM=RET-1.
      REN=REM-1.
      ALRET=ALP*RET
      ALREM=ALP*RET*REM
      DTXA=DTX+ALP
      ERROR=EPS*ASUM
C
C    LINEAR SCHEME TO FIND THE FIRST APPROXIMATION
C
      ITER=0
      IF (QAVE.LE.1.0E-5) GO TO 240
      DAQ=ALRET*QAVE**BEM
      QE=(ALAT+DTX*QUP+DAQ*QPRE)/(DTX+DAQ)
      GO TO 250
240    QE=ASUM/DTXA
C
C    NONLINEAR SCHEME TO REFINE THE SOLUTION
C
250    ITER=ITER+1
      AEST=DTX*QE+ALP*QE**BET
      ADEV=ASUM-AEST
      IF (ABS(ADEV).LE.ERROR) GO TO 300
      IF (ITER.LT.IMAX) GO TO 260
      PRINT 460, IT*K*J
      STOP
260    FDER=DTX+ALBET*QE**BEM
      SDER=ALREM*QE**BEN
      BB=FDER/SDER
      SC=2.*ADEV/SDER
      STEFM=BB*BB+SC
      IF (STEM.GE.0.) GO TO 270
      QE=QE+ADEV/FDER
      GO TO 250
270    STEM=SQRT(STEM)
      IF (ADEV.GT.0.) GO TO 290
      FTEM=BB+STEM
      QE=QE-FTEM
      IF (QE.GT.0.) GO TO 250
280    ETEM=0.5*ETEM
      QE=QE+ETEM
      IF (QE.GT.0.) GO TO 250
      GO TO 280
290    X1=QE-BB-STEM
      X2=QE-BB+STEM
      AD1=ARS(ASUM-DTX*X1-ALP*X1**RET)
      AD2=ARS(ASUM-DTX*X2-ALP*X2**RET)

```

SUBROUTINE ROUT

```

      QE=X1
      IF (AD1.GT.AD2) QE=X2
      GO TO 250

C
C   DETERMINATION OF FLOW CONDITIONS, SUCH AS HYDRAULIC DEPTH, MEAN
C   VELOCITY, AND BOUNDARY SHEAR STRESS
C
300   ARFA=ALP*QE**RFT
      VMEAN=QE/AREA
      WEPER=CPR*ARFA**FPR
      HYRAD=AREA/WEPER
      RN=QE/(SNU*WEPER)
      IF (WEPER.GT.CPR) RPER=WEPER
      IF (ITYPE.EQ.1.OR.ITYPE.EQ.3) GO TO 320
      IF (HYRAD.GT.HHT) GO TO 310
      EWT=ERA
      GO TO 330
310   FWT=1.-CHG-ELG*RHT/HYRAD
      GO TO 330
320   EWT=ERA
330   TAT=62.4*HYRAD*SLP*EWT
      SV=(TAT/1.9379)
      RMV=2.5*VMEAN/SV
      FGRN=GRF/RN**ERF
      TAO=0.24224*FGRN*VMEAN*VMEAN

C
C   DETERMINATION OF THE AMOUNT OF SOIL DETACHED BY RAINDROP IMPACT
C
      IF (RN.GT.900.OR.DIM.EQ.0..OR.ZSUM.GT.CIM) GO TO 340
      SDR=DIM*(1.-ZSUM/CIM)
      ZB=ZB+SDR*PB
      ZW=ZW+SDR*PW

C
C   BED MATERIAL LOAD ROUTING
C
340   TTEM=TAO-CGB
      IF (TTEM.LE.0.) GO TO 370

C
C   DETERMINATION OF RATIO OF SUSPENDED BED MATERIAL LOAD
C
      ZR=FVB/(0.4*SV)
      AR=SMB/HYRAD
      IF (ZR.GT.5.5.OR.AR.GT.0.5) GO TO 350
      CALL POWER (ZR,AR,FJ,SJ,1.0E-2)
      P=AR**((7R-1.)/(11.6*(1.-AR)**ZR))
      SUSP=P*(RMV*FJ+2.5*SJ)
      IF (SUSP.LT.0.) SUSP=0.
      GO TO 360
350   SUSP=0.

C
C   DETERMINATION OF TRANSPORTING CAPACITY OF BED MATERIAL LOAD
C
360   GBC=(1.+SUSP)*ERA*WEPER*AGR*TTEM**REX
      RB(K,J)=GBC/QE

C
C   CHECK THE AVAILABILITY OF BED MATERIAL LOAD
C
      EGB=(GRUP-RB(K,J)*QE)*DTX-RB(K,J)*AREA*BTM*ATEM*BLAT
      IF (EGB.GE.0.) GO TO 380
      EBTM=EGB+7B*WPER
      IF (EBTM.GE.0.) GO TO 380

C
C   DETERMINATION OF THE AMOUNT OF SOIL DETACHMENT BY FLOW
C
      DFR=-ADF*EBTM/WPER
      ZB=ZB+DFR
      ZW=ZW+DFR*PW/PB
      RB(K,J)=(ZR*WPER*BLAT+ATEM*ATEM+GBUP*DTX)/(AREA*QE*DTX)
      EGR=-7B*WPER
      GO TO 380

```


SUBROUTINE ROUT

```

C
C      DETERMINATION OF DEPOSITION DUE TO LACK OF CARRY CAPACITY
C
370      RH(K,J)=0.
          EGB=GRUP*DTX+HTEM*ATEM+RLAT
C
C      DETERMINATION OF AVAILABILITY OF WASH LOAD
C
380      ZWTEM=ZW*RPER
C
C      WASH LOAD ROUTING
C
          TTEM=TAO-CWL
          IF (TTEM.LE.0.) GO TO 420
C
C      DETERMINATION OF RATIO OF SUSPENDED WASH LOAD
C
          ZR=FVW/(0.4*SV)
          AR=SMW/HYRAD
          IF (ZR.GT.5.5.OR.AR.GT.0.5) GO TO 390
          CALL POWER (ZR,AR,FJ,SJ,1.0E-2)
          P=AR** (ZR-1.)/(11.6*(1.-AR)**ZR)
          SUSP=P*(HMF*FJ+2.5*SJ)
          IF (SUSP.LT.0.) SUSP=0.
          GO TO 400
390      SUSP=0.
C
C      DETERMINATION OF WASH LOAD TRANSPORTING CAPACITY
C
400      WCP=(1.+SUSP)*ERA*WEPER*AWP*TTEM**REX
          RW(K,J)=WCP/QE
          WLP=(GWUP-RW(K,J)*QE)*DTX-RW(K,J)*AREA+WTEM*ATEM+WLAT
C
C      CHECK THE AVAILABILITY OF WASH LOAD
C
          IF (WLP.GT.-ZWTEM) GO TO 430
          RW(K,J)=(ZWTEM+WLAT+WTEM*ATEM+GWUP*DTX)/(AREA*QE*DTX)
          WLP=-ZWTEM
          GO TO 430
C
C      DETERMINATION OF DEPOSITION DUE TO THE CEASE OF RUNOFF
C
410      AREA=0.
          QE=0.
          RB(K,J)=0.
          EGP=GRUP*DTX+RTEM*ATEM+RLAT
          IF (DIM.EQ.0.OR.ZSUM.GT.CIM) GO TO 420
          SDR=DIM*(1.-ZSUM/CIM)
          ZB=ZR+SDR*PB
          ZW=ZW+SDR*PW
420      RW(K,J)=0.
          WLP=GWUP*DTX+WTEM*ATEM+WLAT
430      A(K,J)=AREA
          QP(K,J)=QE
          AUP=AREA
          QUP=QE
          GRUP=RR(K,J)*QP
          GWUP=RW(K,J)*QE
C
C      DETERMINATION OF DEGRADATION OR AGGRADATION
C
          ZCHAN=EGB/POPH+WLP/PORW
          ZE(K,J)=ZTFM+ZCHAN/PPER
C
C      DETERMINATION OF AVAILABILITY FOR NEXT TIME STEP
C
          ZR=ZR+EGB/PPER
          ZW=ZW+WLP/PPER

```


SUBROUTINE ROUT

```

      SR(K,J)=ZR
      SW(K,J)=ZW
440    CONTINUE
C
C      DETERMINATION OF WATER, WASH LOAD, BED MATERIAL LOAD DISCHARGE
C
      Q(K)=QUP
      GW(K)=GWUP
      GB(K)=GRUP
450    CONTINUE
      RETURN
C
460    FORMAT (30X,42HDO NOT CONVERGE FOR THE COMPUTATION POINT ,I5,2X,I5
      1,2X,I5)
C
      END

```

SUBROUTINE RAINEX (ITCOM)

```

      SUBROUTINE RAINEX (ITCOM)
C
C      THIS SUBROUTINE DETERMINES THE OVERALL MEAN RAINFALL EXCESS RATE
C      THE RAINFALL EXCESS COMPUTATION IS CARRIED OUT FOR A POINT UNDER
C      CANOPY AND FOR ANOTHER POINT IN THE AREA WITHOUT TREES
C
      DIMENSION RCUM(2), SINT(2), CM(2), EFR(2)
      COMMON /INO/ NSEG,NOV,NT0,NDX,DT,DTN,IT,EPS,IMAX,ITMAX
      COMMON /FLO/ Q(100),A(100,10),DR(300),ER(300),EVP,VIN,AMC,CMC
      COMMON /REF/ PERM,SM,WP,CPW,ETA,CND,GCD,CGC,VOG,SRG,VOR
      IF (PERM.EQ.0.) GO TO 110
      CIF=4.*CPW/(PERM*(SM-WP)*DT)
      GO TO 120
110    CIF=0.
C
C      DETERMINE THE INITIAL INTERCEPTION STORAGES
C
120    SINT(1)=GCD*VOG
      SINT(2)=(VOR+GCD)*VOG
      RCUM(1)=VIN*SINT(1)
      RCUM(2)=VIN*SINT(2)
      CM(1)=AMC
      CM(2)=AMC
      ETFM=EVP*DT
      DO 200 IT=1,ITCOM
C
C      DETERMINE THE RATES OF RAINFALL INPUT
C
      IF (IT.GT.ITMAX) GO TO 130
      DRF=DR(IT)
      GO TO 140
130    DRF=0.
140    DO 190 I=1,2
C
C      DETERMINE THE AVERAGE NET RAINFALL RATE
C
      S=GCD*SRG
      IF (I.EQ.2) S=S+VOR*SRG
      RCUM(I)=RCUM(I)+DRF*DT-ETFM*S
      IF (RCUM(I).LE.SINT(I)) GO TO 150
      RNET=(RCUM(I)-SINT(I))/DT
      RCUM(I)=SINT(I)
      GO TO 160
150    IF (RCUM(I).LT.0.) RCUM(I)=0.
      RNET=0.
C
C      DETERMINE THE AVERAGE INFILTRATION RATE
C

```

SUBROUTINE RAINEX (ITCOM)

```

160      RIF=0.5*PERM*(1.+SQRT(1.+CIF*(SM-CM(I))*2))
C
C      CHECK THE AVAILABILITY OF MOISTURE SUPPLY FOR INFILTRATION
C
      IF (RNET.GE.RIF) GO TO 170
      ERIF=RNET
      GO TO 180
170      ERIF=RIF
C
C      DETERMINE THE AVERAGE RAINFALL EXCESS RATE
C
180      EFR(I)=RNET-ERIF
C
C      ADJUST MOISTURE CONTENT FOR NEXT TIME STEP
C
      IF (ERIF.EQ.0.) GO TO 190
      CM(I)=(CM(I)*ETA+DT*ERIF)/ETA
      IF (CM(I).GE.SM) CM(I)=SM
190      CONTINUE
C
C      COMPUTE THE OVERALL MEAN RAINFALL EXCESS RATE
C
      ER(IT)=(1.-CND)*EFR(1)+CND*EFR(2)
200      CONTINUE
      CMC=(1.-CND)*CM(1)+CND*CM(2)
      RETURN
C
      END

      SUBROUTINE FRIC(IITYPE)

      SURROUTINE FRIC (IITYPE)
C
C      THIS SUBROUTINE DETERMINES THE COEFFICIENT AND THE EXPONENT IN A-Q
C      RELATION
C
      COMMON /REF/ PERM,SM,WP,CPW,ETA,CND,GCD,CGC,VOG,SRG,VOR
      COMMON /FRC/ QN,AN,SNU,SLP,FK1,FK2,FK3,ALP,BET,CPR,EPR,ARF,CRF,GRF
1      ERF,RHT,CHG,CLG,ELG,XIC,XIO
      PW=CPW*AN**EPR
      HR=AN/PW
      RN=QN/(PW*SNU)
      GO TO (110,120,150), IITYPE
110     XIR=1.+XIO*HR*GCD/(1.-GCD)
      GO TO 160
120     IF (HR.GT.RHT) GO TO 130
      EPH=HR
      ASM=CHG*ELG
      GO TO 140
130     ERH=RHT**3/HR**2
      ASM=CHG*ELG*RHT/HR
140     XIR=(1.-CHG*ELG*ELG*XIC*ERH+CHG*XIC*HR)/(1.-ASM)
      GO TO 160
150     XIR=1.
160     SK1=XIR*FK1+27.162*APF**0.407
      SK2=FK2*XIR
      SK3=FK3*XIR
      FK4=FK1+27.162*ARF**0.407
      IF (PN.GT.900.) GO TO 170
      ERF=1.
      CRF=SK1
      GRF=FK4
      GO TO 210
170     IF (PN.GT.2000.) GO TO 180
      ERF=1.25234*ALOG(SK1/SK2)-6.13916
      TEM=900.*(ERF-1.)
      CRF=SK1*TEM
      GRF=FK4*TEM
      GO TO 210

```

SUBROUTINE FRIC(IITYPE)

```

180 IF (RN.GT.25000.) GO TO 190
    ERF=0.25
    CRF=SK2
    GRF=FK2
    GO TO 210
190 IF (RN.GT.100000.) GO TO 200
    ERF=0.72135*ALOG(SK2/SK3)-1.82621
    TEM=100000.*ERF
    CRF=SK3*TEM
    GRF=FK3*TEM
    GO TO 210
200 ERF=0.
    CRF=SK3
    GRF=FK3
210 AEXP=1./(3.-EPR*(1.+ERF))
    ALP=(CPR*(1.+ERF)*CRF*SNU**ERF/(257.6*SLP))**AEXP
    BET=(2.-ERF)*AEXP
    RETURN

```

C

END

SUBROUTINE POWER (Z,A,XJ1,XJ2,CONV)

SUBROUTINE POWER (Z,A,XJ1,XJ2,CONV)

C

THIS SUBROUTINE EVALUATE J1 AND J2 INTEGRALS

C

NOTATIONS

C

XJ1 = VALUE OF J1 INTEGRAL

C

XJ2 = VALUE OF J2 INTEGRAL

C

N = ORDER OF APPROXIMATION + 1

C

CONV = CONVERGENCE CRITERION

C

```

N=1
XJ1=0.
XJ2=0.
ALG=ALOG(A)
C=1.
D=-Z
E=D+1.
FN=1.
AEX=A**E
GO TO 120
110 N=N+1
    C=C*D/FN
    D=E
    E=D+1.
    FN=FLOAT(N)
    AEX=A**E
120 IF (ABS(E).LE.0.001) GO TO 130
    XJ1=XJ1+C*(1.-AEX)/E
    XJ2=XJ2+C*((AEX-1.)/E**2-AEX*ALG/E)
    GO TO 140
130 XJ1=XJ1-C*ALG
    XJ2=XJ2-0.5*C*ALG**2
140 IF (N.EQ.1) GO TO 150
    CJ1=ABS(1.-FJ1/XJ1)
    CJ2=ABS(1.-FJ2/XJ2)
    IF (CJ1.LE.CONV.AND.CJ2.LE.CONV) RETURN
150 FJ1=XJ1
    FJ2=XJ2
    GO TO 110

```

C

END